2013-01-28

Meniscus Structure and Function

Andrews, Stephen

UNIVERSITY OF CALGARY

Meniscus Structure and Function

by

STEPHEN ANDREWS

A THESIS

SUBMITTED TO THE FACULTY OF GRADUATE STUDIES

IN PARTIAL FULFILMENT OF THE REQUIREMENTS FOR THE

DEGREE OF DOCTOR OF PHILOSOPHY

BIOMEDICAL ENGINEERING GRADUATE PROGRAM

CALGARY, ALBERTA

JANUARY, 2013

Abstract

The knee menisci are commonly injured, and do not heal well as a result of their minimal vascularity and severe loading environment. Further, removal of the menisci is detrimental to the long term health of the knee joint. This objective of this body of work was to implement an integrated approach to better understand the function of the menisci as it relates to their fine structure and composition. This approach included mechanical, structural and biochemical analyses, of the menisci using a bovine model.

A thorough assessment of the relevant literature led to the conclusion that menisci do not act as a shock absorber in the knee, as was previously believed. To probe the relations between osmolarity and material properties, it was identified experimentally that meniscal samples swell significantly under iso-osmotic conditions. This swelling results in greatly altered mechanical properties in those samples. The osmolarity independent swelling indicates that the menisci are a pre-stressed structure.

For the first time, a novel imaging modality, optical projection tomography (OPT) was successfully used to examine connective tissue structure. With OPT, the highly complex, three-dimensional collagen matrix organization within the meniscus was revealed. OPT was also capable of visualizing blood vessel organization in meniscal samples.

The localization of the matrix molecules, aggrecan, type II collagen, elastin and proteoglycan 4 were evaluated using various histological and immunofluorescence techniques. The localization was examined as it related to the various architectural subunits of the menisci to further elucidate the composition and organization of those regions. These techniques led to the identification of a new region in the menisci; a proteoglycan-rich, peri-vascular region. It is hypothesized that this region plays a protective role for blood vessels in the menisci. It was further identified that elastin has a region specific distribution which suggests a mechanical role for this protein in the menisci. Collagen II and aggrecan were observed to co-localize in the menisci, indicating similarities with other connective tissues that undergo compressive loading. Finally, these findings were integrated into a novel structural model of meniscal function, which proposes mechanical roles for each of the architectural sub-regions of the menisci.

Preface

Chapters Two through Seven of this thesis are based on the following manuscripts:

Chapter Two: with permissions
Andrews, S, Shrive, N, Ronsky, J. The shocking truth about meniscus. *Journal of Biomechanics* 44, 2737-40.

Chapter Three:
Andrews, SHJ, Rattner, JB, Shrive, NG, Frank, CB, Ronsky, JL. Osmotic and structural influences on meniscal swelling. (Submitted *Journal of Orthopaedic Research)*

Chapter Four:
Andrews, SHJ, Shrive, NG, Ronsky, JL. Relationship between meniscal swelling and the compressive properties of the bovine menisci. (In preparation for *Journal of Biomechanics)*

Chapter Five:
Andrews, SHJ, Ronsky, JL, Rattner JB, Shrive NG, Jamniczky, HA. An evaluation of meniscal collagenous structure using optical projection tomography. (Submitted *Journal of Biomechanics)*

Chapter Six:
Andrews, SHJ, Rattner JB, Ronsky, JL. Distribution of structural proteins in the bovine meniscus. (In preparation for the *Journal of Orthopaedic Research)*

Chapter Seven:
Andrews, SHJ, Samsom, MJ, Schmidt, TA, Ronsky, JL. Rattner JB. Distribution of proteoglycan 4 in the bovine meniscus. (Submitted to the *Orthopaedic Research Society Conference 2013)*

Acknowledgements

Thanks to my parents for their unquestioning support throughout my entire educational career and especially throughout my graduate education. For instilling in me a sense of curiosity and social responsibility, I am forever grateful.

To Heather and Mike, thank you from the bottom of my heart for your unending derision and mockery combined with your care and support.

To my friends, my unending thanks for your support and fellowship throughout this process; I am a better person for having known you all. I have learned as much from all of you as I have in my academic pursuits. To Erik, Brandon and Kyle for our numerous discussions that inevitably led to solutions to problems or at least a chance to get away from them temporarily, I am very appreciative.

To Sarah, thank you so much for your patience and understanding through this seemingly unending process. Your love and encouragement have made this past year far easier than it otherwise would have been.

To my supervisor, Janet, thank you for your support of my academic curiosity and your career guidance throughout this past 7 years. Thanks are also due to the numerous lab group colleagues that I have had the pleasure to work with over the years.

To my committee members, Drs. Frank and Shrive your insightful and challenging questions have made me a better researcher throughout this journey.

To Dr. Rattner, I am so grateful for the seemingly boundless generosity of your time and mentorship. I have learned so much from you in the short time that we have collaborated; it has been a pleasure to see research through your lens. Without your guidance this thesis would not have been possible.

To May Chung, the best technical support anyone could ask for, I am forever indebted. You have been my "lab mom" for the past year and for that I am so grateful.

My thanks is also due to the various agencies that have supported this work: NSERC, CRC Program, CIHR, AITF, AIHS and Zymetrix.

Table of Contents

List of Tables

List of Figures and Illustrations

Epigraph

"I hope all of you have this experience at some time in your life: that something you deeply and profoundly believe in, because it's beautiful and elegant and wonderful; turns out to be wrong. Because then, you can open your mind." ~ Lawrence Krauss

"To strive, to seek, to find, and not to yield" ~Lord Alfred Tennyson

"Discovery consists of seeing what everyone has seen and thinking what nobody has thought."

~ Albert von Szent-Gyorgyi

Chapter 1

Introduction and Review of Literature

Chapter One:

1.1 Introduction

Knee menisci are fibrocartilagenous discs, found in the femorotibial joint of many animals, including humans. The menisci are commonly injured in athletic activities (Roos, Ostenberg et al. 2001), and do not heal well as a result of their minimal vascularity and severe loading environment (Arnoczky and Warren 1982). These semi-lunar, wedge shaped discs deepen the contact surfaces on the tibial plateau and bridge the incongruence between the rounded femoral condyles and the relatively flat tibial plateau. Increasing the congruency in the knee joint results in lower stresses in the articular cartilage on the tibial and femoral surfaces (Shrive, O'Connor et al. 1978; Baratz, Fu et al. 1986; Cottrell, Scholten et al. 2008). Further, the menisci have secondary roles in providing increased joint stability, aiding in joint lubrication and proprioception (McDermott, Masouros et al. 2008).

Meniscal health is integral to long term knee joint health which is repeatedly supported by epidemiologic evidence (Fairbank 1948; Lanzer and Komenda 1990; Roos, Lauren et al. 1998; Lohmander, Englund et al. 2007; Englund 2009; Englund, Guermazi et al. 2009). Injury and subsequent removal of the meniscus, results in a 14-fold increase in the likelihood of developing premature osteoarthritis (Roos, Lauren et al. 1998). Due to their poor healing capacity, injured portions of the menisci are commonly removed by surgical procedures. The proportion of the meniscus that is surgically removed is directly related to the increased risk of developing osteoarthritis and further illustrates the importance of the menisci to knee joint health (Higuchi, Kimura et al. 2000). Since the menisci do not heal, replacement is an option that has been explored. Replacement menisci have been attempted with donor allografts and with

collagen scaffolds that promote tissue ingrowth (Matava 2007; Zaffagnini, Marcheggiani Muccioli et al. 2011). The results of these studies are favorable when compared to meniscectomy alone, but do not restore normal knee function. Current attempts are being made at developing tissue engineered solutions for the meniscus, where meniscal tissue would be grown from cell cultures (Athanasiou and Sanchez-Adams 2009). To date there has been little success at developing these tissues, due to a number of experimental factors. Some of the factors that have been proposed to influence tissue growth include: the cell type and source of these cells, the mechanical loading environment required to induce appropriate matrix production from the cells, the scaffold type on which the cells are seeded, along with quantitative and temporal variations of nutrition and growth factors required by these engineered constructs (Athanasiou and Sanchez-Adams 2009). In order to evaluate the fidelity of such constructs it is necessary to understand the characteristics of normal meniscal tissue. To date, the knowledge of meniscal structure and composition is limited. There are discrepancies amongst studies of the material properties of the tissue in compression, tension and shear. There are further discrepancies amongst studies of the organization, composition and distribution of matrix molecules in the menisci. A more complete understanding of native tissue properties is essential to furthering attempts at meniscal repair or replacement in the pursuit of long-term joint health after meniscal injury.

1.2 Literature Review

In the following literature review I will cover topics relating to the overall structure and function of the knee menisci. The review will include the topics of composition, structure and mechanics of the knee menisci. Further, I will introduce the imaging technique: optical projection tomography (OPT). OPT is an imaging technique that is novel in the analysis of the

microarchitecture of connective tissues. Finally, various animal models in meniscal research and the rationale for the use of bovine menisci for the research contained in this thesis will be covered.

1.2.1   Anatomy

The menisci are fibrocartilagenous structures found in the femorotibial joints of humans, and many other species. The medial and lateral menisci are semilunar in shape and insert into the tibia centrally, along the tibial spine anteriorly and posteriorly (Figure 1.1). At the periphery of the joint, the menisci are thicker than at the inner radius, resulting in a wedge-shaped cross-section. The shape of the menisci result in increased congruency between the rounded femoral condyles and the relatively flat tibial plateau and play a large role in load distribution on the femorotibial joint. At their periphery, the menisci are attached to the joint capsule, sometimes referred to as the coronary ligament. These coronary ligaments limit the motion of the menisci anteriorly and posteriorly and rotationally in the transverse plane. In the mid-sagittal plane the medial meniscus also attaches to the deep medial collateral ligament (Brantigan and Voshell 1943). In the human knee, during flexion the menisci move posteriorly. However, the medial meniscus is less mobile than the lateral meniscus due to its stronger and more complete circumferential peripheral attachment. The menisci are connected to each other at the anterior portion via the geniculate ligament, also known as the intermeniscal or transverse ligament (McDermott 2010). Two ligaments have been identified that attach the lateral meniscus to the medial femoral condyle known as the ligaments of Humphrey and Wrisberg (Kohn and Moreno 1995). Capsular attachments in the anterior compartment that connect the patella to the anterior tibial plateau are also integrated into the anterior portion of the menisci. These attachments may pull the menisci anteriorly during extension of the knee (McDermott 2010). The menisci are

fully integrated into the femorotibial joint as can be seen from their multiple connections to various structures within the joint.

1.2.2   Meniscus Structure

The structure of the meniscus has been described in 5 major architectural subdivisions (Petersen and Tillmann 1998):

1) Main body, which is composed to two major components:

    a) Circumferentially oriented fascicles

    b) Radially oriented tie-fibre sheets.

2) Surface layer

3) Lamellar layer

4) Cartilage-like inner portion.

Ligament of Wrisberg
Posterior cruciate ligament
Ligament of Humphry
Lateral collateral ligament
Capsule
Deep medial collateral ligament
Popliteal tendon
Superficial medial collateral ligament
Popliteal hiatus (recess)
Coronary ligament (meniscotibial)
Medial meniscus
Lateral meniscus
Anterior cruciate ligament
Transverse ligament

Anterior cruciate ligament
Anterior meniscofemoral ligament (ligament of Humphry)
Posterior cruciate ligament
Posterior meniscofemoral ligament (ligament of Wrisberg)
Lateral meniscus
Popliteus tendon (under arcuate ligament)
Medial meniscus
Arcuate ligament
Coronary ligament (meniscotibial ligament)
Superficial medial collateral ligament
Lateral collateral ligament
Popliteus muscle
Soleal line

Figure 1.1 Illustration of the knee joint, showing (Top) Superior view with the femur removed (B) Posterior view, with permissions (Evans 2007).

1.2.2.1 <u>Main Body</u>

Circumferential Bundles

The major structural components of the menisci are the circumferentially oriented bundles. Bullough et al. first described this fibre orientation as it pertained to the mechanics of the tissue in tension (Bullough, Munuera et al. 1970). Similar to other connective tissues, these

bundles of the meniscus, also called fascicles are composed of smaller subunits fibres, which are composed of fibrils (Figure 1.2). Fascicles are on the order of 100 µm in diameter and are thought to be oriented in directions parallel to the outer circumference of the meniscus. Fascicles are composed of bundles of collagen fibres, approximately 5 µm in diameter (Rattner, Matyas et al. 2011). Meniscal cells reside at this hierarchical level and are associated with individual fibres (Rattner, Matyas et al. 2011). Along these fibres the cells contain long cellular projections that connect cells along a fibre and between adjacent fibres (Hellio Le Graverand, Ou et al. 2001). The fibres are comprised of collagen fibril with diameters of approximately 100 nm (Petersen and Tillmann 1998). The constituents of the fibril are collagen molecules.
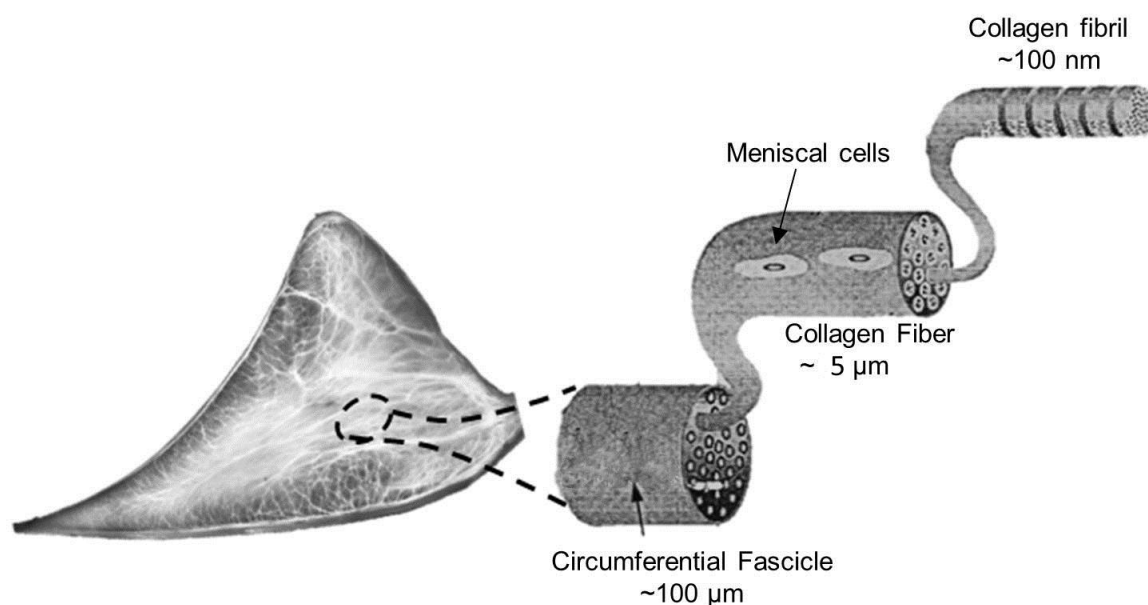
Figure 1.2 Schematic representation of a collagen hierarchy in circumferential direction in menisci. Collagen fascicles are composed of constituent fibres upon which cells reside in a linear organization. Fibres are composed of collagen fibrils approximately 100 nm in diameter. Adapted from (Rosenbloom, Abrams et al. 1993)

Tie-fibres

Bullough et al. proposed that individual tie-fibres were oriented radially in the human meniscus, perpendicular to the circumferential fascicles with the role of tying the bundles together (Bullough, Munuera et al. 1970). Skaggs et al. further described the arrangement of tie-fibres in the bovine meniscus (Skaggs, Warden et al. 1994). They found that the radial tie-fibres increased in prevalence from the anterior to posterior region of the meniscus. The presence of these fibres correlated with increased stiffness of the tissue. Further, serial sections of the menisci demonstrated tie-fibres that persisted over several sections, implying that the tie-fibres may actually form sheets of fibres to resist separation of the circumferential bundles. Rattner et al. modified the paradigm of meniscal structure through a series of electron microscopy (EM), and light microscopy techniques. In summary they found that the fibre bundles, arranged predominantly in the circumferential direction, weave through a honeycomb-like structure formed by a network of radial tie-fibre sheets. These sheets surround the fibre bundles and are composed of laterally integrated 10 µm thick fibril bundles (Figure 1.3) (Rattner, Matyas et al. 2011).

1.2.2.2 <u>Surface Layer</u>

The surface layer is composed of a fine mesh of randomly oriented fibres approximately 35 nm in diameter and is approximately 10 µm thick (Petersen and Tillmann 1998). The surface layer is also populated by a large number of fusiform cells (Ghadially, Lalonde et al. 1983). The cells on the surface have been shown to produce proteoglycan 4, a molecule shown to have lubricating properties in synovial joints (Schumacher, Schmidt et al. 2005; Sun, Berger et al. 2006). This fine mesh combined with cells that produce lubricating molecules result in a surface

capable of providing low-friction, wear resistance properties that are integral to maintaining long term joint health.

1.2.2.3 <u>Lamellar Layer</u>

Beneath the surface is a 150-200 μm thick layer of woven bundles (20-50 μm wide) composed of fibrils approximately 120 nm in diameter (Figure 1.3) (Petersen and Tillmann 1998). This superficial layer surrounds the main body of the meniscus. The fibre direction of this layer may imply that it experiences a stress radially, aligned along the direction of the surface of the meniscus. There are vertical, arborizing, fibres which project from this lamellar layer into the main body of the meniscus (Figure 1.3). These fibres may tie together the lamellar and central portions of the tissue by integrating the two and allow for force transmission between the layers.

1.2.2.4 <u>Inner Cartilage-Like Tip</u>

The structure of the inner tip of the meniscus is similar to that of articular cartilage. The tissue in this region has a homogeneous, fine collagenous structure (McDevitt and Webber 1990). Cells in this region are chondrocytic in appearance (McDevitt and Webber 1990; Hellio Le Graverand, Ou et al. 2001) and lie in lacunae of type VI collagen (Vanderploeg, Wilson et al. 2012).

1.2.3 Composition

The menisci are hydrated soft-tissues, composed of approximately 65% water (Djurasovic, Aldridge et al. 1998). The solid matrix is composed of a network containing primarily collagen type I (the most abundant solid component), collagen type II in smaller amounts, proteoglycan (PG), elastin and other non-collagenous proteins (McDevitt and Webber 1990).
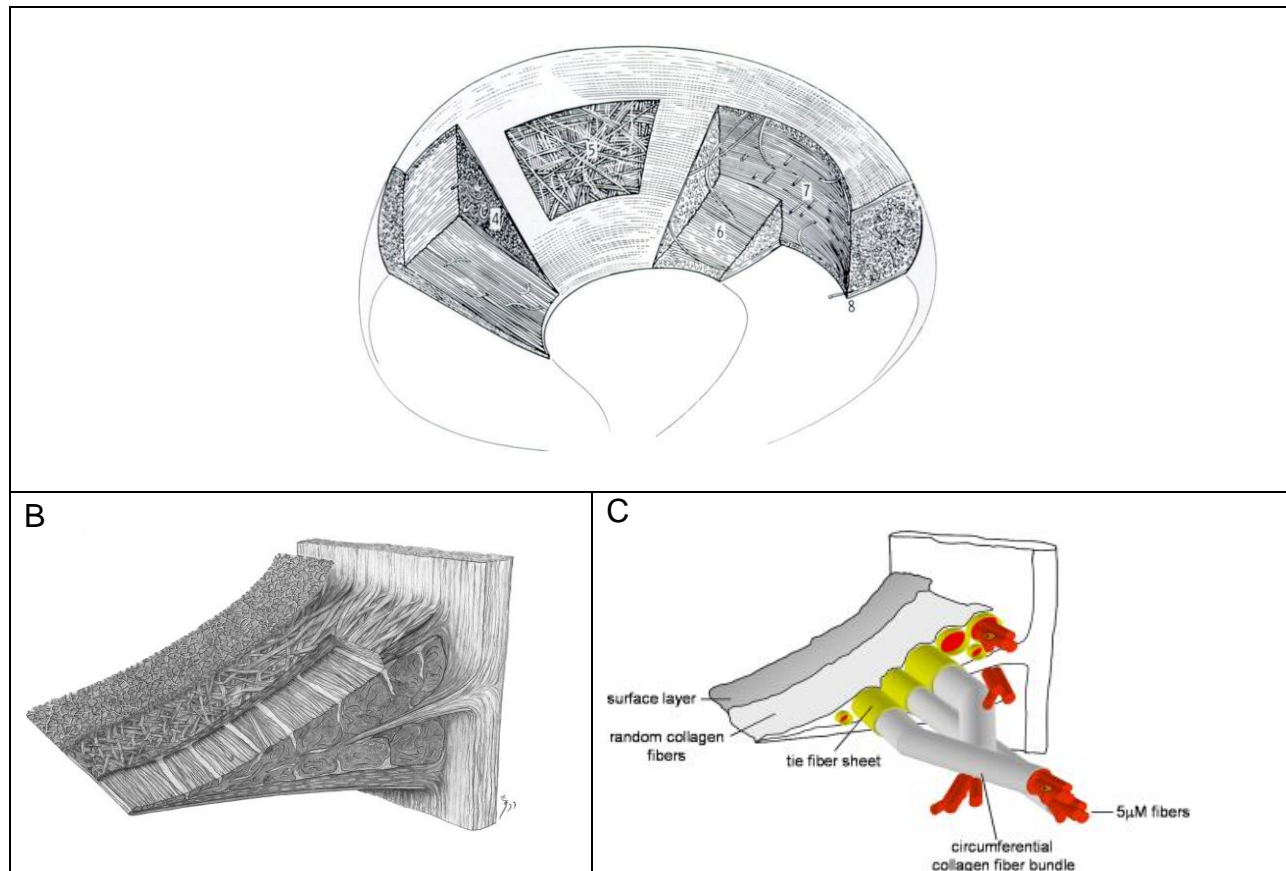
Figure 1.3 Images taken from previous models of meniscal structure from Bullough et al. (A) (Bullough, Munuera et al. 1970), Peterson and Tillman (B) (Petersen and Tillmann 1998) and Rattner et al. (C) (Rattner, Matyas et al. 2011), with permissions. Figure A is predominantly circumferentially oriented fibres with few radially oriented fibres and a disorganized surface layer. Figure B shows a distinction between the surface layer, and radially oriented lamellar layer beneath the surface layer with large circumferentially oriented fascicles in the main body. The model of Rattner et al. (Figure C) includes the idea of tie-fibre sheets wrapped around fascicles with the fascicle orientation weaving in the circumferential direction. This model also proposes a constituent 5 μm fibre in the circumferential fascicles.

1.2.3.1 Collagens

Collagen is the most abundant human protein, composing two-thirds of all protein in the body (Kadler 1994). It is the structural backbone of many connective tissues. Collagen structure is varied, and to-date 25 collagen types have been identified (Sun, Luo et al. 2002). This

discussion will deal with the predominant collagens found within the menisci. Eyre and Wu (1983) were the first to quantify the collagens found in menisci (Eyre and Wu 1983). In their study menisci were obtained from skeletally immature bovine stifles. The menisci were diced (1 mm) for pepsin digestion; sections were also digested from the surfaces to identify site-specific variation in composition. Type I collagen was determined to be the dominant form (98%), with smaller proportions of collagen type II, type III and type V. A follow-up study evaluated spatial differences in collagen content by location, as it was observed that inner one-third of the menisci is hyaline-like (containing more type II collagen), while the outer two-thirds is fibrocartilagenous (O'Connor 1976). Collagen content as a percent of dry weight is higher in the outer two-thirds than in the inner two-thirds, 82% versus 66% (Cheung 1987). Type II collagen was seen to be in higher proportions (4% of the total collagen) than the previous study with significant portions in the inner meniscus (60%). A major limitation of these studies is their use of pepsin tissue digestion to quantify the collagen components. Cheung noted that only 20% of the collagen in outer meniscus was pepsin soluble and 34% in the inner meniscus. Consequently, approximately 80% of the total collagen is insoluble to pepsin digestion in meniscal samples. This finding leaves some question as to the actual percentage of each collagen type in the meniscus.

Kambic and McDevitt evaluated the spatial organization and co-localization of the two major collagens (Type I and II) in the canine meniscus using indirect immunofluorescence (Kambic and McDevitt 2005). This study identified that circumferential fibres contained predominantly type I collagen with some bundles containing both type I and II fibres and others containing only type I fibres. Type II collagen was seen co-localized with type I fibres within the tie-fibres that separate the circumferential fascicles in radial sections. Collagen II was not seen in the surface or lamellar layers previously identified by Peterson and Tillman but was seen

extensively in the inner, cartilage-like portion of the meniscus (Petersen and Tillmann 1998). The authors also stated that similar patterns were observed in both bovine and lapine menisci.

More recently, the organization of these collagens, as well as collagen VI was studied in the juvenile bovine meniscus (Vanderploeg, Wilson et al. 2012). Collagen VI was evaluated as it had previously been identified in the pericelluar matrix (McDevitt and Webber 1990). Findings were similar to those previously reported in the canine model however, collagen II was seen in greater abundance in the outer portion of the meniscus surrounding the circumferential fascicles. This difference was hypothesised to be due to the young age of the bovine specimens which could change during maturation and warrants further investigation.

1.2.3.2 <u>Proteoglycan</u>

Proteoglycans (PGs) are heavily glycosylated proteins which consist of a core protein with covalently bound glycosaminoglycans (GAGs). PGs play important roles in connective tissues including contributions to compressive stiffness through osmotic swelling pressure (Kempson, Muir et al. 1970; Venn and Maroudas 1977; Williamson, Chen et al. 2001; Sanchez-Adams, Willard et al. 2011), governing fibril formation (Kadler, Holmes et al. 1996), and aiding in joint lubrication (Swann and Radin 1972; Schmidt, Gastelum et al. 2007). Various PGs have been identified in the knee menisci, including aggrecan, biglycan, fibromodulin, decorin and proteoglycan 4 (Ingman, Ghosh et al. 1974; McNicol and Roughley 1980; Schumacher, Schmidt et al. 2005). These molecules vary in their function and abundance from the inner to outer regions of the menisci (Nakano, Dodd et al. 1997; Valiyaveettil, Mort et al. 2005).

Nakano et al. identified increased PG content in the inner third compared to the outer two-thirds of the tissue (Nakano and Scott 1986). This finding was further expanded to show that

generally, the total amount of proteoglycan decreases with increasing distance from the inner tip in the direction of the outer edge, however not all of the component PGs follow this trend. Aggrecan decreases toward the outer edge, while fibromodulin and biglycan are most prevalent in the mid portion of the menisci and decorin is most abundant in the outer third (Nakano, Dodd et al. 1997; Valiyaveettil, Mort et al. 2005). This variation in the PG of the menisci is also related to variation in the material properties within these regions (Sanchez-Adams, Willard et al. 2011).

Aggrecan is a PG that has been specifically identified in its role in contributing to compressive stiffness in tissues, including menisci and articular cartilage. The large aggregating molecule is composed of negatively charged GAGs (keratan sulphate and chondroitin sulphate) which are hydrophilic (meaning they readily bind with and attract water), resulting in a swelling pressure in tissues with significant aggrecan content (Figure 1.4) (Maroudas 1976). The degeneration of aggrecan has also been linked with changes associated with osteoarthritis, signifying the important role this protein plays in tissue function (Huang and Wu 2008).
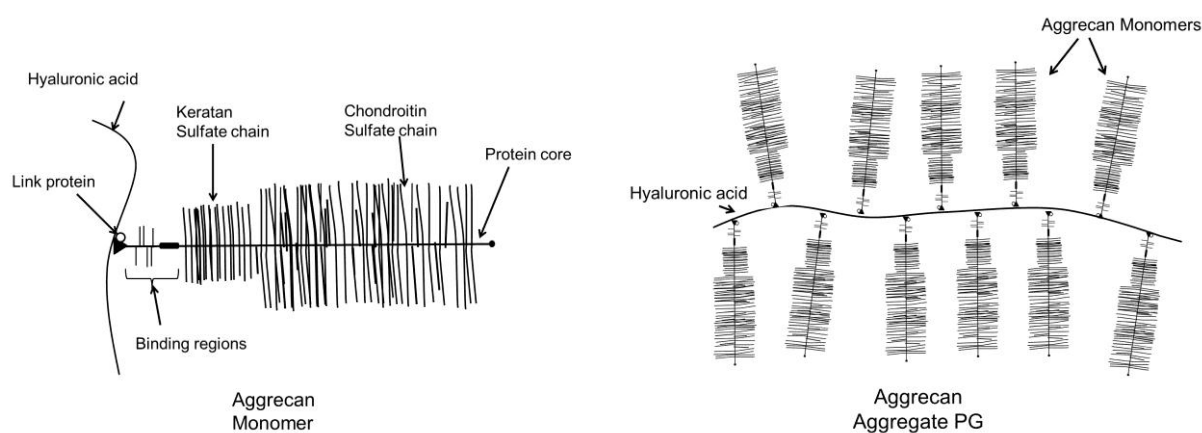
Figure 1.4 Schematic representation of an aggrecan monomer (left) and an aggrecan PG aggregate right. Aggrecan is composed of a protein core with a keratin sulfate rich region and a chondroitin sulfate rich region bound to it. Link protein stabilizes the bond between the aggrecan and hyaluronic acid. Aggrecan forms large PG aggregates by binding to a hyaluronic acid chain. Recreated from (Kelly 1990).

1.2.3.3 <u>Elastin</u>

Elastin molecules comprise 90% of the composition of elastin fibres found in connective tissues, including the menisci as well as in lung and blood vessels (Hopker, Angres et al. 1986; Rosenbloom, Abrams et al. 1993). Elastin fibres can elongate up to 100-150% of their length prior to failure (Carton, Dainauskas et al. 1962). They are theorized to contribute to the elastic mechanical behaviour of the tissues in which they reside. Isolated elastin fibres exhibit a non-linear stress-strain relationship, with increasing stiffness at higher levels of strain (Carton, Dainauskas et al. 1962).

Within the menisci the composition of elastin is low (0.6%), despite the diffuse vascularization which is known to contain significant amounts of the protein (Peters and Smillie 1972). There is contradictory information on elastin's orientation within the meniscus extracellular matrix (ECM). One study identified that elastin is oriented obliquely to the collagenous matrix in human menisci (Hopker, Angres et al. 1986), while another identified elastin parallel to tie-fibre sheets (Rattner, Matyas et al. 2011). Other observations of the menisci have identified a network of tie-fibres through which the circumferential fibres pass, making the idea of obliquely oriented elastin fibres counter-intuitive, as they would have to follow a path through the tie-fibre sheets, separate from the collagen with which they are associated (Rattner, Matyas et al. 2011). Further, elastin fibrils have been observed within cross-sections of collagen fibres of lapine and human menisci using electron microscopy (Ghadially, Lalonde et al. 1983; Ghadially, Wedge et al. 1986) . This result indicates that elastin may be directly associated with individual collagen fibres or fascicles. The findings of these previous studies are conflicting and the orientation of elastin fibres with respect to the collagenous matrix requires clarification.

1.2.3.4 <u>Cells</u>

The cells of the meniscus are diverse. Cells from the inner portion of the meniscus are rounded and lie in lacunae and resemble chondrocytes from articular cartilage (Figure 1.5) (McDevitt and Webber 1990; Hellio Le Graverand, Ou et al. 2001). The cells from the outer portion are elongated with several projections and have a similar morphology to fibroblasts. Cells from the intermediate region identified by McDevitt and Webber as fibrochondrocytes have an intermediate morphology between fibroblasts and chondrocytes (McDevitt and Webber 1990). These cells are rounded or oval shaped with few cellular projections (McDevitt and Webber 1990; Hellio Le Graverand, Ou et al. 2001). Meniscal cells may also be classified by the matrix molecules they produce. The previous sections identified that the localization of matrix molecules varies with the location in the meniscus. The more chondrocyte-like cells produce more type II collagen and aggrecan than the outer fibroblast-like cells which produce predominantly type I collagen (Eyre and Wu 1983; McDevitt and Webber 1990; Nakano, Dodd et al. 1997). In the transitional zone fibrochondrocytes make a combination of the molecules produced by the other cell phenotypes (Verdonk, Forsyth et al. 2005). At the surface, cells have a fusiform morphology and are known to produce the lubricating molecules, hyaluronic acid and proteoglycan 4 (PRG4). Meniscal cells are a combination of four distinct phenotypes that are integral to the development and maintenance of the complex matrix that compose the tissue.
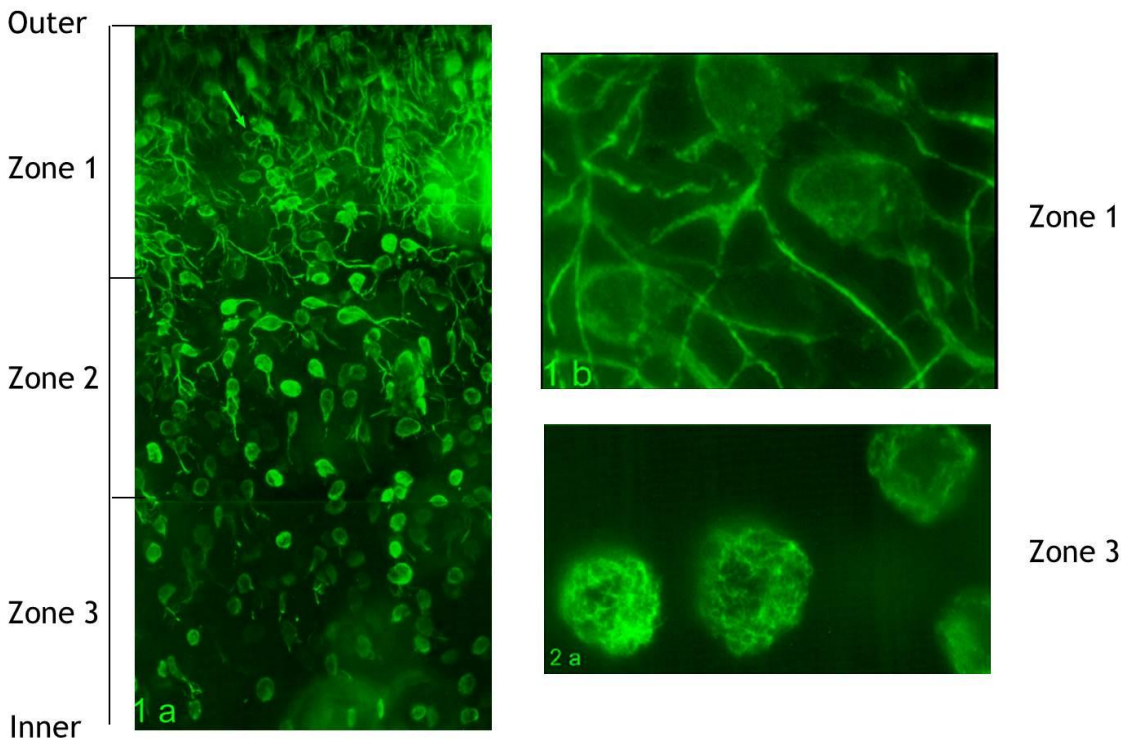
Figure 1.5 Immunofluorescence image of meniscal cells from the inner middle and outer zones of the rabbit meniscus, demonstrating the different cell phenotypes expressed in the meniscus. Reprinted with permissions (Hellio Le Graverand, Ou et al. 2001). Cells from zone 1 exhibited long cellular processes and fibroblastic morphology. Zone 3 contained cells which were rounded without projections, similar to chondrocyte morphology. Zone 2 contained an intermediate phenotype, and are considered fibrochondrocytes. Cells near the surface displayed a fusiform morphology.

1.2.4 Optical Projection Tomography

The structural models previously described here were developed using two-dimensional imaging techniques. The inherent limitation with all of these techniques, is that the structure of the meniscus is heterogeneous and complex in three dimensions. Consequently, the 3-D models previously developed have made conclusions about the 3-D structure by extrapolation of 2-D images. Optical projection tomography (OPT) is a promising technique which could overcome the inherent difficulties in imaging a highly heterogeneous structure (Sharpe, Ahlgren et al.

2002). It is a technique capable of imaging samples on the 'mesoscopic scale' (1-10 mm) at a micro-scale resolution (Sharpe, Ahlgren et al. 2002) but to date has not been used to evaluate the structure of connective tissues. The technique takes two-dimensional images of objects from multiple angles and reconstructs them using a back projection algorithm to determine its three-dimensional structure (Figure 1.6). It is optically similar to computed tomography (CT), but uses white or fluorescent light rather than x-ray to image the object of interest. The technique requires for the tissue to be cleared using a benzyl alcohol, benzyl benzoate (BABB) mixture to allow light to pass through the object. This technique has primarily been used to evaluate development and gene expression in mouse embryos (Sharpe, Ahlgren et al. 2002). To date, no study has attempted to evaluate collagenous structure of connective tissues using OPT. As collagen and elastin both autofluoresce at similar wavelengths (325 nm) (Richards-Kortum and Sevick-Muraca 1996) in the fluorescent spectrum, this technique may be useful in the evaluation of meniscal tissue structure.
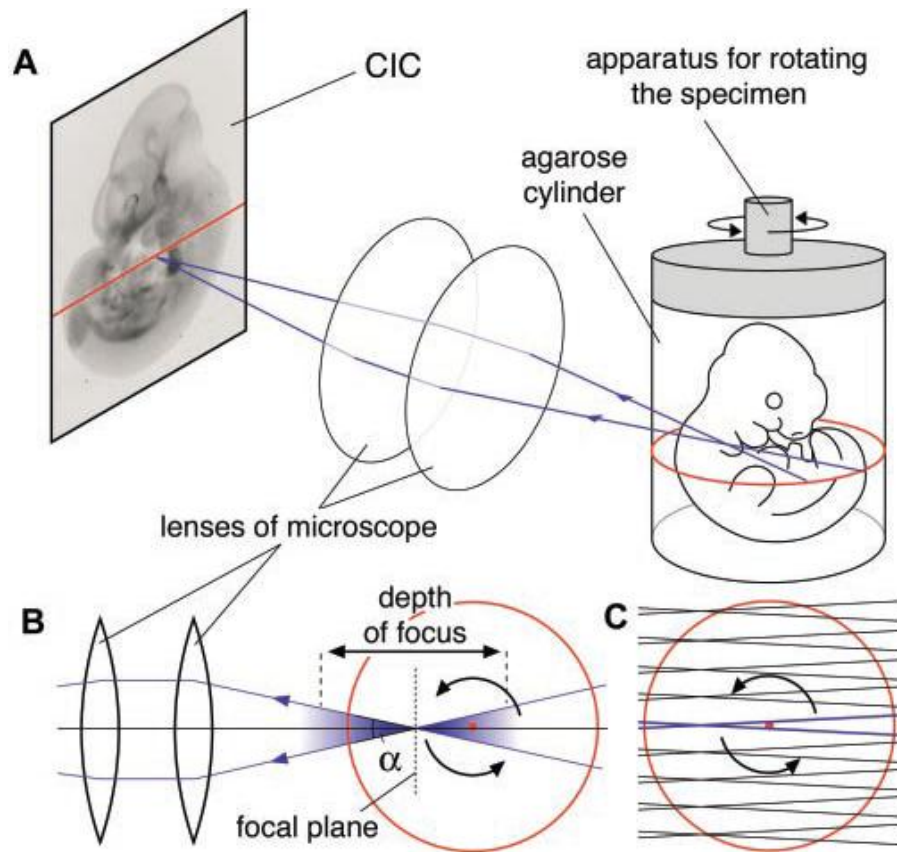
Figure 1.6 OPT microscopy. (A) A schematic of the OPT microscopy setup. The specimen is rotated within a cylinder of agarose while held in position for imaging by a microscope. Light transmitted from the specimen (blue lines) is focused by the lenses onto the camera-imaging chip (CIC). The apparatus is adjusted so that light emitted from a section that is perpendicular to the axis of rotation (red ellipse) is focused onto a single row of pixels on the CIC (red line). The section highlighted as a red ellipse in (A) is seen as a red circle in (B). The region of the specimen sampled by a single pixel of the CIC is shown as a double inverted cone shape (blue region). Modified from Sharpe et al. with permissions (Sharpe, Ahlgren et al. 2002)

1.2.5 Mechanics

In order to describe the mechanical behaviour of the meniscus, this review will discuss several mathematical and mechanical foundational principles. This background information will cover the topics required for the following review of meniscal mechanics.

Constitutive material properties are those that describe the behaviour of a material irrespective of its structure; which includes the relationship between stress and strain. Stress is a

measure of the internal forces per unit area within a body caused by the application of external forces. Strain is a measure of the normalized deformation caused by the forces applied to a deformable body. Stress and strain can have two main forms, volumetric and deviatoric. Volumetric stresses are those that act normal to a surface and tend to change the volume of the material. These stresses can be either tensile or compressive. Deviatoric, or shear, stresses act tangential to a surface and tend to deform the body without inducing a volumetric change.

Relationships between the stress and strain for a material define the general material type. Two types of materials are discussed here: linear and non-linear. Linear materials have a linear relationship between stress and strain. Non-linear materials, as the name suggests, have a non-linear relationship between stress and strain (Figure 1.7). Very few materials display a truly linear relationship, however some standard engineering materials such as steel, carbon fibre and glass are approximately linear. The modulus of a linear material is constant until it fails (or yields) and is typically defined by Young's Modulus which is equal to the slope of the stress-strain relationship. Most musculoskeletal materials are non-linear including, bone, ligament, tendon, cartilage and menisci (Røhl, Larsen et al. 1991; Woo, Abramowitch et al. 2006). The typical stress-strain curve for these materials is approximately sigmoidal in shape, with an initial low stiffness 'toe-region', followed by an approximately linear region until failure begins to occur (Figure 1.7).

There are many ways of characterizing the modulus of a non-linear material. The two most commonly accepted techniques are: tangent modulus and secant modulus. The tangent modulus is defined by the instantaneous rate of change of the stress-strain curve. In practical applications with discrete data measurements, finite difference approximations are used to calculate this tangent modulus value. The secant modulus is defined as the ratio of stress to strain

at any given strain (Figure 1.7). In many studies the 'linear' stiffness is used which is a modified version of the tangent modulus; a portion of the stress-strain curve is approximated as linear and a line of best fit is used to calculate is slope.
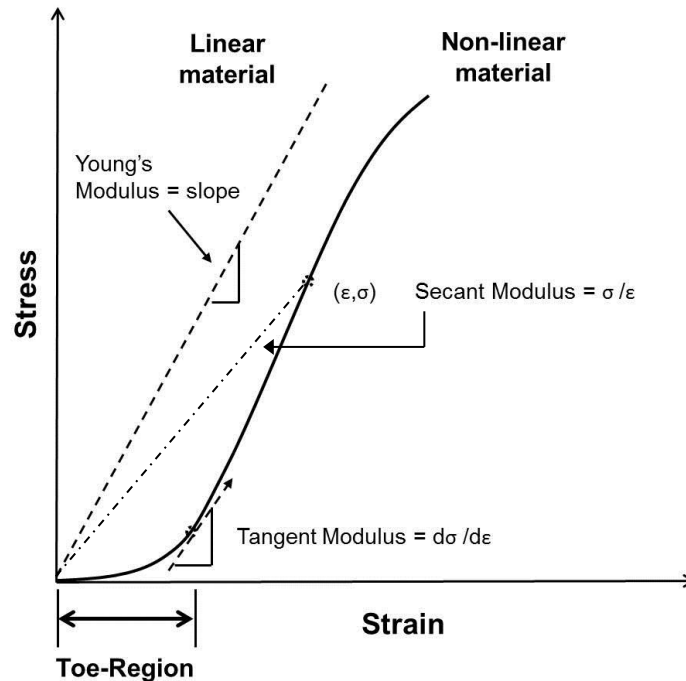
Figure 1.7 Schematic describing stress-strain relationships in linear and non-linear material behaviour. The definitions of Young's modulus, tangent modulus and secant modulus as they relate to the material behaviour are indicated.

Anisotropy, meaning that the material properties are direction dependent, is a property of many musculoskeletal materials. Most of these materials have directionality to the matrices that compose them and this determines the material behaviour in those directions (Mow, Ratcliffe et al. 1992; Augat, Link et al. 1998; Chia and Hull 2008). Anisotropic behaviour is particularly prevalent in the menisci (Proctor, Schmidt et al. 1989). Viscoelasticity is another material property common in musculoskeletal tissues. Viscoelastic materials exhibit both viscous and elastic material behaviour, meaning that they have time dependent behaviour. Two of these time

dependent properties are stress relaxation and creep. In stress relaxation, a displacement is applied and held constant, and the resultant stress decreases over time. Creep occurs when displacement increases over time under a constant applied load. These time-dependent behaviours occur as a result of fluid movement and redistribution coupled with rearranging of the solid matrix under changing load or displacement (Mow, Kuei et al. 1980).

Biphasic theory is used to describe the viscoelastic behaviour of fluid saturated materials. Biphasic theory is an adaptation of poroelastic theory which was developed by Biot in 1941 to describe the material behaviour of hydrated soils (Biot 1941). Mow et al. applied this same theory to hydrated soft tissue, specifically articular cartilage (Mow, Kuei et al. 1980). The theory explains the behaviour of poroelastic materials by describing the combined effects of movement of a fluid medium through an interconnected set of pores within a solid matrix. In soft tissues, such as cartilage, meniscus, ligament and tendon the theory describes the intrinsic behaviour of the solid matrix and synovial fluid, as well as the interaction caused by movement of the fluid through the tissue (Mow, Kuei et al. 1980).

The original mathematical theory describing the behaviour of cartilage applied only to the assumption of infinitesimal strain, where the permeability was assumed constant for small strain and the material was linear elastic and isotropic. This theory was later adapted for finite deformation with changing permeability due to consolidation of the matrix as well as including hyperelastic material properties (Holmes 1986; Holmes and Mow 1990) and further adapted to include anisotropy (Scowen, Brailsford et al. 1948).

Biphasic theory has been used extensively to describe the normal material properties of both cartilage and meniscus in many species of animals (Mow, Kuei et al. 1980; Proctor, Schmidt et al. 1989; Fithian, Kelly et al. 1990; Joshi, Suh et al. 1995; Tissakht and Ahmed

1995). The two main properties reported by this method are bulk modulus (H_A) and permeability (k). Mow et al. evaluated the results of this theory against the direct permeation method to determine permeability (Mow, Kuei et al. 1980). In this method, a hydrostatic pressure is applied across the tissue specimen and the resulting flow is used to determine the permeability using Darcy's Law; a constitutive law for fluid flow in a porous medium. The results of the direct permeation experiment were shown to be comparable to those results obtained by curve fitting the equations obtained by biphasic theory. This finding demonstrated the applicability of the theory to connective tissues.

1.2.6 Meniscal Mechanics

The mechanics of the menisci are integral to the overall mechanics of the femorotibial joint. The menisci transmit approximately 50% of the load in the femorotibial joint (Seedhom, Dowson et al. 1974; Krause, Pope et al. 1976). By increasing the joint congruency between the femur and tibia, the menisci are integral to decreasing stresses on the articular surfaces of the tibia and femur (Baratz, Fu et al. 1986; Cottrell, Scholten et al. 2008). Under a vertically applied load, the wedge-shape contour of the menisci introduces a radially extrusive force, which would tend to push the menisci from the joint. This radial force is resisted by the strong ligamentous attachments to the anterior and posterior tibial spine and is converted into a tensile hoop stress (Figure 1.8) (Fairbank 1948; Krause, Pope et al. 1976; Shrive, O'Connor et al. 1978). Loading of the femorotibial joint results in a complex state of stress in the tissue: (1) the aforementioned hoop stress (2) a radial tensile stress which tends to splay the tissue (3) a vertical compressive stress (4) shear stress.
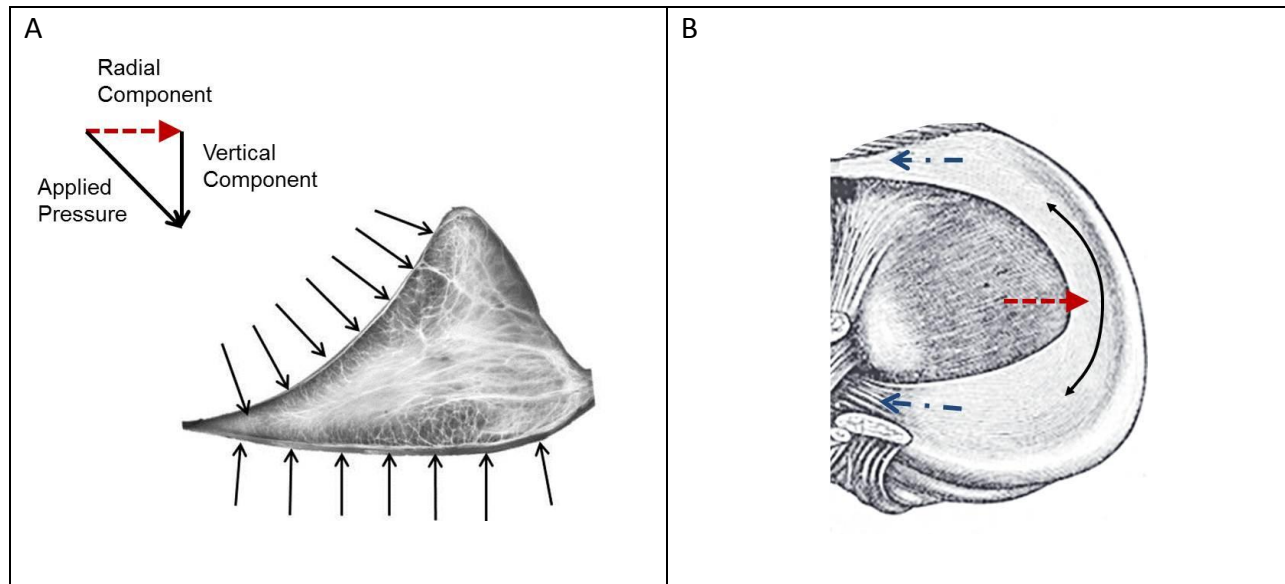
Figure 1.8 Schematic representation of the load bearing in the meniscus. A: The applied pressure results in a vertical compressive force and a radially extrusive force. B: The radially extrusive force (red dashed arrow) is resisted by the strong attachments at the tibial spine (blue dash-dot arrows) resulting in a circumferential hoop stress in the tissue (black arrow)

The shape of the distal end of the femur, which contacts with the meniscus, varies throughout flexion. In extension, the radius of curvature of the contact surface is large and decreases for increasing flexion angle (Figure 1.9). In addition, the femur is narrower in the medio-lateral direction at extension, and increases for increasing flexion. As a consequence of this shape, when the femur contacts the menisci in extension, the large radius of curvature forces the anterior and posterior horns of the menisci apart from each other. As the knee flexes, the larger medio-lateral aspect of the femur forces the menisci outward radially, which pulls the anterior and posterior horns closer together. This narrowing of the anterior-posterior gap accommodates the reduced radius of curvature of the posterior femur. The shape of the femur combined with the compliance of the menisci, results in a dynamic congruency throughout varying degrees of flexion.
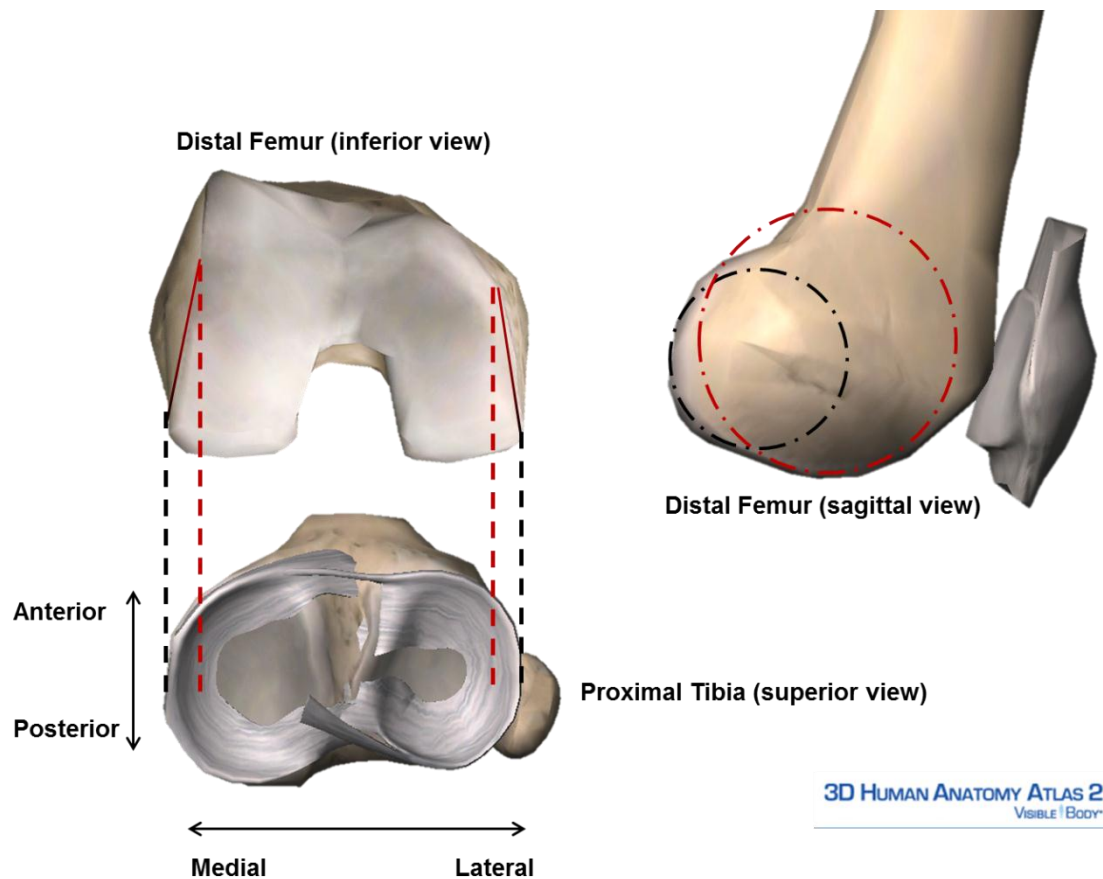
Figure 1.9 Illustration of the varying geometry of the femur from extension to flexion as it relates to meniscus geometry. The femur is narrower in the medio-lateral direction and has a larger radius of curvature in extension than in flexion.

The menisci are also purported to act as shock absorbers in the femorotibial joint (Kurosawa, Fukubayashi et al. 1980; Voloshin and Wosk 1983). However, this paradigm is non-intuitive due to the low permeability (Proctor, Schmidt et al. 1989) and minimal deformation of the menisci under physiological loads (Jones, Keene et al. 1996). Further investigation of this paradigm is required to confirm the role of the menisci as shock absorbers.

1.2.7 Compression

1.2.7.1 <u>Whole joint compression</u>

Seedhom et al. were the amongst the first groups to quantify the approximate load in the menisci (Seedhom, Dowson et al. 1974). This study loaded the entire joint axially from 2-100 kg and measured the resultant displacement. The meniscal attachments were detached, one at a time. The resultant displacements measured from the intact experiment were then applied to the joint and the resultant loads were measured. The theory of superposition was then used to calculate the loads in the meniscus. In this theory, if a tissue is removed from a previously measured test and the joint position is recreated in a subsequent test, then any change in measured load would be load carried by the excised tissue. This study showed that the menisci transmit 50% of the load experienced in the medial compartment and 70% of the load experienced by the lateral compartment (Seedhom, Dowson et al. 1974). The stress in the knee joint has been evaluated using pressure sensitive films (Fuji films) placed on the tibial plateau to evaluate changes in the stress of the femorotibial joint after meniscectomy (Fukubayashi and Kurosawa 1980). Under a load of 1000 N, the contact area was 2.2 times greater in the intact joint. Further, the peak contact pressure was 3 MPa intact, compared to 6 MPa in the meniscectomized case. These studies illustrate the important role the menisci play in load distribution in the femorotibial joint and demonstrate a chondroprotective effect by reduction of contact stress. Various other studies had previously evaluated changes in contact area using other measurement techniques. While the results of these studies are variable in terms of absolute contact areas, there is always a significant decrease in the contact area, and by analogy increased contact stress in all of these reports (Kettelkamp and Jacobs 1972; Walker and Erkman 1975; Maquet, Van De Berg et al.

1976). More recently, the effects of partial meniscectomy were studied using a newer version of pressure sensitive films (K-Scan 4000) on the tibial plateau (Lee, Aadalen et al. 2006). This study found an approximately linear relationship with the amount of meniscus removed and the decrease in the contact area in the femorotibial joint for 3 different flexion angles (0˚, 30˚, 60˚).

Implantable strain transducers on the peripheral (outer) edge of the meniscus provide another modality with which to test in situ mechanics of the menisci. Measuring the compressive strain in the body of the tissue is impracticable; while measuring the tensile strain at the peripheral edge is possible. However, the "zero position" of the tissue is not known, so the in vivo reference length is difficult to define. The results of Jones et al. indicate an average strain of 2.9%, 2.7%, and 1.5% for the anterior, mid and posterior portions of the meniscus respectively under a load of 3 times bodyweight at full extension (Jones, Keene et al. 1996). This study identified that vertical loading does indeed result in hoop stress in the meniscus. There is also a differential strain experienced regionally in the menisci, which may aid in identifying discrete structural properties throughout the menisci. Experimentally induced radial and longitudinal tears in the body of the meniscus, caused changes in the strain measured on the circumference. This finding identifies the interconnected structure of the meniscus and its relationship with the tissue's mechanical properties. Altering the structure in the body of the meniscus directly affected the circumferential strain.

1.2.7.2 <u>Compression of test samples</u>

Measuring the in vivo or in situ compressive properties of the menisci is not feasible with current technologies due to its complex shape and the inability to deconstruct the complex stress

state in the vertical direction. Consequently, test samples of known dimension are typically prepared to test the compressive properties directly. The meniscus is anisotropic, but this anisotropy has been approximated as orthotropic; meaning that the material properties can be described in 3 orthogonal directions that describe the bulk of the behaviour in the tissue. These three directions are axial, radial and circumferential (Figure 1.10). The only direction which would experience significant compressive loads is the axial direction. Many studies have tested samples prepared in this direction to determine this constitutive material property (Proctor, Schmidt et al. 1989; Joshi, Suh et al. 1995; Sweigart, Zhu et al. 2004; Gabrion, Aimedieu et al. 2005; Chia and Hull 2008; Bursac, Arnoczky et al. 2009). The results of compression testing are variable, and depend on the test protocol (i.e. rate of loading and magnitude of loading or displacement applied) and the animal model used. The results for human and bovine studies that including both bulk modulus and permeability were summarized by Masouros et al. (Masouros, McDermott et al. 2008) (Table 1-1).
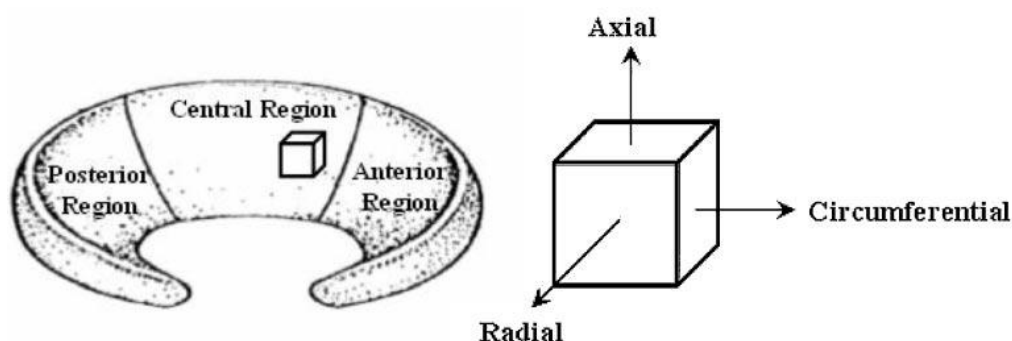
Figure 1.10 Schematic representation of the directions of the orthotropic description for the anisotropic material properties of the meniscus. From Chia and Hull with permissions (Chia and Hull 2008)

It is interesting to note that there is a 4 fold difference between the studies of Proctor et al. (Proctor, Schmidt et al. 1989) and Joshi et al.(Joshi, Suh et al. 1995) using the same animal

model. The former study applied approximately 25% strain to their samples while the latter used less than 10%. This difference in protocol may be a reason for this significant discrepancy. Increased strains can result in tissue compaction and greater swelling pressure, resulting in an increase in material stiffness (Ateshian, Warden et al. 1997). Proctor et al. revealed that the permeability of meniscal samples was almost $1/10^{th}$ that of articular cartilage (Proctor, Schmidt et al. 1989). As fluid pressurization is responsible for a large portion of the load bearing in articular cartilage, this result identifies a significant role for fluid pressurization in the load bearing mechanism of the meniscus as well. The studies of Joshi et al. and Sweigart et al. included many other species including baboon, monkey sheep, rabbit, dog and pig and the reader is referred to these articles for a full review of these animal models.

Table 1-1 Summary of compressive properties of human and bovine menisci as calculated using biphasic theory. Reproduced from Masouras et al. (Masouros, McDermott et al. 2008).

Study	Number of samples	Type	Location	Aggregate Modulus (MPa)	Permeability $(x10^{-15} \text{ m}^4\text{N}^{-1}\text{s}^{-1})$
Proctor et al. (1989)	63	Bovine	Medial	0.41	0.8
Joshi et al. (1995)	5	Bovine	Medial	0.11	3.3
	5	Human	Medial	0.22	2.0
Sweigart et al (2004)	10 Menisci	Bovine	Medial	0.14	5.6
	9 Menisci	Human	Medial	0.12	1.8

1.2.8 Tension

The wedge-shaped profile of the meniscus leads to generation of a circumferential hoop stress under applied compressive load. Due to the strong ligamentous attachments at the anterior and posterior horns, this hoop stress is manifested as tensile stress in the circumferentially oriented fibres (McDermott, Masouros et al. 2008). The constituent tensile properties in the

circumferential direction have been studied extensively. Tensile properties have also been evaluated in the radial direction, as it is believed that the tie-fibres resist tension in that direction to inhibit separation of the circumferential fibres (Bullough, Munuera et al. 1970; Skaggs, Warden et al. 1994). The tensile properties of the meniscus are strongly influenced by the fibre direction. Circumferentially oriented samples are an order of magnitude stiffer than radially oriented samples (Fithian, Kelly et al. 1990). Further, Skaggs et al. identified that the radial stiffness was influenced by presence of tie-fibres within the sample (Skaggs, Warden et al. 1994). Tensile properties of several species have been evaluated and have demonstrated large variability within and between animals (Table 1-2). In the studies of Goertzen et al. (Goertzen, Budney et al. 1997) and Proctor et al. (Proctor, Schmidt et al. 1989) in bovine menisci, a 3-fold difference in the stiffness was reported in the circumferential direction, but similar results were reported in the radial direction. Results of Lechner et al. (Lechner, Hull et al. 2000) was in response to the large differences in stiffness observed in the studies of Tissakht et al. (Tissakht and Ahmed 1995) and Fithian et al. (Fithian, Kelly et al. 1990) in human menisci. Their hypothesis was that sample thickness affected the results from these two previous studies. Results indicated that stiffness decreased with increased sample thickness, which was speculated to be caused by a sampling bias when testing thinner samples. The speculation identified that thin samples with few collagen fascicles would have low structural integrity and not be able to be tested, whereas thicker samples with few collagen fascicles would maintain enough integrity to be tested but would be less stiff.

Results from our lab have also identified significant strain-rate dependence in meniscal testing samples (Andrews 2011). Stiffness increased by almost 40% from the slowest strain rate

(comparable to the strain rates in the studies summarized here) to a physiologic strain rate; 100 times faster than the slowest strain rate (Appendix A).

Table 1-2. Summary of the tensile properties of the menisci of several animal species. From Masouras et al. with permissions (Masouros, McDermott et al. 2008)

Study	Number of samples	Thickness × width (mm × mm)	Test speed	Shape	Type	Orientation	Location	Tensile modulus (MPa)
Proctor et al. (1989)	72 (six menisci)	0.4 × 1.0	0.5 mm/min	Dumbbell	Bovine	Circumferential	Medial	129
						Radial		26
Fithian et al. (1990)	56 (seven knees)	N/A	0.3%/min	Rectangular	Human	Circumferential	Lateral	220
							Medial	118
Tissakht and Ahmed (1995)	31 knees	1.5–2.0 × 1.75–3.0	5.0%/min	Rectangular	Human	Circumferential	Lateral	112
							Medial	83
		0.8–2.0 × 1.75–3.0				Radial	Lateral	12
							Medial	10
Goertzen et al. (1997)	5 menisci	0.75 × 2.6	0.6 mm/min	Rectangular	Bovine	Circumferential	Medial	316
						Radial		25
Muratsu et al. (2000)	501 (six knees)	1.0 × 1.0	N/A	Rectangular	Porcine	Circumferential	Lateral	125
							Medial	162
Lechner et al. (2000)	10 menisci	0.5 × 1.0	0.36 mm/min	Dumbbell	Human	Circumferential	Medial	121
	10 menisci	1.5 × 1.0						85
	10 menisci	3.0 × 1.0						60

1.2.9 Shear

Shear stiffness is a measure of a material's resistance to changes in shape. The menisci have a low shear stiffness relative to articular cartilage (Zhu, Chern et al. 1994). Bovine menisci have been found to be $1/6^{th}$ to $1/10^{th}$ as stiff as bovine articular cartilage under conditions of oscillatory torsion (Kelly 1990). Like all material properties in the meniscus, the stiffness is direction dependent. The shear stiffness perpendicular to the circumferential fascicles is 20-33% stiffer than parallel to them in the bovine meniscus (Zhu, Chern et al. 1994). More recently, Nguyen and Levenston (Nguyen and Levenston 2012) identified a 40% greater shear stiffness perpendicular to the circumferential fascicles in bovine menisci. This same study also found that

articular cartilage was almost 150 times stiffer in shear than the menisci. This is a significant discrepancy when compared to the previous from Kelly et al. (1990) where it was reported that articular cartilage is 6-10 times stiffer than menisci in shear. The reason for the discrepancy between these results was not addressed in the study. Variable results within animal species for all of the mechanical properties described here identify the effect that test protocol, sample location, animal age and species could have on the results obtained.

1.2.10 Osmotic Influences

Osmolarity is a measure of the number of moles of solute in a solution. In the presence of an osmotic gradient across a membrane, fluid pressure is required to prevent the flow of water from the high to low osmolarity solutions. An osmotic pressure, known as Donnan osmotic pressure, is present in articular cartilage due to the high concentration of polyanionic GAGs associated with relatively high amounts of aggrecan (Maroudas 1976). This osmotic pressure is believed to pre-stress the cartilage and to play a role its compressive properties.

Altering the osmotic environment of hydrated soft tissues has been shown to induce changes in the water content in ligaments, cartilage and intervertebral discs (IVD) (Galante 1967; Maroudas and Venn 1977; Parsons and Black 1979; Eisenberg and Grodzinsky 1985; Chimich, Shrive et al. 1992; Best, Guilak et al. 1994). In full-depth samples of healthy articular cartilage swelling has been shown to be minimal under isotonic solution (as defined by synovial fluid osmolarity of 300 mOsm/L) (Brandt, Brière et al. 2010). However, when these full-depth samples were subsequently sectioned into 250-400 μm and placed in the same iso-osmotic solution, significant swelling in occured. Further, these samples were then placed in a hypotonic saline solution and subsequently imbibed more fluid (Maroudas and Venn 1977). Similarly, IVD samples, prepared for mechanical testing, swelled in a solution of iso-osmotic saline (Best,

Guilak et al. 1994). In whole ligament preparations, increased water content has been demonstrated under hypotonic conditions, while decreased water content was demonstrated under hypertonic conditions and no swelling was observed under isotonic solution (Chimich, Shrive et al. 1992). The iso-osmotic swelling of articular cartilage and IVD indicate that they are pre-stressed structures which may be constrained by the ECM in their intact state. These findings indicate a load bearing mechanism in these tissues where compressive forces are borne by hydrostatic pressure. To date the osmotic effects on meniscal swelling have not been evaluated and require investigation.

1.2.11 Meniscal Kinematics

Meniscal kinematics are important to proper function of the knee joint. Since the menisci are attached at the anterior and posterior aspects of the tibia by ligaments, and have only minor attachments at their periphery, they are able to move relative to the tibial plateau (Shrive, O'Connor et al. 1978). Throughout increasing flexion, the menisci tend to move posteriorly and rotate relative to the tibial plateau (Vedi, Williams et al. 1999). The ends of the menisci tend to move closer together in increasing flexion. Being more pronounced on the medial side, the anterior horn moves more relative to the tibia than does the posterior horn, resulting in a narrowing of the gap between the two ends (Vedi, Williams et al. 1999). As described previously, this mechanism yields a dynamic congruency in the joint, as the posterior condyles of the femur have a smaller radius of curvature than the more anterior aspects, resulting in a wrapping of the menisci around the condyles during flexion. This wrapping mechanism may result in protection of the tibial articular cartilage, as it may aid in greater load distribution throughout a dynamic range of motion. Further, meniscal motion is reportedly reduced in

osteoarthritic joints, where the movement and wrapping of the menisci has be shown to decrease (Scarvell, Smith et al. 2007).

1.2.12 Animal Models

Basic scientific investigations of the normal structural and biological behaviour of human meniscal tissue require a supply of healthy, uninjured tissue from relatively young subjects. Obtaining this type of tissue is difficult and makes examining the normal properties of human tissue difficult. Further, the study of specific surgical or medical interventions requires the use of a translational animal model to ensure the safety and efficacy of the treatment for human patients (Arnoczky, Cook et al. 2010). Several animal models for meniscal research have been discussed here, including bovine, lapine, ovine and canine. Each animal model has advantages and disadvantages with respect to its comparison to the human condition, including anatomy, biology, mechanical properties, size, cost and availability. It is often concluded that the more basic the phenomena being compared, the more valid translational models can be (Arnoczky 1990). The work described in this dissertation involves the use of bovine menisci. Bovine specimen have been used extensively in studies of the mechanical and compositional properties the menisci (Proctor, Schmidt et al. 1989; Goertzen, Budney et al. 1997; Schumacher, Schmidt et al. 2005; Nguyen and Levenston 2012; Vanderploeg, Wilson et al. 2012). All of the evaluations contained in this dissertation have been in the bovine meniscus from specimens of similar age and the same supplier. This approach has allowed for direct comparisons between the various studies that were conducted. Further, bovine specimens were easily and inexpensively obtained and did not require any additional animal sacrifice for this work.

1.3 Purpose

The overall purpose of this body of work was to expand the knowledge about meniscus structure and function by using a multifaceted approach, incorporating structural, compositional and mechanical studies of the tissue. The goal of this integrated approach was increase the knowledge of the function of the meniscus as it relates to their fine structure and composition.

1.4 Thesis Outline

This dissertation focuses on various aspects of the meniscus using a multifaceted approach in order to fill gaps in the current knowledge regarding meniscus structure, function and composition. This integrated approach has led to the development of a new model of meniscal function that will be discussed in Chapter 8. This dissertation has been formatted in a manuscript based format. Chapter 2 is the first manuscript of the dissertation, entitled "*The Shocking the Truth About Meniscus"*, which is a perspective article published in the Journal of Biomechanics in 2011 (Andrews, Shrive et al. 2011); included with permissions. This paper re-evaluated the paradigm of the meniscus as a shock absorber, in an attempt to clarify the function of the meniscus in the femorotibial joint. The experimental findings from this body of work are included in Chapters 3 to 7. In Chapter 3 the effects of osmotic gradients on swelling in meniscal testing samples were evaluated. The structural basis for the observed swelling was also assessed in this chapter. The manuscript is entitled "*Osmotic and structural influences on meniscal swelling"* and has been submitted to Journal of Orthopaedic Research. In Chapter 4 a mechanics based study that evaluated the effect of swelling on the properties of meniscal samples in compression was conducted. The manuscript is in preparation to be submitted to the Journal of Biomechanics. The study included in Chapter 5 evaluated the three-dimensional structure of the

meniscus using an imaging technique, optical projection tomography (OPT), not previously used for the evaluation of connective tissue structure. The manuscript of this work is entitled "*An evaluation of meniscal collagenous structure using optical projection tomography*" and has been submitted the Journal of Biomechanics. Chapters 6 and 7 contain studies on the organization of the proteins that have a structural role in meniscal function including; type II collagen, aggrecan, elastin and proteoglycan 4 (PRG4). The manuscript for Chapter 6 is in preparation for the Journal of Orthopaedic Research and Chapter 7 was modified from an abstract submitted to the Orthopaedic Research Society Conference 2013. A discussion is included in Chapter 8 in which key findings from this collection of studies are summarized and a new model for the function of the bovine meniscus is proposed. This model has built upon previous models of both the structure and function of the tissue by incorporating the findings from the following studies. Based on the findings from this body of work, future studies are also proposed in Chapter 8.

1.5 Specific Hypotheses

The hypotheses for the studies contained in this dissertation were as follows:

Chapter 2: The menisci do not act as shock absorbers within the knee joint.

Chapter 3: Swelling would be osmolarity dependent, with increased swelling under decreased osmolarity conditions. It was also hypothesized that there will be swelling under isotonic conditions; similar to the behaviour of articular cartilage and IVD (Venn and Maroudas 1977; Best, Guilak et al. 1994).

Chapter 4: Meniscal samples will be less stiff and more permeable in a swollen state than when they are compressed to the 'fresh', thickness prior to test initiation. It was also hypothesized that a test protocol which compressed the tissue to its fresh height would result in material behaviour that was similar to those of fresh tissue samples.

Chapter 5: OPT would be able to visualize the collagenous network in meniscal samples due to the autofluorescent properties of collagen.

Chapter 6: Type II collagen and aggrecan would be strongly colocalized in meniscal sections, similar to that seen in articular cartilage. It was hypothesized that elastin fibres would be oriented parallel to both tie-fibres and circumferential fascicles in the meniscus.

Chapter 7: Proteoglycan4 (lubricin) is conserved as the animal ages and would be distributed wherever major architectural elements of the tissue interact, including between fascicles, fibres and along tie-fibres.

Chapter 2

The shocking truth about meniscus

Chapter Two:

Abstract

The menisci of the knee are structures integral to the long term health of the knee joint. The primary function of these tissues is to distribute load across the tibiofemoral joint by increasing the congruency of the joint, thereby decreasing the resultant stress experienced by the articular cartilages. The menisci also play a secondary role in stabilizing the joint, particularly in the anterior cruciate ligament deficient knee, and also have roles in joint lubrication and proprioception. Also, an oft-cited role of this tissue is that of a shock absorber. We will review the literature supporting this shock absorption paradigm and describe the limitations and errors in the conclusions made by these studies. Consequently, we will show that the literature is inconclusive with no support for the shock absorption paradigm which should therefore not be stated as a function of the menisci. We will describe how one of the three articles in support of this paradigm actually could be interpreted to the contrary and support the idea that the menisci may play no significant role in shock absorption at the knee at all, with the two remaining papers being inconclusive.

2.1 Introduction

The menisci of the knee are complex structures, whose health is strongly correlated with the long term health of the knee; specifically the health of the articular cartilage (Roos, Lauren et al. 1998; Roos, Ostenberg et al. 2001; McDermott and Amis 2006). The common description of the menisci is that they are semi-lunar fibrocartilagenous discs whose main function is to increase the congruency of the tibiofemoral joint, thereby decreasing the stress in the joint through an increase in contact area (McDermott, Masouros et al. 2008). The role of the menisci in the joint is also commonly stated as being that of a shock absorber and secondary stabilizer with possible roles in aiding joint lubrication, proprioception and nutrition of articular cartilage (Mow, Gu et al. 2005; McDermott, Masouros et al. 2008; Chevrier, Nelea et al. 2009; Englund, Guermazi et al. 2009). While shock absorption is a role commonly stated in papers and textbooks describing the menisci, this function of the menisci is not intuitive. Moreover, upon further review of the literature, there is little evidence that shock absorption is indeed a significant function of the menisci. We will review the three most commonly cited studies which support this shock absorption paradigm and attempt to refine the current knowledge of the role of the menisci in the joint.

Mechanically, a shock absorber is defined as a device that dissipates energy to modify the response of a mechanical system to applied shock (Piersol 2010). One of the most common examples of shock absorbers would be those found in automobile suspension systems. In such systems, when vertical impulses are imparted to the vehicle, the resultant kinetic energy is dissipated via heat energy in a viscous fluid. In viscoelastic media such as soft tissues, energy dissipation can occur from fluid movement in the tissue that generates heat, or through rearranging of the molecular structure of the solid components (Mak 1986). Physiologically,

shock absorption is necessary to reduce the magnitude of the forces transmitted and the energy imparted to the skeletal system during everyday activities such as heel strike during gait or landing from the flight phase of running. For example, during heel strike in gait, the head experiences only one-tenth of the accelerations experienced at the shank (Light, McLellan et al. 1980). This attenuation of acceleration through the skeletal system provides a protective mechanism for the head and vestibular system (Cappozzo 1978a). Significant energy is absorbed at the knee during gait: throughout load acceptance, 6.3 J of energy are absorbed (Winter 1983). The knee joint functions effectively to absorb this energy, the proposal here however, is that this is accomplished with minimal contribution from the menisci.

2.2 Critique of the existing literature

An early paper discussing the shock absorption capacity of the menisci was *Mechanical Changes in the knee after meniscectomy* (Krause, Pope et al. 1976). In this study, canine and human knees were excised, and tested in an Instron universal testing machine. Load-deformation behaviour was measured at varying flexion angles, strain rates and rotational alignments. The intact joints were then tested. Subsequently, a medial meniscectomy was performed and finally a lateral meniscectomy. Joint testing was repeated at each stage of dissection. To determine the energy absorbed in the meniscus, the integral of the force displacement curve was calculated for each condition and the difference in the curves was considered to be the energy absorbed by the menisci (Figure 1). The results indicated less energy absorbed by the meniscectomized joints than the intact joints. The problem with this approach is that, while the integral of this curve is equal to the energy required to deform the joint, it is not equivalent to energy absorbed by the joint. In an elastic material, the energy used to deform the material is equal to the integral of the

force-deformation curve, however, this energy is then released when the material is unloaded resulting in no net damping or energy absorption. Since the tissues of the knee joint are viscoelastic, they exhibit hysteresis in the force-displacement plots (i.e. the loading and unloading paths are not the same). This energy loss phenomenon is due to movement of fluid and/or the rearranging of molecular structure of the tissue itself (Fithian, Kelly et al. 1990) (Figure 2). Consequently, as the unloading curves were not reported in this study, it does not show any change in shock absorbing capabilities of the knee at various stages of meniscus removal.
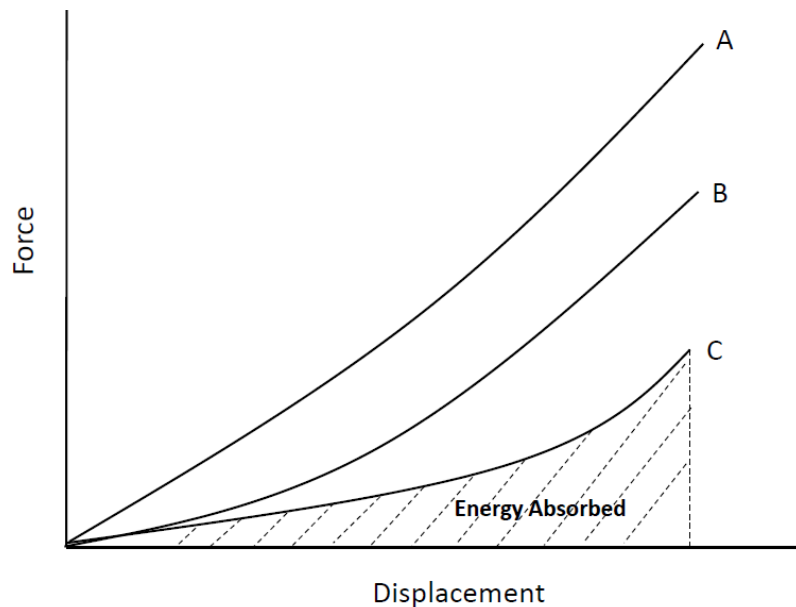
Figure 2.1 Representation of data reported, recreated from Krause et al. 1976, Force displacement curves (A) Intact joint (B) Medial Meniscectomy (C) Total Meniscectomy. Hatched area represents the energy absorbed for curve C (Krause, Pope et al. 1976)
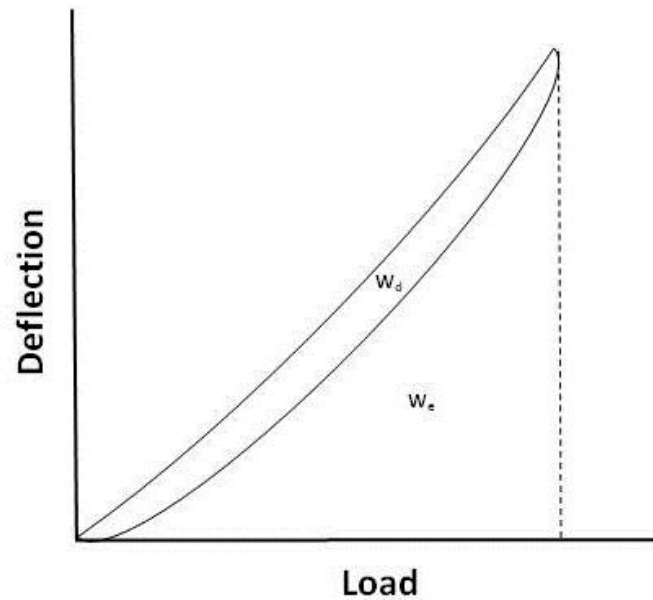
Figure 2.2 Load-deflection plot illustrating the hysteresis loop in loading and unloading a viscoelastic material. W_e is the elastic energy and W_d is the dissipated energy, and the total work done to deform the material is $W = W_e + W_d$

Kurosawa *et al.* also evaluated the role of the menisci in energy absorption in the knee (Kurosawa, Fukubayashi et al. 1980). In this study, 14 knee joints were tested at 0° of flexion at four load levels (200N, 500N, 1000N and 1500N) at a rate of 5 mm/min and the resulting displacements were measured. In these experiments, the unloading force-displacement curves were also recorded. While this study is often quoted to support shock absorption properties of the meniscus, (Rodeo 1994; McDermott, Masouros et al. 2008; Englund 2009) it is done so incorrectly. The results presented in Table 1 show the energy dissipation at the knee. The variables are W (the total work done to deform the whole joint), W_e (the elastic energy of deformation for the joint) and W_d (the energy dissipated by the joint). It is important to note the scale of the total work variable is 10^{-1} Joules (indicated by N·m). These results from this study identified two main points. First, meniscectomized joints actually dissipated more energy and

composed a higher percentage of the deformation energy than intact joints, reported by W_d/W. This suggests that the menisci retard the ability of the joint to dissipate energy. Second, the magnitude of energy dissipated by the passive structures in the intact joint is very low. In the 1000 N case, only 0.04 J are absorbed by all of the passive structures (bone, cartilage and meniscus). Only a portion of this energy can be attributed to the meniscus, making it clear that the meniscus is not contributing significantly to shock absorption under physiological conditions, i.e the 6.3 J absorbed in load acceptance of gait (Winter 1983). Moreover, the small magnitude of energy dissipated by all of the passive tissues combined reveals that muscles are likely to be the most significant absorbers of energy at the knee in physiological scenarios. Eccentric muscle contractions do negative work on joints, degrading the mechanical energy to heat (Alexander 1991) and are therefore capable of absorbing energy from impacts in physiological loading. The strain rate in this study is low, approximately $1/10^{th}$ of the rate seen during load acceptance (White, Yack et al. 1998). However, it gives an insight to the magnitude of energy dissipated in the soft tissues of the knee under physiological load magnitudes. Race et al. demonstrated decreasing energy absorption at increased loading rates in intervertebral disc (Race, Broom et al. 2000), so the values obtained in the study of Kurosawa et al. can likely be considered an overestimate of the magnitude of energy absorbed. The clear implication of the data in Table 1 is that the menisci are not significant shock absorbers in the knee joint. In fact, their presence in the joint reduced the energy absorption capabilities of the joint.

Table 2-1 Energy ratios, recreated from Kurosawa et al. (1980)

Loads	Intact Knees			Knees Without Menisci		
	$W\ (10^{-1}\ \text{N·m})$	W_e/W	W_d/W	$W(10^{-1}\ \text{N·m})$	W_e/W	W_d/W
500N	1.00+/-0.26	0.81+/-0.02	0.19+/-0.02	1.11+/-0.23	0.74+/-0.23	0.26+/-0.03
1000N	2.62+/-0.51	0.85+/-0.03	0.15+/-0.01	2.69+/-0.51	0.73+/-0.10	0.27+/-0.03
1500N	5.41+/-0.61	0.77+/-0.06	0.23+/-0.03	5.76+/-0.50	0.67+/-0.08	0.37+/-0.02

The final paper commonly used to support the proposal that the menisci are shock absorbers is *Shock absorption of meniscectomized and painful knees: A comparative in vivo study* (Voloshin and Wosk 1983). In this paper, attenuation of vibration was measured across the knee joint in healthy patients, those with painful but intact knees and those with meniscectomy, during gait. Accelerometers were strapped firmly to the tibia and femur, and the attenuation of signal amplitude was determined from the ratio of signal intensities at sites inferior and superior to the knee joint. There was a decrease of approximately 20% in signal attenuation in both painful intact knees and meniscectomized knees when compared to healthy knees. The authors suggest that the lack of menisci is responsible for the decrease in attenuation. However, the fact that there was the same decrease in signal attenuation in painful knees with intact menisci, as there was in meniscectomized knees, indicates that the absence or presence of menisci may not be a factor in the overall attenuation of signal across the knee. Since muscles have shock absorption capacity (Alexander 1991), the timing and magnitude of the muscle forces crossing the knee joint would have to be controlled in order to conclude that the meniscal tissue was responsible for shock absorption differences. Moreover, with altered kinematics (Allen, Wong et al. 2000) and load distribution within the joint (Kurosawa, Fukubayashi et al. 1980), the transmission of forces across the joint could have been affected by changes in alignment or

kinematics at the knee, resulting in altered signal attenuation. Consequently, this study's results are inconclusive with respect to the meniscal role in shock absorption.

2.3 Conclusion

The menisci are important structures in the knee joint and their functions vary from their primary role as a load distributor to more secondary roles in stabilization, lubrication, nutrition and proprioception (McDermott, Masouros et al. 2008). However, the oft-cited description of the menisci as a shock absorber is not supported by the literature. In the study by Krause et al., the assumption that the difference in force-deformation behaviour of the joint between intact and meniscectomized specimens was due to energy absorption of the menisci is flawed based on mechanical theory of elastic deformation. Elastic energy storage is not a form of shock absorption and as such cannot be used as evidence to support energy absorption by the menisci. Kurosawa et al. actually showed more energy absorbed in meniscectomized knees, implying that menisci retard shock absorbing capacity, yet their results have been cited in support of the paradigm. This study also identifies that if the menisci do absorb any energy, the magnitude of the energy absorbed would not be significant in physiological loading scenarios. Finally, Voloshin and Wosk's attempt to describe the menisci as shock absorbers, while different in approach, does not support the shock absorption paradigm. While the attenuation of signal across the knee joint is less in meniscectomized joints, the inability to control for muscular action and changes in kinematics does not show whether or not the meniscus is responsible for the shock absorption differences in the subject groups. The similar loss of dissipation in non-meniscectomized, but painful, joints identifies the shock absorbing capacity of the knee is largely independent of the menisci. These three studies therefore do not demonstrate the shock absorbing

capacity of the menisci and in one of them, an argument can be made against the shock absorbing capacity in the tissue (Kurosawa, Fukubayashi et al. 1980). While these studies may not support the paradigm of the menisci as a shock absorber, the role of the meniscus in the joint is an extremely important one. Both the studies of Krause and Kurosawa as well as many others have shown that load distribution across the joint in largely governed by the meniscus (Walker and Erkman 1975; Krause, Pope et al. 1976; Shrive, O'Connor et al. 1978; Kurosawa, Fukubayashi et al. 1980; Donahue, Hull et al. 2002). Epidemiologically, the importance of the meniscus to long term joint health is irrefutable (Fairbank 1948; Lanzer and Komenda 1990; Roos, Lauren et al. 1998; Lohmander, Englund et al. 2007; Englund 2009; Englund, Guermazi et al. 2009). With this knowledge of the tissue's importance, research regarding tissue engineered constructs or artificial replacements should focus on its role as load distributor and secondary stabilizer, not its ability to absorb shock.

Chapter 3

Osmotic and structural influences on meniscal swelling

Chapter Three:

Abstract

Osmotic swelling effects have been studied in many hydrated soft tissues. However, the quantity of and structural basis for swelling of meniscal fibrocartilage has not been evaluated. Understanding this behaviour is vital to understanding structure-function relationships in the menisci. This study evaluated the swelling associated with varied osmotic conditions on samples prepared from bovine menisci. A further purpose was to elucidate a structural basis for any observed swelling through the use scanning electron microscopy (SEM) and histological staining. The swelling of meniscal samples was independent of bathing solution in a range of osmolarities (50 mOsm/L - >1000 mOsm/L). The direction of swelling was dependent on the orientation in which the sample was prepared. SEM revealed collagen fibril separation, leading to swelling perpendicular to the orientation of circumferential bundles. Histological staining identified that the presence of the proteoglycans coupled with the microarchitecture of the collagen network likely determine the amount and direction of swelling in meniscal samples. This is the first study to evaluate the quantity, direction and structural basis of swelling in meniscal fibrocartilage. Our results may have application in understanding changes that occur due to injury or disease and may help influence protocols that preserve meniscal architecture during surgery.

3.1 Introduction

The knee menisci are semilunar, fibrocartilagenous structures that undergo complex loading, including axial compression, radial and circumferential tension and shear (Adeeb, Sayed et al. 2004). The menisci have an extracellular matrix architecture composed primarily of collagens, proteoglycans (PG), and water (McDevitt and Webber 1990); proteoglycans are hydrophilic glycoproteins which contribute to the water content of the tissue. The menisci are highly hydrated, with a water content of approximately 65% (Djurasovic, Aldridge et al. 1998). These structural components are arranged in an intricate matrix with a strong directionality, particularly in the collagen network, which has a predominantly circumferential orientation at the macroscopic level (Bullough, Munuera et al. 1970; Rattner, Matyas et al. 2011).

Altering the osmotic environment of hydrated soft tissues has been shown to induce changes in the water content of these tissues. Experimentally, these swelling effects are induced by osmotic changes in the bathing solution of the tissue; most commonly by varying the concentration of saline solutions (Maroudas and Venn 1977; Nguyen and Levenston 2012) or sucrose solutions (Parsons and Black 1979; Chimich, Shrive et al. 1992; Thornton, Shrive et al. 2001). Sucrose is an osmotically active, non-ionic, and tissue neutral solution that has been used to alter tissue water content (Canatrow 1978). The effects of osmotic swelling have been studied extensively in many hydrated soft tissues, including articular cartilage, intervertebral disc (IVD), and ligament (Galante 1967; Maroudas and Venn 1977; Parsons and Black 1979; Eisenberg and Grodzinsky 1985; Chimich, Shrive et al. 1992; Best, Guilak et al. 1994). To date, no study has evaluated the swelling of the menisci in altered osmotic environments.

It has been demonstrated that in full-depth samples of healthy articular cartilage, swelling is minimal under isotonic solution (as defined by synovial fluid osmolarity of 300 mOsm/L

(Brandt, Brière et al. 2010)). However, when these full-depth samples were subsequently sectioned into 250-400 μm slices there was significant swelling in the same isotonic solution. Further, when these samples were placed in a hypotonic saline solution they subsequently imbibed more fluid (Maroudas and Venn 1977). Similarly, IVD samples, prepared for mechanical testing, swelled in a solution of isotonic saline (Best, Guilak et al. 1994). In whole ligament preparations, increased water content was demonstrated under hypo-osmotic conditions, while decreased water content was demonstrated under hyper-osmotic conditions and no swelling was seen under isotonic solution (Chimich, Shrive et al. 1992).

The purposes of the study reported here were three-fold. The first purpose was to determine the swelling associated with altered osmotic environments of cylindrical samples prepared from bovine menisci. Second, due to the complex fibre orientation of the menisci (Rattner, Matyas et al. 2011), we evaluated the effect of sample orientation (vertical versus circumferential, Figure 1) on the amount and direction of swelling. Finally, to investigate a structural basis for the observed swelling, scanning electron microscopy (SEM) and histological staining techniques were used to observe changes in the microarchitecture of the tissue. Cylindrically cut samples were chosen as these are commonly prepared for mechanical testing to determine the compressive properties of menisci (Proctor, Schmidt et al. 1989; Fithian, Kelly et al. 1990; Joshi, Suh et al. 1995; Nguyen and Levenston 2012). We hypothesized that swelling would be osmolarity dependent, with increased swelling under decreased osmolarity conditions. We also hypothesized that there will be swelling under isotonic conditions; similar to the behaviour of articular cartilage and IVD (Venn and Maroudas 1977; Best, Guilak et al. 1994). We also proposed that observation of the microarchitecture of the tissue would allow us to suggest a mechanism for any observed swelling of bovine meniscal samples.

3.2 Methods:

Meniscal samples (n=120) were obtained from 5 bovine stifles (age 18-30 months, n=24/animal) from animals slaughtered for consumption at a local abattoir. Biopsy punches (4 mm) were used to excise cylindrical plugs from the medial and lateral menisci in two orientations. "Vertical" plugs were punched in the direction normal to the tibial plateau in the mid portion of each meniscus, between the inner and outer circumferences from the anterior, central and posterior portions. Circumferential plugs were extracted by cutting a 5 mm thick slice of the meniscus perpendicular to the circumference of the tissue using a custom-made dissecting jig. The tissue was then punched perpendicular to the cut surfaces to create the circumferential samples (Figure 3.1). A second custom jig was used to slice the plugs into approximately 1.5 mm thick samples. Six vertical and six circumferential specimens were prepared from each meniscus. The specimens in this "fresh" condition were then weighed and measured. From each meniscus, there were 2 samples from each location (anterior, central and posterior), in each orientation (vertical and circumferential) from each meniscus (medial and lateral), for 24 samples per animal (2x3x2x2). This number of samples was chosen to allow even distribution of samples in the varied osmotic solutions.
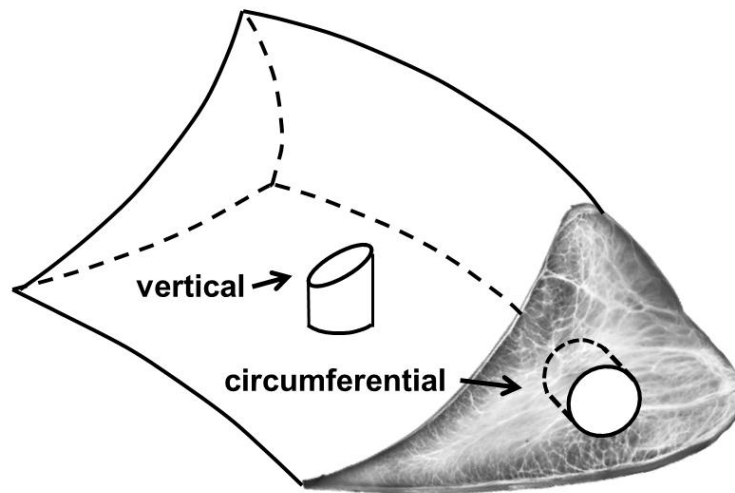
Figure 3.1 Schematic of sample orientation. Samples were harvested in both the vertical (axial) and circumferential directions using a 4 mm biopsy punch and a custom designed cutting jig. Samples were harvested similarly for both medial and lateral menisci.

3.2.1 Dimension Measurement

Specimen dimensions were measured with a photogrammetric technique using a dissection microscope and digital camera (Zeiss Stemi SV8 Microscope with moticam 5.0M Pixel camera). This technique was implemented to avoid the compression of the tissue that can occur when using a contact measurement device such as a caliper. Photographs were taken of the top view of the specimen to determine its radius. Two photographs of the specimen side were obtained in orthogonal directions to determine the thickness of the tissue (Figure 3.2). A calibration object was used to determine the conversion from pixels to millimeters using a custom written Matlab program (The Mathworks Inc, Natick, USA). The specimen images were then used to determine specimen dimensions. The top-image pixel area was approximated as a circle, and an equivalent radius was calculated. The edges of the side images were manually digitized in four locations on each edge and an average thickness calculated from the eight

measurements (2 photos x 4 thickness measures). The system accuracy was determined using a separate calibration object, a cylindrical disc of similar dimension to the meniscal specimen (3.97 mm radius x 1.94 mm thick). The accuracy was determined to be 0.03 mm and the intra-user repeatability was determined to be ($\pm$ 0.02 mm). The accuracy results were determined to be acceptable as they represent less than 1% of the average specimen radius and less than 2% of average specimen thickness dimensions.
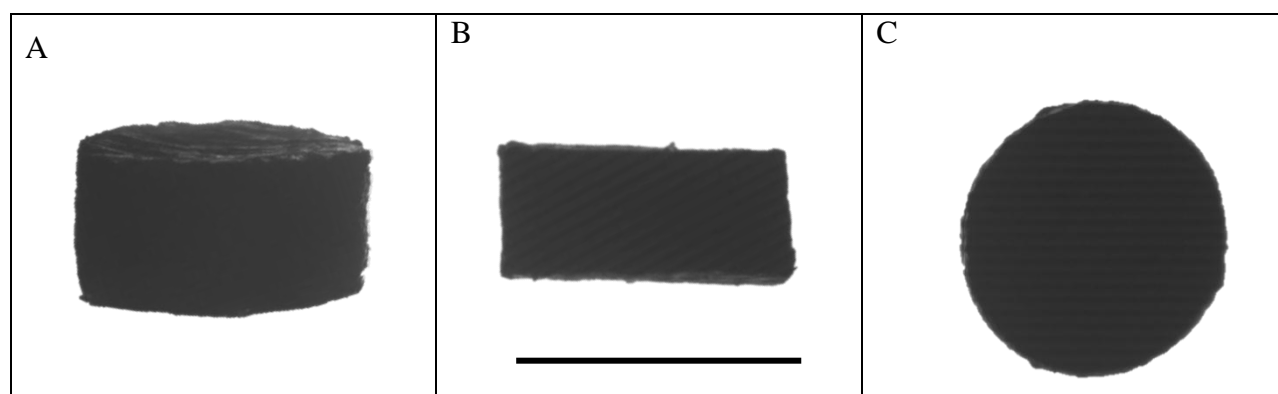
Figure 3.2. Photograph of meniscal tissue samples using a digital camera attached to a dissection microscope. A. 3 Dimensional view of a representative sample. B. Side view C. Top view. Scale bar ~ 4 mm

After the fresh weights and measurements were determined, the samples were assigned randomly into one of four solutions: deionized water (DW), phosphate buffered saline (PBS), 6.5% w/v sucrose or 25% w/v sucrose solution. The assignation led to an equal number of samples in the solutions from each meniscus and orientation. These solutions were used to determine the effect of osmolarity on the swelling of the prepared samples. Deionized water represented a strongly hypo-osmotic solution, while both PBS and 6.5% sucrose were approximately iso-osmotic with osmolarities of approximately 300 mOsm/L. Twenty-five percent sucrose represented a strongly hyperosmotic solution with a measured osmolarity of greater than 1000 mOsm/L. The osmolarity was compared to that of synovial fluid which has an

osmolarity of approximately 300 mOsm/L (Brandt, Brière et al. 2010). All solutions were prepared with protease inhibitors (PI), (complete Protease Inhibitor Cocktail Tablets, Roche Applied Science) to reduce the effects of tissue degradation over time. The samples were allowed to equilibrate in the solution for one hour, weighed and dimensional measurements repeated (wet condition).

One hour was deemed an appropriate equilibration time, as 30 minutes was previously found to achieve a mechanical equilibrium in response to changes in osmolarity of meniscal samples (Nguyen and Levenston 2012). Pilot studies confirmed this finding; showing no difference in swelling between 1 hour and 24 hours in solution for the samples tested in this study. Subsequently, the tissue was dehydrated in a vacuum drying centrifuge for 24 hours and the dry weight measured to allow determination of the water content in both the fresh and wet conditions. The volume of each sample was determined in both the fresh and wet conditions using the values obtained from the dimension measurement technique. Volumetric measurements allowed for comparison of measurements to evaluate swelling.

3.2.2 Scanning Electron Microscopy (SEM)

Vertically and circumferentially oriented samples were cut and prepared for SEM. Several pairs of adjacent samples were prepared from one animal (n=8, 2 vertical and 2 circumferential samples from the central portions of the medial and lateral menisci), with one fixed immediately in 2.5% glutaraldehyde (GA) and the other allowed to swell freely in PBS with PI for one hour and then fixed in 2.5% GA. PBS was chosen based on the results of the first portion of the study and due to its ubiquitous use in mechanical testing of tissues. The samples were then dehydrated in graded ethanol series (25%-100%), and placed in a graded hexamethyldisilazane (HMDS) series (50-100%) (Bray, Bagu et al. 1993). The samples were

subsequently dehydrated overnight in a desiccant chamber, sputter-coated with gold-palladium and imaged using a Phillips XL 30 scanning electron microscope. Qualitative analysis was conducted to evaluate changes in fibre organization between immediately fixed and swollen samples. This smaller number of samples was chosen due to limited access to and budget for the SEM operations and was conducted as a scoping study to evaluate structural changes caused by swelling in the tissue.

3.2.3 Histology

Representative samples from both menisci from one animal were stained for collagen and PG content to evaluate the internal extracellular matrix (ECM) architecture and composition qualitatively. After a swollen sample (1 hour in PBS with PI) had been measured with the photogrammetric technique, a thin section was cut from the middle of the specimen and stained using a Fast Green and Safranin O protocol for collagen and PG respectively. Samples were washed in PBS, placed in Fast Green for 5 minutes, followed by 1% (V/V) acetic acid for 1 minute, dipped in PBS, placed in Safranin O for 3 minutes and washed in PBS again for 1 minute. The resulting sections were then photographed for qualitative analysis of their structure and composition. These images facilitate qualitative analysis of the location of the matrix molecules as well as structure of the collagen matrix.

3.2.4 Statistical Analysis

An analysis of variance (ANOVA) was used to evaluate swelling differences between animals. Swelling was defined by the percentage increase in volume from the fresh volume. Based on the results of this analysis (i.e. no animal dependence), a multifactor ANOVA was used on the grouped sample data (all animals grouped n = 120) to determine the effect of harvest location medial vs lateral meniscus, orientation (vertical vs circumferential) and solution on

swelling (n= 6/group). Student's t-tests were used to determine differences identified by the ANOVA. T-tests with post-hoc Bonferroni adjustments were also used to determine differences in the direction of swelling (thickness vs. radius) for vertical and circumferential samples. The level for statistical significance was set at $p \leq 0.05$ in all cases.

3.3 Results

The solution dependence was assessed by evaluating the change in volume in meniscal samples in various osmolarity solutions. The results indicate that the sample swelling was independent of the solution they were placed in after they were cut from the meniscus ($p > 0.05$, Figure 3.3). Swelling was significantly greater in the medial meniscus (34.4%) than in the lateral meniscus (20.0%), $p < 0.001$. Sample orientation also did not affect the total swelling ($p > 0.05$) but did affect significantly the direction of swelling. Vertically cut samples swelled more in the thickness (vertical) dimension than in the radial direction, whereas the circumferentially oriented samples swelled significantly more in the radial direction (Figure 3.4). Average vertical swelling in vertically oriented samples was 17.3% versus 4.2% in the radial direction ($p < 0.001$). Conversely, in circumferentially oriented samples the average radial swell was 10.7% in the radial direction versus 3.0% in the thickness dimension ($p < 0.001$). Water content for samples placed in PBS, was $63.2 \pm 4.0\%$ fresh and $72.3 \pm 4.4\%$ in the wet condition. Taken together, these results indicate a lack of solution dependence but a strong dependence of sample orientation on the direction of swelling after 1 hour in solution.

Changes in the collagen structure in the meniscal samples after 1 hour in solution was evaluated qualitatively through SEM. There are marked differences in the samples fixed in GA immediately after dissection (Figure 3.5A and 3.5C), when compared to samples allowed to

swell for 1 hour in PBS with PI prior to fixation (Figures 3.5B and 3.5D). The images in 3.5A

and 3.5B are oriented looking toward the cut end of a circumferentially oriented fibre bundle. In

Figures 3.5C and 3.5D, the images contain a radial tie-fibre in the foreground of the image with

the cut ends of circumferential bundles in the background. The circumferential fibre bundles

appear to be composed of the ~100 nm fibres demonstrated by Peterson and Tillman (Petersen

and Tillmann 1998). In the samples fixed immediately after cutting (Figures 3.5A and 3.5C), the

fibres are closely packed, whereas in the specimens allowed to swell, the fibres appear to have

separated from each other (Figures 3.5B and 3.5D). Further, immersion in solution resulted in the

ends of fibres appearing to have splayed and lost structural integrity (Figure 3.5D), in contrast to

the immediately fixed fibres which remain tightly packed together (Figure 3.5C). The SEM

results indicate changes in structure between fresh and swollen samples.
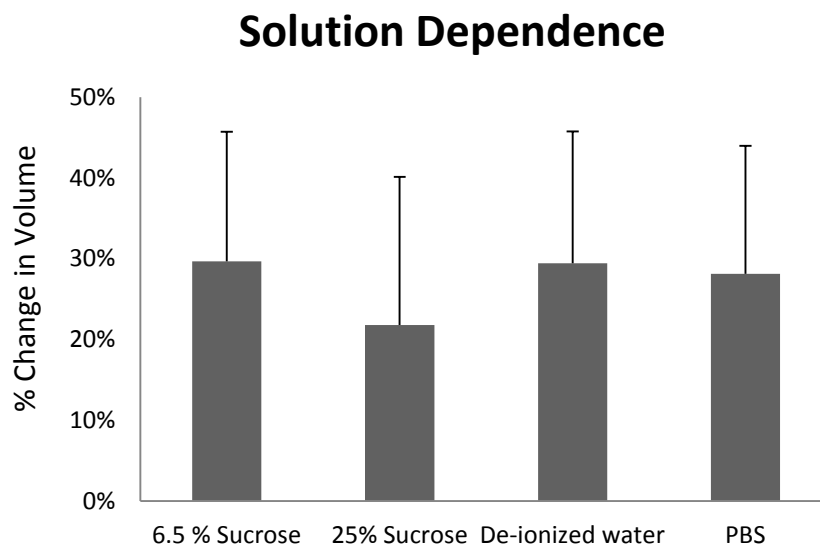
Figure 3.3. Meniscal sample percent increase in weight + standard deviation after one hour in various solutions n=30 per group. There were no significant differences due to solution (p > 0.1).
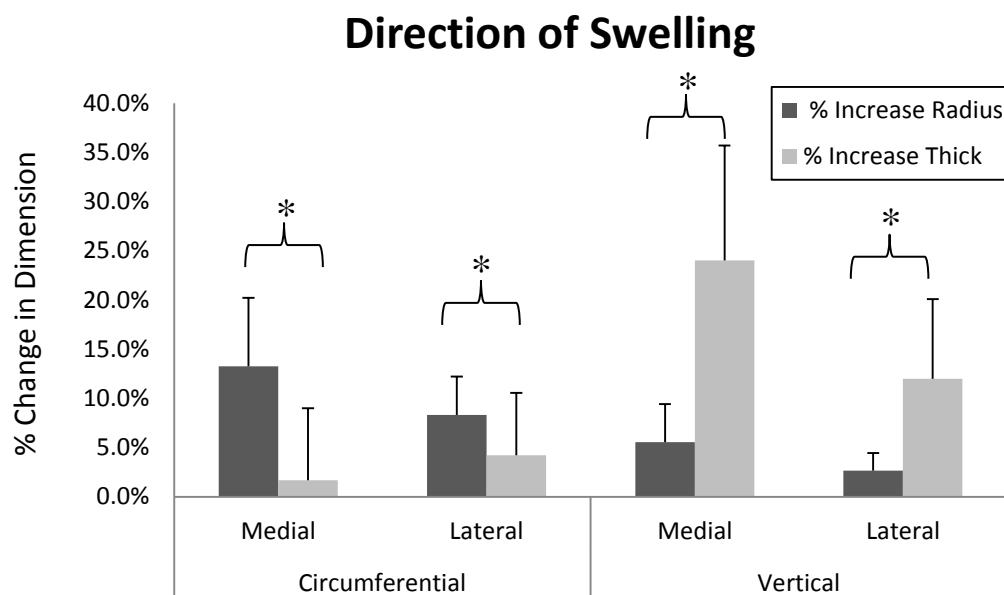
Figure 3.4. Direction of swelling based on the sample location n=15 per group. '*' denotes significance (p < 0.05). Data presented as mean + standard deviation.

Histological staining was evaluated to understand the structural basis for swelling within meniscal samples. A substantial range of architectures was observed across samples harvested from the bovine menisci (Figure 3.6). The pink color identifies areas rich in PG, while the blue-green areas are collagen rich. These samples represent some of the various collagen architectures and staining that can be seen within the menisci. It is apparent that the samples are highly heterogeneous, both within and between samples. This heterogeneity can be seen in the amount of and location of PG staining in cross-section as well as the complex tie-fibre arrangement in the samples. Moreover, the resultant shape after one hour of swelling also varies between samples. These samples would all have been approximately rectangular in shape prior to allowing them to swell in PBS. The swelling is clearly non-uniform in some cases (Figure 6A), whereas more uniform swelling is evident in the other cases (Figures 6B-6D). The relative

swelling in the vertical direction was 52%, 17%, 26%, and 13% for samples A through D respectively. These example images demonstrate large structural and compositional variation amongst samples from within the same joint. Refer to Appendix B for additional images illustrating the heterogeneity within and between samples.
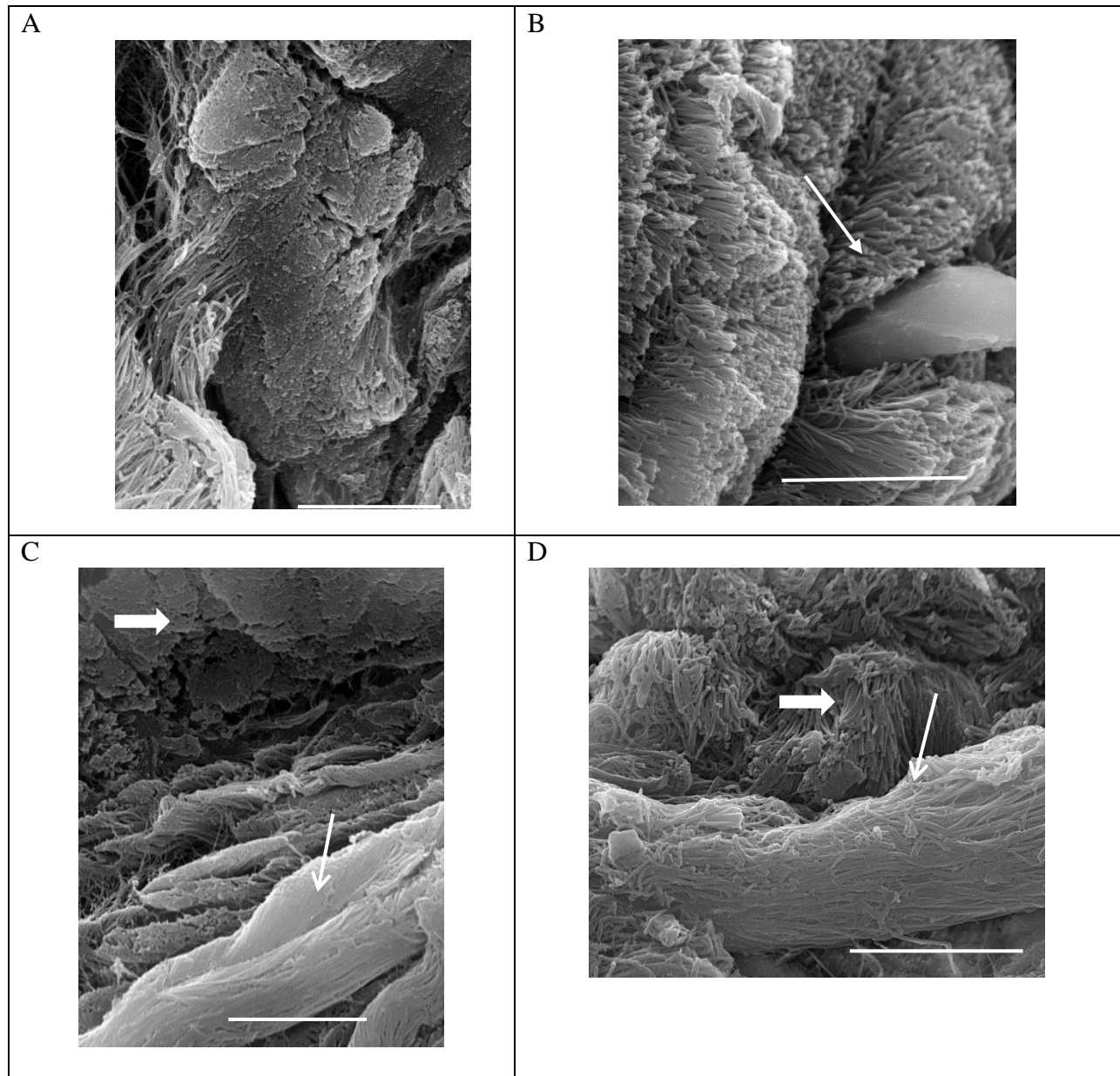
Figure 3.5. **SEM images of meniscal samples. Scale bars are 10 µm in all images. Image A and C show samples fixed immediately after dissection and B and D show those samples allowed to swell for 1 hour prior to fixation. Figure A shows the cut end of a circumferential bundle with tightly bound fibrils whereas in the ends of the fibres are less tightly bound packed. In B elastin fibre imbedded is imbedded along that bundle (arrow). Note the stark difference in the swollen circumferential fibre ends (D large arrow) compared to the tightly packed fresh-fixed sample (C large arrow). The uncut radial tie-fibres appear similar in their structure in both samples (C and D small arrows).**
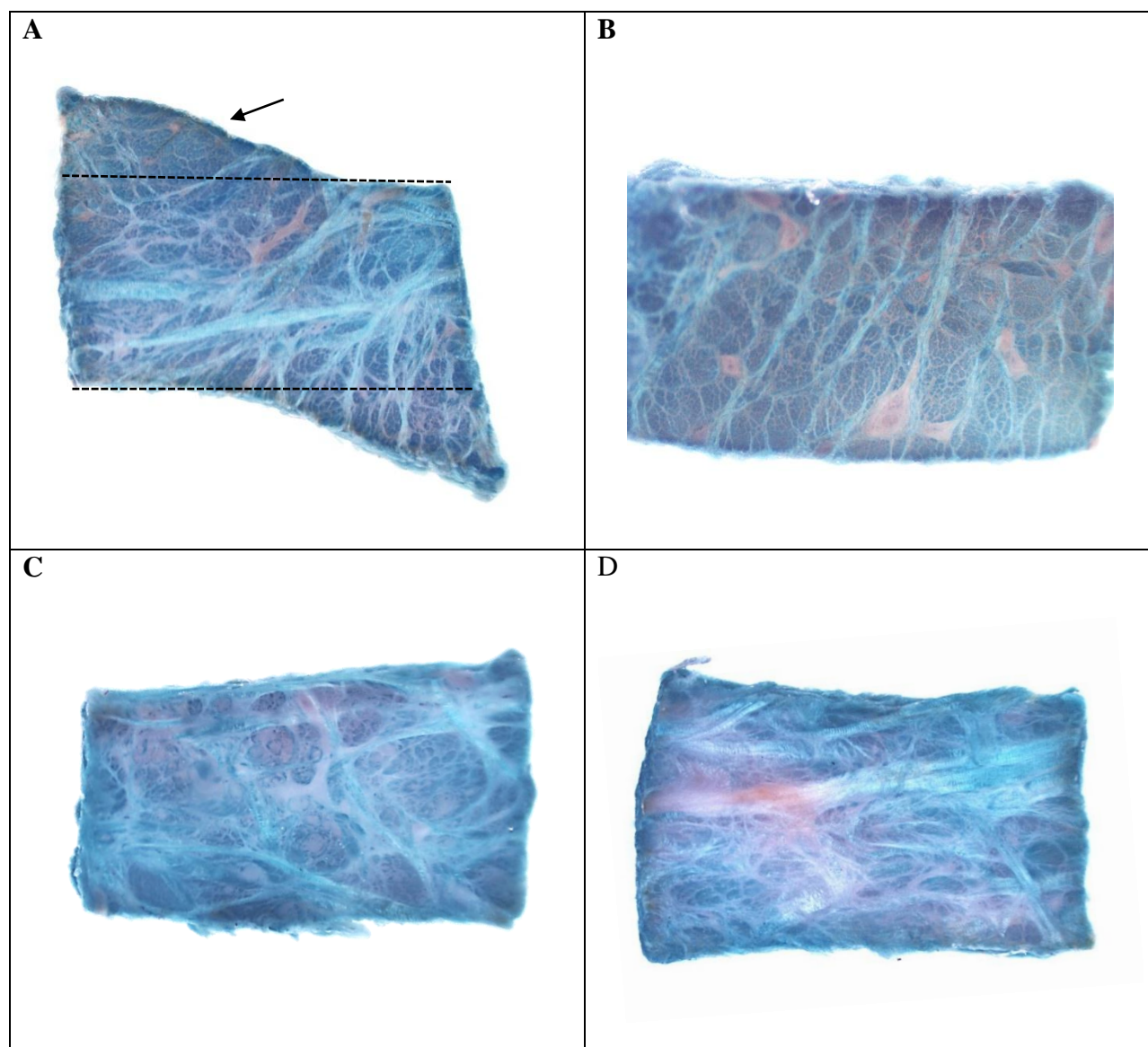
Figure 3.6. Example cross sections of 4 samples after swelling for 1 hour in PBS with PI stained with Fast Green (collagen) and Safranin O (proteoglycan). In 6A the dashed lines represent the approximate fresh shape. The arrow points to a large area of asymmetric swelling.

3.4 Discussion

This study has evaluated the effect of osmolarity on the swelling of meniscal samples. The swelling was not significantly different in any of the four solutions tested, with an osmolarity range from approximately 50 mOsm/L to greater than 1000 mOsm/L. This result is different from those seen in whole ligament preparations, where a decrease in water content was seen in 25% sucrose solution (Chimich, Shrive et al. 1992). However, recent unpublished results from our lab indicate that ligament samples cut from intact tissue do swell similarly to the meniscus. Thus, cutting the collagenous structure of connective tissues may facilitate swelling within that tissue. These findings may indicate that the mechanical damage to the tissue from cutting of the ECM is greater than the osmotic influence on swelling. This potential influence of mechanical damage implies that the collagen matrix is under a state of pre-stress in the intact meniscus, as the tissue will draw in more fluid, even in highly hyperosmotic conditions. This finding is also supported by the findings of Rattner et al., which identified that some fibres tended to be released from the tissue and uncoil in thin sections (Rattner, Matyas et al. 2011). This uncoiling could only occur if the fibres were under some state of pre-stress. Results from Maroudas and Venn indicated no swelling of intact cartilage in an isotonic saline solution. However, when these full-depth samples were subsequently sectioned into 250-400 μm slices there was significant swelling in the same solution (Maroudas and Venn 1977). This finding demonstrates that samples cut from menisci and articular cartilage, behave similarly in isotonic solution. This finding may have future implications to our understanding of the types of meniscal injuries that occur (buckle-handle, radial, etc.) and the consequences to the remaining intact tissue. Since each type of injury would disrupt the collagen matrix differently, the effects on the intact tissue may vary with injury type.

A limitation of this study is the large variability seen in the amount of swelling between samples. This limitation may have led to the insignificant findings for solution dependence. However, despite this limitation, samples swelled on average 20% in a highly hyperosmotic solution. This indicates that while specific osmolarity dependence may have been masked by the large variation, the results do indicate a pre-stressed structure that will swell when the matrix is disrupted. An accurate understanding of the material properties of the meniscus is crucial to developing accurate computer models, bioengineered replacements or synthetic material replacements for damaged or diseased menisci. Further, if meniscus function is altered by cutting alone during surgery, then one must be mindful of the amount, location and orientation of the tissue that is removed in surgery as it may have consequences for the remaining, intact tissue. The solutions tested here spanned a range from 50 to greater than 1000 mOsm/L which encompasses that of synovial fluid and surgical irrigation fluids and is an important finding to future understanding of meniscal changes after injury.

Understanding the quantity of swelling, and its direction, is of fundamental importance to understanding the mechanics of the meniscus in compression. In most compressive studies of the meniscus, tissue thickness is measured after some time in solution, and therefore, may not be indicative of the original cut thickness of the tissue (Proctor, Schmidt et al. 1989; Sweigart, Zhu et al. 2004; Nguyen and Levenston 2012). Several samples in this study swelled more than 50% in the thickness; thus without a compressive offset of at least that magnitude, the properties determined may not be indicative of in vivo material behaviour. As is demonstrated in biphasic theory, large compressive deformations can cause stiffening of the fibre matrix and a decrease in matrix permeability (Ateshian, Warden et al. 1997). Consequently, large changes in the size of the tissue would likely affect the material properties determined. Moreover, if the samples are

measured fresh and not after swelling, the strain values (as defined by change in thickness divided by the original thickness) and resultant material behaviour may also not represent in vivo properties.

The water content results of 72% for swollen samples in PBS compare very well with previous results of 71.8% and 73.8% in compressive meniscal specimens also placed in PBS for 1 hour or more (Proctor, Schmidt et al. 1989; Nguyen and Levenston 2012). The result of 63% for fresh specimen compares favorably with results from Djurasovic et al. of 64.8% where tissue water content was also evaluated fresh (Djurasovic, Aldridge et al. 1998).

The histological sections confirmed a complex structural architecture and compositional variation within the tissue. This architecture may have a significant influence on the ability of PG to absorb water and physically expand the matrix. PG is a hydrophilic component of the tissue ECM that is strongly correlated with the swelling pressure within these tissues (Eisenberg and Grodzinsky 1985). This swelling pressure, coupled with the collagen matrix in which PG is embedded, may determine the amount of swelling in the tissue samples. The significant effect of sample orientation on the direction of swelling may indicates a link between damage to the structure of the ECM and the resulting swelling. As PG induced swelling likely not be directional in nature, the anisotropy of the surrounding matrix would directly influence the direction in which swelling would occur; i.e. a hydraulic swelling pressure would expand the tissue in the direction of the weakest collagen matrix. The orientation of the samples significantly impacted the direction of the swelling (vertical vs. radial) (p<0.001). In both cases however, the predominant direction of the swelling is perpendicular to the large circumferential bundles. The SEM results supported this finding. These images demonstrated that the individual fibres that compose the circumferential bundles appear to have separated in the samples that were allowed

to swell prior to fixation; whereas bundles in the immediately fixed samples remained tightly packed and organized. The histological findings further identify the structural and compositional influences on swelling. In one example (Figure 3.6A) there is a large tie-fibre network originating in the upper right hand corner of the sample which runs obliquely down to the bottom left of the sample. The significant change in shape and thickness in this particular sample appear to be correlated with the sparse tie-fibre matrix coupled with the presence of PG in the upper left quadrant where the specimen has swelled so dramatically. Contrarily, the swelling could be resisted by the collagen fibre matrix that runs from the upper right and lower left quadrants resulting in little shape change in those areas. The variation in the amount of swelling of the histological samples (Figure 3.6) would support the hypothesis that the swelling of these samples was determined by presence of PG coupled with the local arrangement of the collagen fibres in the sample. The structural basis proposed here regarding the swelling of the meniscus is similar to that in cartilage, which was thought to be due to the osmotic pressure due to the total PG content coupled with loss of the elastic restraint from the collagen matrix due to cutting (Bray, Bagu et al. 1993).

3.5 Conclusion

There was significant swelling in all of the solutions used in this study across a wide range of osmolarity, with a grouped average of approximately 30% across all solutions. The direction of swelling was strongly related to orientation of the sample. A possible structural basis for the swelling has been identified, via separation of the individual fibres within the large fibre bundles which is accommodated by the cutting of the restraining structures in the presence of PGs. This is a novel finding in the meniscus and the first time that the quantity and directionality of

swelling has been quantified for meniscal samples. These results combined with the implication that the menisci are a pre-stressed structure are important to better understanding the material properties of the knee menisci and understanding of the in vivo structure-function relationships in this tissue.

Chapter 4

Relationship between meniscal swelling and the compressive properties

of bovine menisci

Chapter Four:

Abstract

Understanding the in vivo material properties of the menisci in compression is important to understanding their overall function in the joint and gives a benchmark for tissue engineered construct development. Recently, the swelling behaviour of the meniscal testing samples was demonstrated in various osmotic environments. This study evaluated the effects of swelling on the material properties of meniscal samples using stress relaxation tests under confined compression conditions. Further, the material properties of fresh tissue were compared to tissue allowed to swell freely in phosphate buffered saline for 1 hour. Free-swollen tissue was one third as stiff at equilibrium as those that were recompressed to their original thickness prior to testing. Secant moduli at peak stress, at a loading rate of 0.5 mm/s, were nine times greater in the recompressed samples than the free-swollen samples. Relaxation times were faster in swollen samples, indicating increased permeability compared to recompressed specimen. Fresh samples had significantly higher bulk moduli than the swollen tissue but were not different from the recompressed samples. However, the secant modulus of fresh samples was significantly lower than the recompressed condition. This is the first study to quantify the differences amongst fresh, swollen and recompressed samples to determine the effects of swelling on the material properties of the menisci in compression.

4.1 Introduction

The mechanics of the menisci are integral to the overall mechanics of the femorotibial joint. The menisci transmit approximately 50% of the load in the femorotibial joint (Seedhom, Dowson et al. 1974; Krause, Pope et al. 1976). By increasing the joint congruency between the femur and tibia, the menisci are integral to decreasing stresses on the articular surfaces of the tibia and femur (Baratz, Fu et al. 1986; Cottrell, Scholten et al. 2008). The menisci are anisotropic, but this anisotropy has been approximated as orthotropic; meaning the material properties can be described in 3 orthogonal directions that describe the behaviour in the tissue. These three directions are axial, radial and circumferential. In menisci, compression would only be experienced in the axial direction, and as such, many studies have tested samples in the axial direction to determine the compressive properties (Proctor, Schmidt et al. 1989; Joshi, Suh et al. 1995; Sweigart, Zhu et al. 2004; Gabrion, Aimedieu et al. 2005; Chia and Hull 2008; Bursac, Arnoczky et al. 2009).

The menisci are hydrated soft-tissues, composed of approximately 65% water (Djurasovic, Aldridge et al. 1998). The solid matrix is composed of a network of primarily collagenous proteins with smaller amounts of non-collagenous proteins, including various proteoglycans (McDevitt and Webber 1990). The material behaviour of the menisci has been described as biphasic, meaning the response of the tissue to applied load is time dependent and determined by both the solid constituents and their interaction with the fluid component (Proctor, Schmidt et al. 1989). Due to the low permeability of the tissue, deformation results in relative movement of the solid matrix and the fluid it contains, resulting in the creation of large drag forces between the two phases. Fluid exudation from the matrix governs the viscoelastic behaviour of the tissue, including stress relaxation and creep (Kwan, Lai et al. 1984).

The swelling behaviour of meniscal samples in varying osmotic environments was evaluated in our lab [Chapter 3]. Meniscal samples swelled significantly, approximately 30% volumetrically in iso-osmotic phosphate buffered saline (PBS). Further it was seen that the predominant direction of swelling was vertical, which is the direction that would be compressed during mechanical testing. It was hypothesized in that study, that the material properties of the tissue would be affected by this significant swelling. However, no study has evaluated the effect of sample swelling on the behaviour of the menisci in compression. Therefore, the purposes of this study were two-fold: first to evaluate the effect of swelling on the material behaviour of the menisci in compression and second; to evaluate the ability of a testing protocol to recapitulate the material behaviour of fresh samples, using samples stored in PBS. We hypothesized that meniscal samples would be less stiff and more permeable in a swollen state than when they are compressed to the 'fresh', non-swollen, thickness prior to initiation of the protocol. We also hypothesized that a test protocol which compressed the tissue to its fresh height would result in material behaviour that was similar to those of fresh tissue samples.

4.2 Methods:

4.2.1 Sample preparation

Meniscal samples (n=30) were obtained from 5 immature bovine stifles (n=6/animal. Biopsy punches (4 mm) were used to excise cylindrical plugs in the anterior, central and posterior portions of the medial and lateral menisci in the vertical direction. Vertical plugs were punched in the direction normal to the tibial plateau in the central (inner to outer direction) of each portion of the meniscus (Figure 4.1). A custom jig was used to slice the plugs into approximately 1.5 mm thick samples perpendicular to the tibial surface.
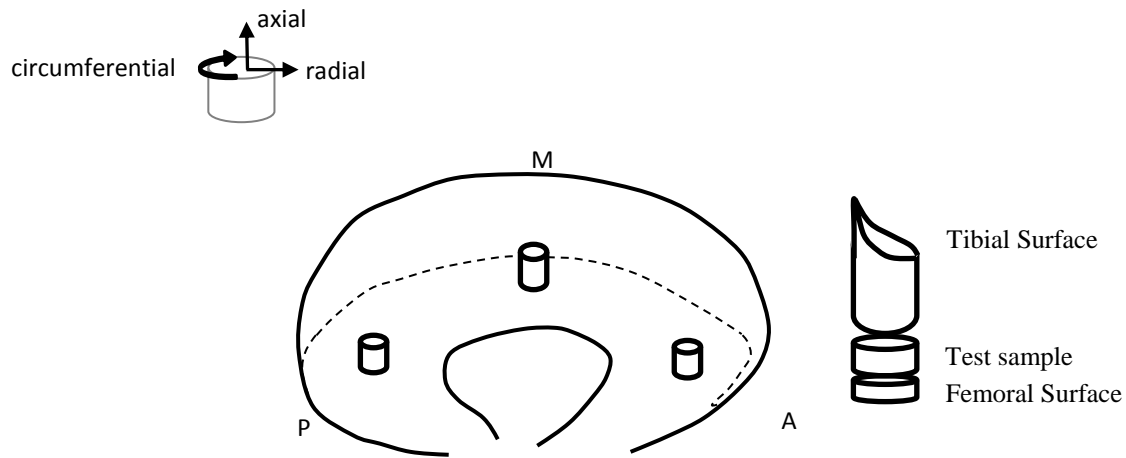
Figure 4.1 (a) Illustration showing the location of samples harvest: anterior (A), mid (M) and posterior (P) and the location of the sample within the punch taken perpendicular to the tibial plateau

4.2.2 Dimension Measurement

Dimensional measurements were taken using the method previously described for evaluating swelling of meniscal samples under osmotic challenge [Chapter 3]. Briefly, specimens were dimensionally measured with a photogrammetric technique using a dissection microscope and digital camera (Zeiss Stemi SV8 Microscope with moticam 5.0M Pixel camera). This technique was implemented to avoid the compression of the tissue that can occur when using a contact measurement device such as a caliper. Photographs were taken of the top view of the specimen to determine its radius. Two photographs of the specimen side were obtained in orthogonal directions to determine the thickness of the tissue. A calibration object was used to determine the conversion from pixels to millimeters using a custom written Matlab program (The Mathworks Inc, Natick, USA). The top-image pixel area was approximated as a circle, and an equivalent radius was calculated. The edges of the side images were manually digitized in four locations on each edge and an average thickness calculated from the eight measurements (2

photos x 4 thickness measures). The accuracy and repeatability of this technique was determined to be 0.03 mm and ±0.02 mm respectively.

The harvested samples (n=6 /animal x 5 animals) were measured using the above technique. The samples were then placed in PBS + protease inhibitors (PI) for 1 hour and subsequently measured again. The vertical swelling was then calculated as the difference between the swollen and fresh measurements. Samples were frozen at -80 ˚C until the day of testing.

4.2.3 Compressive Testing

Samples were allowed to thaw at room temperature for 1 hour on the day of testing. All samples were tested in a custom-designed uniaxial confined compression apparatus. The samples were placed into a tight fitting non-porous steel chamber which was seated on a porous sintered steel disc. A non-porous steel disc was used to compress the top of the specimen to confine fluid flow to one direction. The porosity of the sintered steel disc was 60 μm, much greater than the 80 Å of meniscal extracellular matrix, thus fluid flow was not restricted during compression (Joshi, Suh et al. 1995) . A Bose ElectroForce 3200 testing machine with a 250 gram load-cell (Honeywell Sensotec, accuracy ± 0.07%) and axial displacement transducer (±6.5 mm range, accuracy ± 0.08%) were used for all tests. Two separate compressive protocols were tested in this study.

4.2.3.1 <u>Swollen protocol</u>

Each sample was subjected to a 0.01 N pre-load for 600 seconds; then a rapidly applied strain of 2% (at a rate of 0.5 mm/s) of the swollen thickness was applied and held constant for 3600 seconds. A second, slower displacement was then applied (.0005 mm/s) to compress the sample back to its 'fresh' thickness. This displacement was then held for 5000 seconds to allow

the sample to stress-relax to an equilibrium state. Finally, another rapid displacement of 2% of the fresh sample thickness was then applied to the recompressed sample.

4.2.3.2 Fresh protocol test

One sample from each animal, taken from the central portion of the lateral meniscus (n=5 from different bovine specimen than above) was measured, as described above, and tested in compression in its fresh condition. The compression chamber was humidified and sealed to prevent dehydration during the test. A pre-load of 0.01 N was applied for 600 seconds to ensure proper seating of the sample in the chamber and to allow interdigitation with the sintered steel disc. A rapidly applied displacement (0.5 mm/s) to 2% strain (approximately 0.03 mm) was then applied and held constant for 3600 seconds and the resultant stress relaxation was recorded. This small displacement was used to allow for the approximation of constant permeability for the test (Ateshian, Warden et al. 1997). The sample was then removed from the test chamber and allowed to recover in PBS for 2 hours. The sample dimensions were then measured again, to evaluate the amount of swelling [Chapter 3]. Subsequently, the samples were tested using the swollen test protocol to evaluate differences between the fresh, swollen and recompressed conditions.

4.2.3.3 Mathematical Modeling

The stress relaxation data was modeled using a 3 term Prony model. This model uses a series of 3 Maxwell bodies and a simple spring in a parallel arrangement (Figure 4.2). The mathematical equation describing the behaviour of the Prony series is shown below (Equation 4.1) (Fernández, Lamela Rey et al. 2011).

$$\sigma(t) = \sum_{i=1}^{3} \sigma_i e^{-t/\tau_i} + \sigma_\infty \qquad \textbf{Equation 4.1}$$

Where:

$\sigma(t)$ = compressive stress (kPa)

σ_i = spring constant for each Maxwell body (kPa)

τ_i = relaxation time constant for each Maxwell body (seconds)

t = time (seconds)

σ_∞ = equilibrium stress
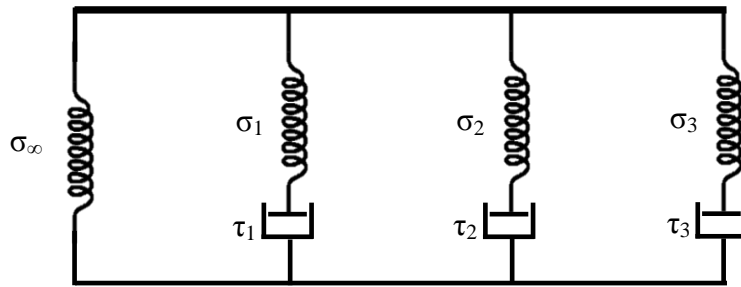
Figure 4.2 A schematic of a 3-term Prony model, including three spring-dashpot elements (Maxwell bodies) and a parallel spring used for stress relaxation modeling of viscoelastic materials

Raw data from the confined compression test were imported into Matlab (R2010a, The MathWorks Inc.) and processed using custom written code. The data were smoothed using a 5 Hz Butterworth recursive filter. Raw and filtered data were plotted to ensure the data were not over-smoothed. Smoothed data were then fit to Equation 4.1 using Matlab curve fitting tool, implementing a Levenberg-Marquardt least squares algorithm. For each stress relaxation curve, the following data were calculated: maximum stress (σ_0), equilibrium stress (σ_∞), as well as the 3 time constants from the Prony series (τ_{1-3}). Bulk modulus (H_A) describes the stiffness of the tissue under equilibrium conditions and was defined by: the equilibrium stress, divided by the applied strain. Further, the secant modulus at peak stress was defined by the peak stress divided by the applied strain and represents the apparent stiffness under a rapidly applied load. The swelling pressure was defined as the equilibrium stress required to return the tissue to its fresh

thickness from its swollen state. This pressure was calculated using the Prony model curve fitting technique for the intermediate compression.

4.2.4 Statistical Analysis

For the swollen protocol tests, Kolmogorov-Smirnoff tests were run to determine the normality of each variable's distribution determined from the Prony series curve fit. Due to technical errors in testing, 28 of 30 samples were included in analysis. For normally distributed data, paired student's t-tests were performed between the swollen and recompressed conditions. Anterior, middle and posterior moduli were compared using non-parametric Wilcoxon rank-sum tests in a sub-analysis to determine the effect of location on stiffness. For non-normally distributed data, Wilcoxon rank-sum tests were performed and the results were compared to the parametric results for the same data set. Further, linear regression modeling was used to evaluate correlations between variables of interest including; swollen versus recompressed bulk moduli, and secant modulus and swelling versus swelling pressure. Statistical significance was set at $p \leq 0.05$ for all tests. Planned linear comparisons were conducted to evaluate differences between fresh and swollen as well as the fresh and recompressed results for bulk modulus and secant modulus. Due to the small sample size in the fresh protocol test (n=5), non-parametric statistics (Wilcoxon rank-sum) were used in these analyses.

4.3 Results

4.3.1 Swollen protocol

The material properties of meniscal samples were significantly different between swollen and recompressed configurations. There were no differences in the stiffness amongst anterior

mid and posterior samples ($p > 0.05$). A representative load versus time curve, illustrates the loading protocol (Figure 4.3). The bulk moduli of recompressed samples were on average 3.2 times stiffer than in the swollen samples $p < 0.001$ (50 kPa swollen vs 156 kPa recompressed, Table 4-1). Further, the secant moduli at peak stress were on average 8.1 times greater in the recompressed samples $p < 0.001$ (327 kPa fresh vs 2656 kPa recompressed). Each of the time constants, τ_{1-3} were significantly smaller in the swollen samples than in their recompressed counterpart (i.e. τ_1 swollen vs τ_1 recompressed) $p < 0.001$ for all comparisons. The average swelling in these samples was $17 \pm 7\%$ in the vertical direction (range 3 - 32%). The swelling pressure was also variable with an average of 14.4 ± 11.1 kPa (range 2.3 - 44.8 kPa). Linear regression analysis showed a strong positive correlation between the swollen and recompressed bulk moduli, $R^2 = 0.77$, $p < 0.001$ (Figure 4.4). The secant moduli were moderately correlated with an $R^2 = 0.36$, $p < 0.001$ (Figure 4.4). The amount of swelling and the swelling pressure were only weakly correlated with $R^2 = 0.11$, $p > 0.05$ (Figure 4.4)

Table 4-1 Summary results of swollen protocol tests. Data columns are bulk modulus (H_A), Secant modulus at peak stress (SM), and the three time constants from the Prony series curve fit (τ_{1-3})

	H_A (kPa)	SM (kPa)	τ_1 (s)	τ_2 (s)	τ_3 (s)
Swollen	50 ± 30	327 ± 146	0.4 ± 0.6	9.0 ± 11.6	202.7 ± 238.1
Recompressed	156 ± 100	2656 ± 1519	4.3 ± 8.6	44.3 ± 52.5	564.4 ± 436.7
p-value (1 tailed paired t-test)	< 0.001	< 0.001	N/A	N/A	< 0.001
p-value (Rank-sum test)	N/A	N/A	< 0.001	< 0.001	N/A

4.3.2 Fresh protocol test

The fresh protocol test yielded average bulk moduli of 89.2 kPa fresh, 32.5 kPa swollen and 82.2 kPa recompressed (Figure 4.6). The absolute value of the differences between fresh and swollen samples averaged 62%, while it was 21% between fresh and recompressed samples. There was a statistically significant difference between the fresh and swollen samples (p = 0.032), but not between the fresh and recompressed samples p > 0.05. Secant modulus at peak stress was not significantly different between fresh and swollen samples p > 0.05, however the recompressed secant modulus was greater than fresh modulus (p = 0.032).
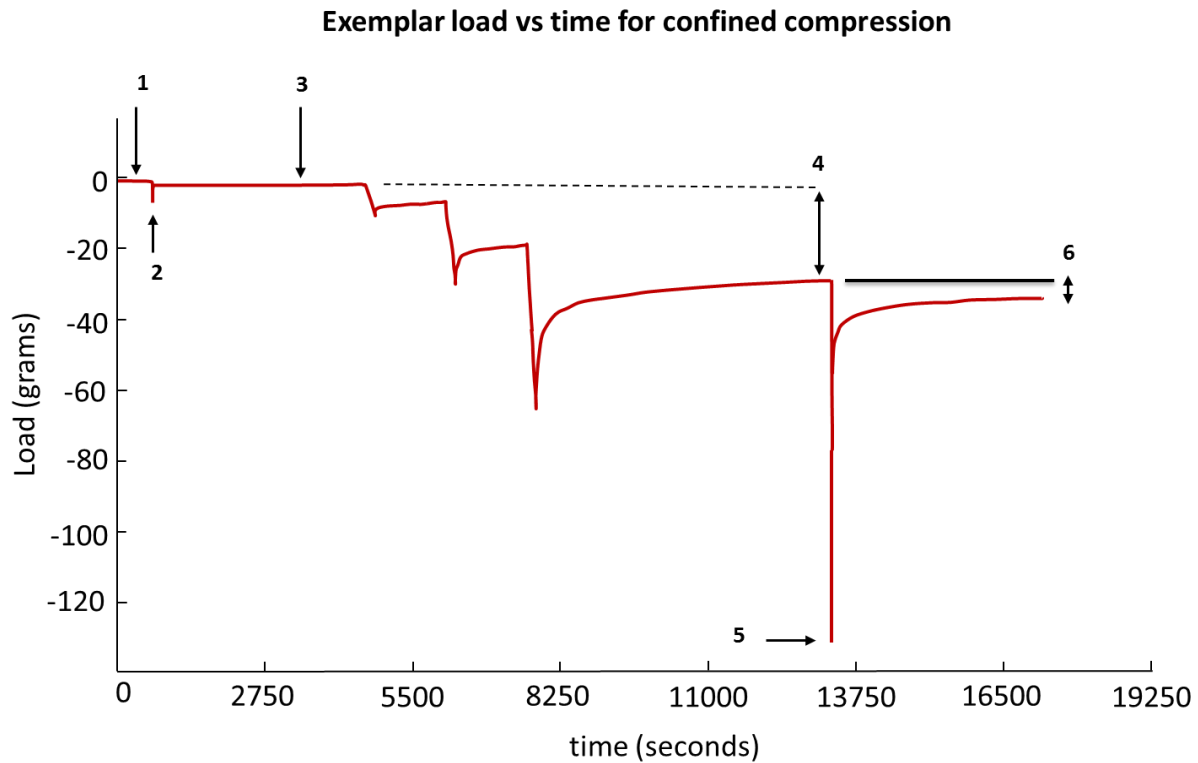
Figure 4.3 Exemplar load vs time curve for confined compression of meniscal samples. (1) An initial pre-load of 0.01 N (1 gram mass) was applied, followed by a step displacement of 2% of the swollen thickness and allowed to stress relax (2-3). The samples was the recompressed to its fresh to its fresh height in 3 steps to avoid tripping the load cell, allowed to stress relax (4) and then strained to 2% of the fresh thickness and allowed to stress relax again (5-6).
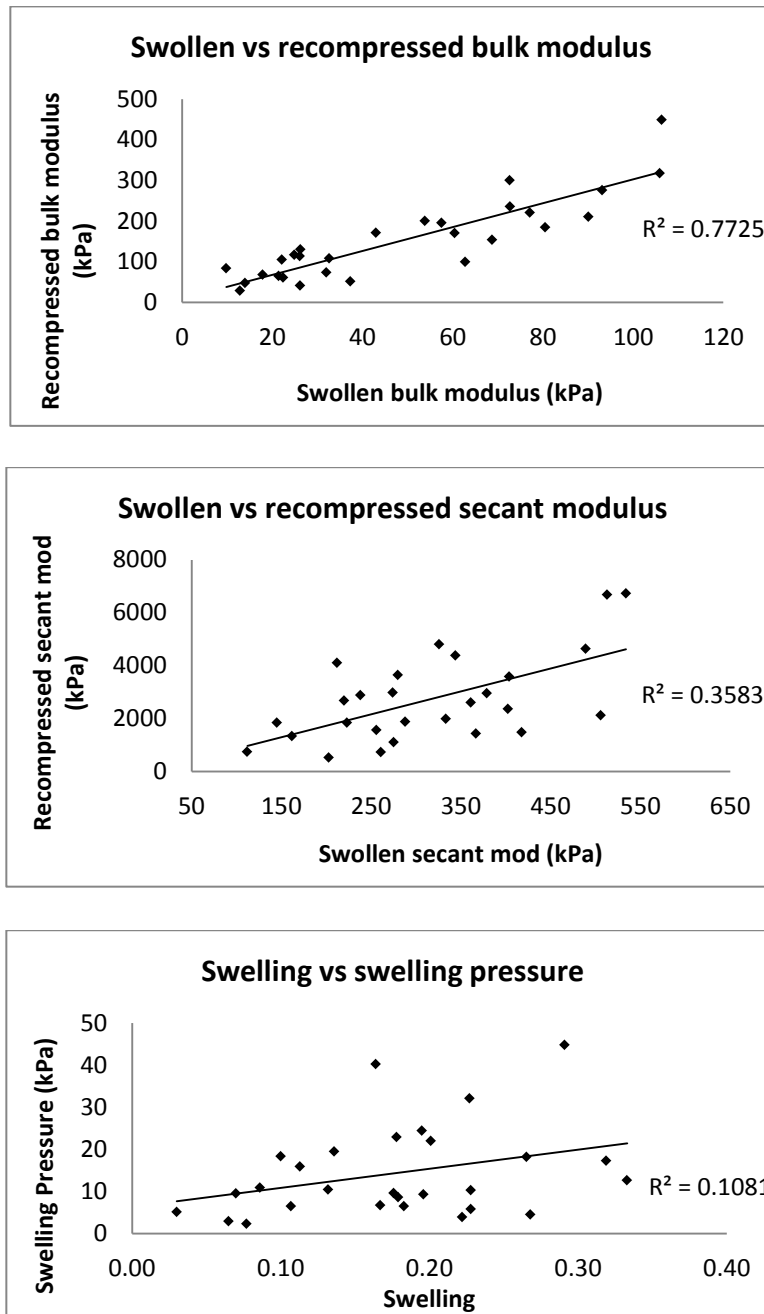
Figure 4.4 Linear regression analyses for swollen and recompressed bulk moduli (top) swollen and peak secant moduli at peak stress (middle) swelling and swelling pressure (bottom). Coefficients of variation (R^2) presented for each correlation.
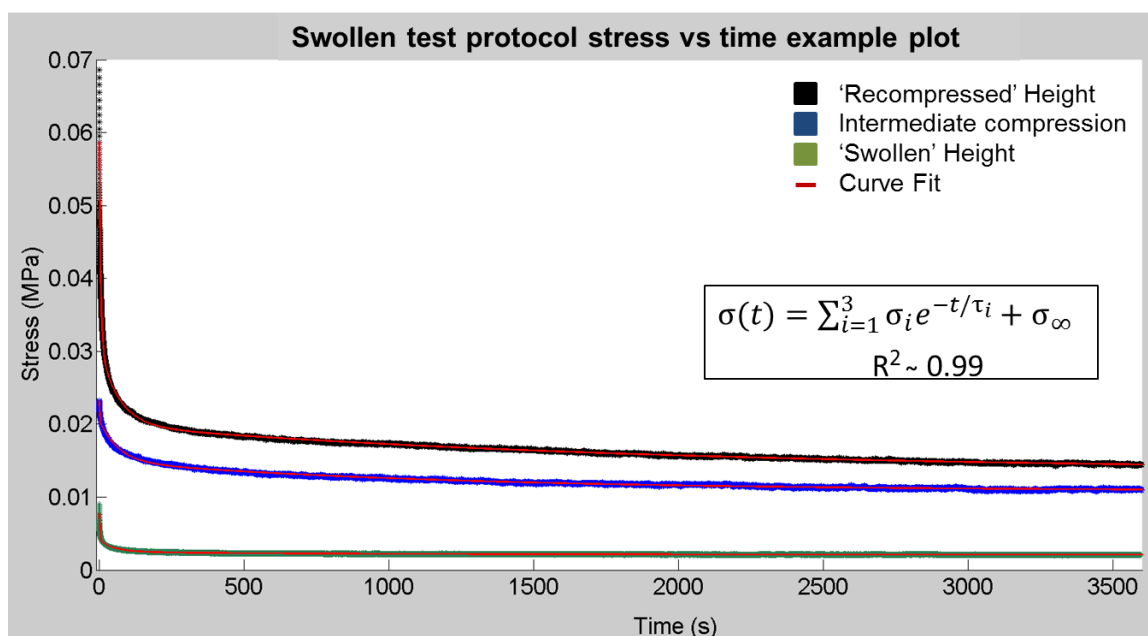
Figure 4.5 Sample data for swollen and recompressed stress relaxation data including the Prony series curve fitting results. Data has been normalized such that time for each stage begins at t=0. Curve fits are overlaid on the filtered raw data.
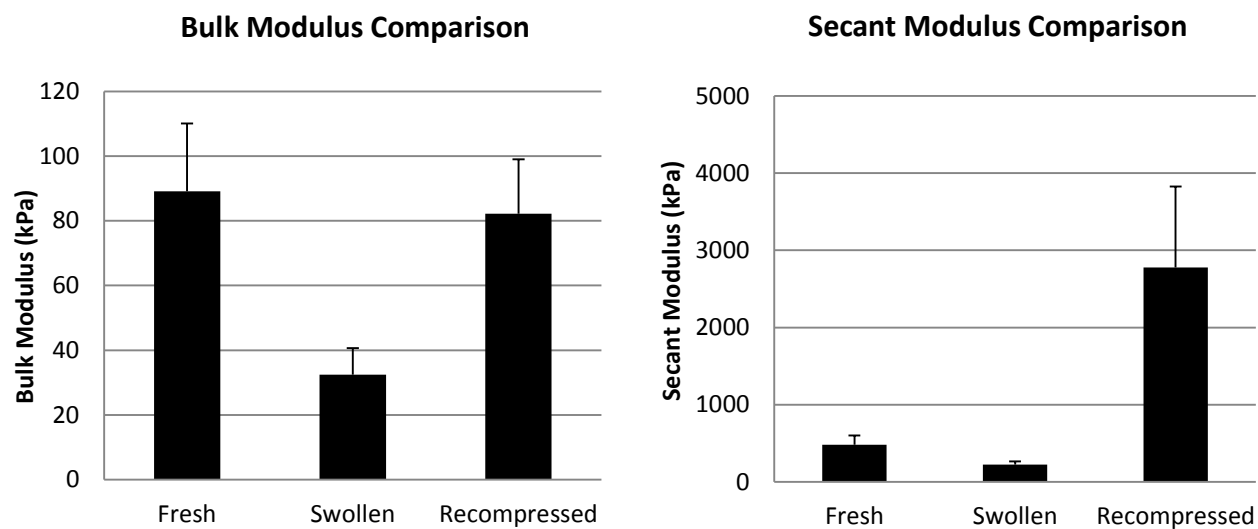
Figure 4.6 Bar graphs showing results from the fresh protocol tests. Bulk modulus + SEM (left) and secant modulus + SEM (right)

4.3.3 Mathematical Model

The 3 term Prony model performed very well for the stress relaxation tests. Curve fits were both qualitatively and quantitatively strong. Qualitative analyses demonstrated a good agreement between the filtered data and curve fits. Quantitative analyses resulted in coefficients of determination for all curves greater than 0.9, with the majority greater than 0.97 (Figure 4.5).

4.4 Discussion

The relationship between swelling and the compressive properties compressive properties of bovine meniscal samples were evaluated in this study. The bulk moduli of samples allowed to free-swell were three-fold lower than when the same samples were recompressed back to their fresh thickness prior to testing. An average bulk modulus of approximately 50 kPa was observed in the swollen samples compared to 156 kPa in the recompressed samples. Joshi et al. showed an average bulk modulus of approximately 120 kPa for bovine specimen (Joshi, Suh et al. 1995). Their reported modulus is higher than swollen samples in this study; however that study tested the sample in creep, not stress relaxation, and also applied a greater strain than this study (approximately 7% equilibrium strain, calculated from their reported applied load and bulk modulus). The differences between creep and stress relaxation have been demonstrated in tension. However, the recompressed samples in this study, with an average compression of 17% prior to testing, resulted in a larger bulk modulus. Proctor et al. reported much higher bulk moduli of 410 kPa, but once again, this study was a creep study with an average equilibrium strain of approximately 25%. Since the bulk modulus is strain dependent due to compaction of the solid matrix, it is not surprising that the results of this study are much greater than those reported here (Ateshian, Warden et al. 1997). More recently, the effects of osmolarity on the

material properties of bovine meniscal samples were evaluated (Nguyen and Levenston 2012).

Average bulk modulus was 13.6 kPa after applying a 10% compressive offset which is quite low

when compared with other literature; this was noted in the study however, no rationale for this

discrepancy was provided. The reported modulus values are also highly variable (Table 4.1). As

was seen in Chapter 3, there is large local heterogeneity in collagen organization and PG content.

As a consequence of this heterogeneity, one would expect the variability observed in the

mechanical testing results.

The secant modulus at peak stress reported here was applied at near physiological loading

rates for human walking (Chia and Hull 2008). The secant modulus at peak stress was 6.6 and

17.0 times greater than the bulk modulus for the swollen and recompressed samples respectively.

This result illustrates the large role that fluid pressurization plays in the dynamic behaviour of

the menisci. Further, this data supports the findings from Chapter 2, where it was shown that the

menisci do not act as a shock absorber in the knee. The high stiffness and linear behaviour

observed under physiological loading supports this assertion. For biphasic materials, with

relatively low permeability, rapidly applied loads result in additional fluid pressure due to drag

forces between the solid and fluid phases, which may protect the solid matrix and associated

cells from large deformations (Mow, Kuei et al. 1980; Ateshian, Warden et al. 1997). The

increase in the secant modulus in samples under increasing strain is in accordance with finite

deformation theory, which predicts decreased permeability and increased fluid pressurization for

increased strain (Kwan, Lai et al. 1990; Ateshian, Warden et al. 1997). This was also supported

by the mathematical models which showed statistically slower relaxation times in the

recompressed tissue, implying lower permeability in the tissue. While the values reported for the

secant modulus in the recompressed bovine samples (2.7 MPa) are higher than previously

reported results for human tissue under similar loading rates (1.1 MPa), they are still likely an underestimation of the in vivo properties of the menisci. Normal loading in the knee joint results in stress on the order of 1 MPa on the tibial plateau, and the menisci carry approximately 50% of this load. Consequently, strain in the menisci would be large, approximately 20% under normal loading conditions, which would be an aberration when compared with other knee joint tissues where strains are less than 10% under normal loading (Sheehan and Drace 2000; Fleming, Renstrom et al. 2001). A reason for this reduced stiffness could be due to preparation of the test samples. Cutting samples from the intact tissue condition would compromise the network of circumferential fibres and would prevent stiffening the matrix by these fibres that could occur in vivo.

A strong correlation was observed between the bulk moduli in the swollen and recompressed samples. This correlation implies that despite the highly variable amount of swelling between samples, the relative change in the bulk modulus from the swollen to recompressed condition is relatively consistent. The weaker correlation between the secant modulus values indicates that the predominantly fluid-mediated, dynamic properties are only weakly linearly related. Previous work on finite deformation theory predicts that permeability is non-linearly related to compression as both the porosity and the permeability of the tissue change due to tissue compaction, which could explain this result (Ateshian, Warden et al. 1997). Interestingly, the swelling pressure and measured swelling were very weakly correlated ($R^2 =$ 0.14). Variability of the matrix organization, including collagen architecture and proteoglycan content, may be responsible for this lack of correlation and illustrates the importance of local tissue organization and composition in the material behaviour in the menisci [Chapter 3].

Results from the fresh protocol test indicate that the bulk modulus of fresh specimens was greater than free-swollen specimens. Swollen samples were only 1/3 as stiff as when tested fresh. The moduli when the samples were recompressed to their original thickness were not statistically different than their fresh orientation and were on average 92% as stiff as in the fresh condition. This indicates that the equilibrium properties of the fresh specimen may be restored by recompressing the sample to its fresh thickness after swelling has taken place. A post hoc power analysis showed that 231 samples would be required to demonstrate no difference between the fresh and recompressed groups with 80% power. The fresh test protocol was approximately 2 hours until the sample were removed. Consequently, only one specimen per animal could be tested in the fresh condition, as the samples would need to be kept hydrated, resulting in swelling in the tissue. Because of this logistical difficulty, testing the number of samples required to power the study appropriately is not practical. However, the large number of samples required indicates the small effect size between the fresh and recompressed conditions and demonstrates the ability of the protocol to restore the equilibrium behaviour more representative of fresh tissue. Secant modulus results were different between the fresh and recompressed conditions. The results for the fresh specimen are low (450 kPa) which may be due to limitations in the test chamber design and small strain protocol. At low strains, samples may initially behave unconfined due to gaps between the samples and the chamber walls, allowing fluid flow both radially and axially, thereby increasing permeability and decreasing the dynamic fluid pressurization. Buschmann et al. demonstrated that at low strains, interdigitation with the porous disc and incomplete confinement impacted the compression behaviour of articular cartilage significantly (Buschmann, Soulhat et al. 1998).

4.5 Conclusion

The material behaviour of meniscal tissue was greatly affected by the swelling that occurs during sample preparation and storage. Swollen samples had a lower bulk modulus and secant modulus at peak stress, and had faster relaxation times, supporting our hypotheses of decreased stiffness and increased permeability. This study also indicated that the equilibrium behaviour of test samples could be restored if the swelling behaviour of the samples is taken into account. These results are important in the development of testing protocols and to evaluating the in vivo properties of the menisci more accurately.

Chapter 5

An evaluation of meniscal collagenous structure using optical projection

tomography

Chapter Five:

Abstract

The collagenous structure of menisci is a complex network of circumferentially oriented fascicles and interwoven radially oriented tie-fibres. To date, examination of this micro-architecture has been limited to two-dimensional imaging techniques. In this study the collagenous structure of the meniscus was evaluated using optical projection tomography (OPT). OPT is an imaging technique capable of imaging samples on the meso-scale (1-10 mm) at a micro-scale resolution. The technique, similar to computed tomography, takes two-dimensional images of objects from incremental angles around the object and reconstructs them using a back projection algorithm to determine three-dimensional structure. Meniscal samples were imaged from several locations to determine the variation in collagen orientation throughout the tissue. Results indicate a highly variable collagenous orientation at the contact surfaces and in the inner third of the main body of the meniscus. The variability in fibre orientation identified transition zones where fascicles were found to have a woven or braided appearance. The outer-third of the main body was composed of fibres oriented predominantly in the circumferential direction. Blood vessels were also visualized using this technique, as they fluoresce more brightly than collagen at the 425 nm wavelength used by the OPT scanner. This is the first study to evaluate the collagenous structure of connective tissue using OPT. Collagenous structure variability, not previously described in the meniscus, was identified which may help elucidate the load bearing function of the menisci in the knee joint.

5.1 Introduction

The menisci are complex three-dimensional structures with a heterogeneous structure. The semi-lunar, wedge shapes of the menisci increase the contact area between the rounded femoral condyles and the relatively flat tibia plateau, thereby protecting the articular cartilage from excessive stresses (Shrive, O'Connor et al. 1978; Baratz, Fu et al. 1986; Cottrell, Scholten et al. 2008). Menisci are fibrocartilages, which have been described as having intermediate structural and functional properties between those of dense, fibrous connective tissue (i.e. ligament, tendon) and hyaline cartilage (Benjamin and Evans 1990).

The composition and structure of the meniscus has been studied extensively since Fairbank discovered the relationship between meniscal removal and the observation of degenerative changes in the knee (Fairbank 1948). An early investigation of the menisci by Bullough et al. in 1970, described the structure of human menisci as consisting predominantly of circumferentially oriented fibres (Bullough, Munuera et al. 1970). The study also identified the presence of radially oriented tie-fibres that the authors supposed acted to tie the circumferentially oriented fibres together to prevent longitudinal splitting of the tissue. The conceptual model of a predominance of circumferentially oriented fibres has subsequently been supported in numerous studies (Cameron and Macnab 1972; McDevitt and Webber 1990; Skaggs, Warden et al. 1994; Petersen and Tillmann 1998; Rattner, Matyas et al. 2011)

The structural, mechanical model proposed by Bullough et al. remained relatively unchanged for almost 25 years. Skaggs et al. (1994) further described the arrangement of tie-fibres in the meniscus of the bovine stifle. Serial sections of the menisci demonstrated tie-fibres that persisted over several sections, implying that the tie-fibres may actually form sheets of fibres to resist separation of the circumferential bundles (Skaggs, Warden et al. 1994). Peterson and

Tillman evaluated the structure of adult human menisci using SEM combined with mechanical and chemical removal of layers of the menisci to reveal the layered, heterogeneous structure and direction of the collagen fibres (Petersen and Tillmann 1998). The resultant model developed from this work agreed with those of Bullough et al. and Skaggs et al. and also included details on the size and arrangement of the fibres in various regions. Briefly, the surface layer was reported to be composed of a fine meshwork of fibres approximately 35 nm in diameter and is 10 μm thick. Beneath the surface is a 150-200 μm thick layer of woven fibre bundles (20-50 μm wide). This lamellar layer surrounds the main body of the meniscus, which is composed of predominantly circumferentially oriented fibre bundles of varying size. These large circumferential bundles are interspersed with radial tie-fibres. In the external circumference, the fibres originate from the joint capsule within a radial orientation between the fibre bundles. Also, vertically oriented tie-fibres emanate from both the tibial and femoral surfaces and penetrate between the fibres. Finally, Rattner et al. modified the current paradigm of meniscal structure through a series of electron microscopy (EM), and light microscopy techniques (Rattner, Matyas et al. 2011). They found the fibre bundles to be arranged predominantly in the circumferential direction and weave through a honeycomb-like structure formed by the intersections of radial tie-fibre sheets. These sheets surround the fibre bundles and are composed of laterally integrated 10 μm fibres. This paper altered the paradigm surrounding the tie-fibres by showing that the radial tie-fibres form a three-dimensional network which contains the circumferentially oriented bundles.

The major limitation of all of these previous models is the use of two-dimensional (2D) imaging techniques to evaluate a highly three-dimensional (3D) structure. One can section and image 2D structures sequentially and subsequently reconstruct 3D models, but this technique is

time consuming and difficult, and to date has not been completed for the meniscus. Optical sectioning using confocal microscopy can yield 3D structures, but the maximum sample depth of a few hundred microns is a limitation in this technique.

Optical projection tomography (OPT) is a promising technique which could overcome the inherent difficulties in imaging a highly heterogeneous structure (Sharpe, Ahlgren et al. 2002), as it is an imaging technique capable of imaging samples on the meso-scale (1-10 mm) at a micro-scale resolution. The technique takes two-dimensional images of objects from multiple angles and reconstructs them using a back projection algorithm to determine its three-dimensional structure. Previously, this technique has primarily looked at developmental studies, which have evaluated the timing and localization of gene expression (Sharpe, Ahlgren et al. 2002). The study described here was exploratory in nature. The purpose was to determine the ability of OPT to visualize the collagenous matrix organization of the meniscus.

5.2 Methods

5.2.1 Sample preparation

Bovine stifle joints (n=2) were obtained from a local abattoir within 48 hours of slaughter (18-30 months age) and the medial menisci were carefully dissected. The menisci were fixed in 100% methanol at 4˚C for 48 hours. Several samples from one stifle were used in sample preparation and system optimization (n=6). For the second stifle, four specimen (approximately 3-4 mm in each of three dimensions) were dissected systematically from a radial section cut from the anterior portion of the medial meniscus and prepared for OPT (Figure 5.1). The four specimens were prepared from different locations in order to observe site-specific variation in

the structure. The specimens were prepared from: 1) Outer third of the main body 2) Inner third of the main body 3) Femoral surface 4) Tibial Surface.

5.2.2 Optical Projection Tomography

Specimens were scanned using fluorescence optical projection tomography (Sharpe et al. 2002) on a Bioptonics 3001M OPT scanner (Bioptonics Microscopy, Edinburgh). Each tissue sample was embedded in a block of 1.5% low melting point agarose (Invitrogen). Blocks were trimmed and glued to mounts, and dehydrated through three washes of 100% methanol (Fisher) over 24 hours. Specimens were then cleared for 24 hours in BABB (1 part benzyl alcohol (Fisher): 2 parts benzyl benzoate (Sigma) in a fume hood, allowing any remaining methanol to evaporate.

Native autofluorescence was imaged using the GFP-1 channel (exciter 425nm/40 nm; emitter LP475 nm) at a resolution of 13.6-20 µm. Raw images were reconstructed into greyscale slices using NRecon (Skyscan NV, Kontich), and further manipulations were carried out using ImageJ (NIH open source software). Each reconstruction results in a stack of 250-500 images, based on the sample size and resolution used. The stacks of images were imported and visualized using the 3D Viewer plugin and the Volume Viewer plugin. The 3D viewer renders a three-dimensional image of the sample from the slices while the volume viewer allows visualization of sections through the sample in a user defined plane. Images of interest were exported to Adobe Photoshop Elements 9.0 (Adobe Inc.) and filtered with a despeckling filter.
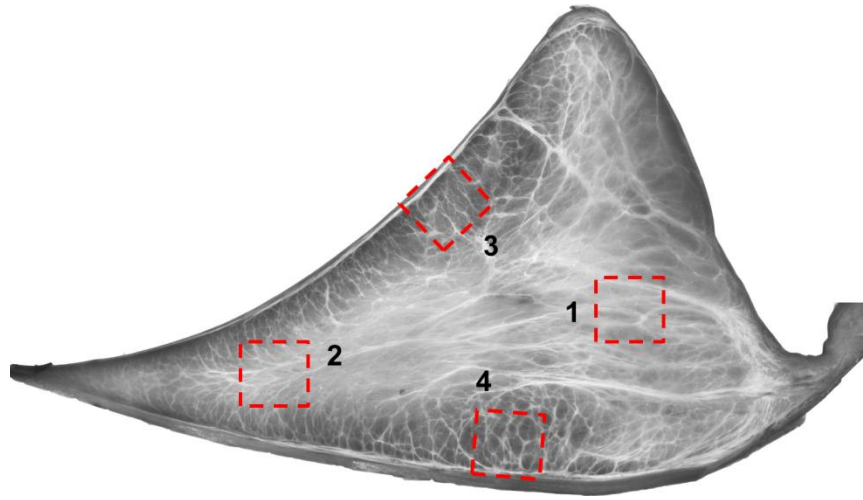
Figure 5.1. Illustration of sample locations obtained for OPT. 1) Outer-third main body 2) Inner third main body 3) Femoral surface 4) Tibial Surface

5.3 Results

Optical projection tomography was capable of imaging collagen fascicle orientations in 3D within a specimen. We were also able to identify blood vessels in multiple specimens. Specimens imaged with OPT each showed different fibre pattern orientations. Specimen 1, taken from the outer third of the main body, contained a highly aligned fibre structure. Sections through the middle, and the extreme ends of the specimen all showed the same predominant fibre direction (Figure 5.2). Blood vessels, which fluoresce more brightly than the surrounding collagen, were seen to persist throughout the specimen. Multiple vessels appear to be situated in an area of low collagen density (Figure 5.2). Blood vessels were seen in many samples taken from both the surfaces and outer portion of the menisci (Figure 5.3). Specimen 2 was taken in the same orientation as specimen 1, but from the inner third of the tissue. This specimen showed a distinctly different fibre orientation pattern than specimen 1. The top surface of this sample was composed of a woven pattern with fibres oriented perpendicular to others within the same plane

(Figure 5.4). Moving through this section in the superior/inferior direction revealed high variability in the fibre direction. The most superior plane contained aligned fibres. Moving through the section revealed an intricately woven arrangement with fibres oriented in multiple directions. The most inferior section through this specimen showed an aligned arrangement, oblique to the arrangement seen in the superior portion of the specimen. The samples from the femoral and tibial surfaces (specimen 3 and 4) demonstrated similar fibre orientation patterns throughout (Figure 5.5). The contact surfaces contained fibres oriented in the direction parallel to the surface in the radial direction. Moving in the direction normal to the contact surfaces, the fibres changed alignment and in some sections became woven, and in others appeared to be braided. The braided appearance is defined by fibres running obliquely to one another, rather than perpendicular as in the woven arrangement (Figure 5.6). Surface samples also revealed fluorescence indicative of blood vessels located beneath the lamellar layer.
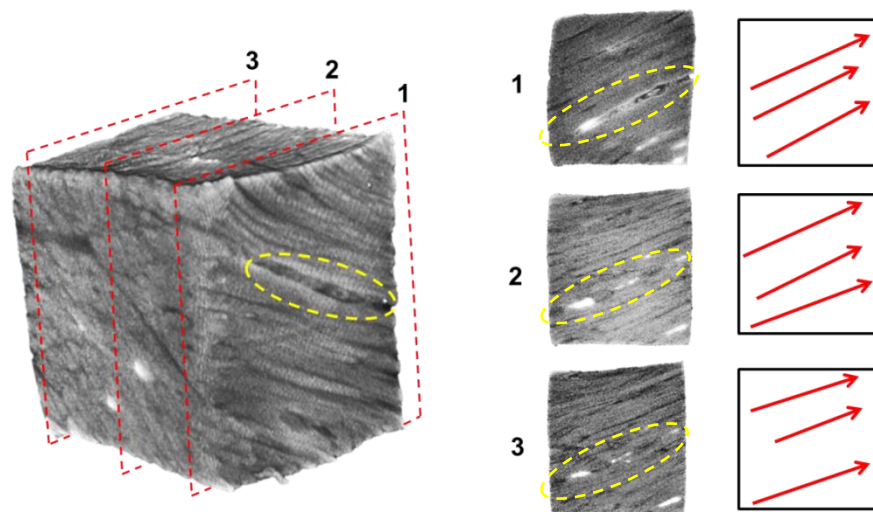
Figure 5.2 A meniscal sample taken from the outer one-third of the main body of the meniscus. The planes identified by the red dashed lines are shown in the breakout images to the right. Predominant fibre directions

are illustrated by the red arrows. All planes showed similar fibre orientations. The collagen sparse void space containing blood vessels are indicated by the yellow dashed ellipses.
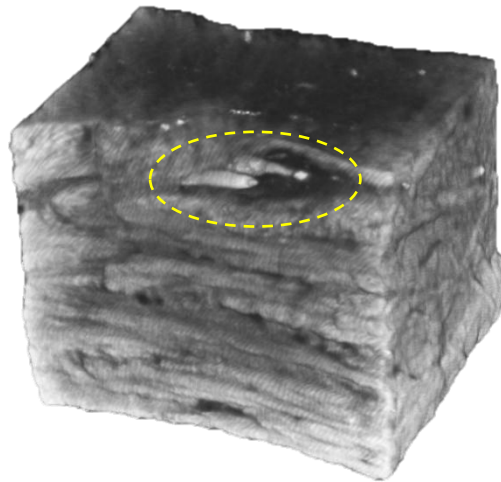
Figure 5.3 A meniscal specimen taken from the femoral surface of a medial meniscus. Two blood vessels can be seen running parallel inside an area devoid of collagen fibres.
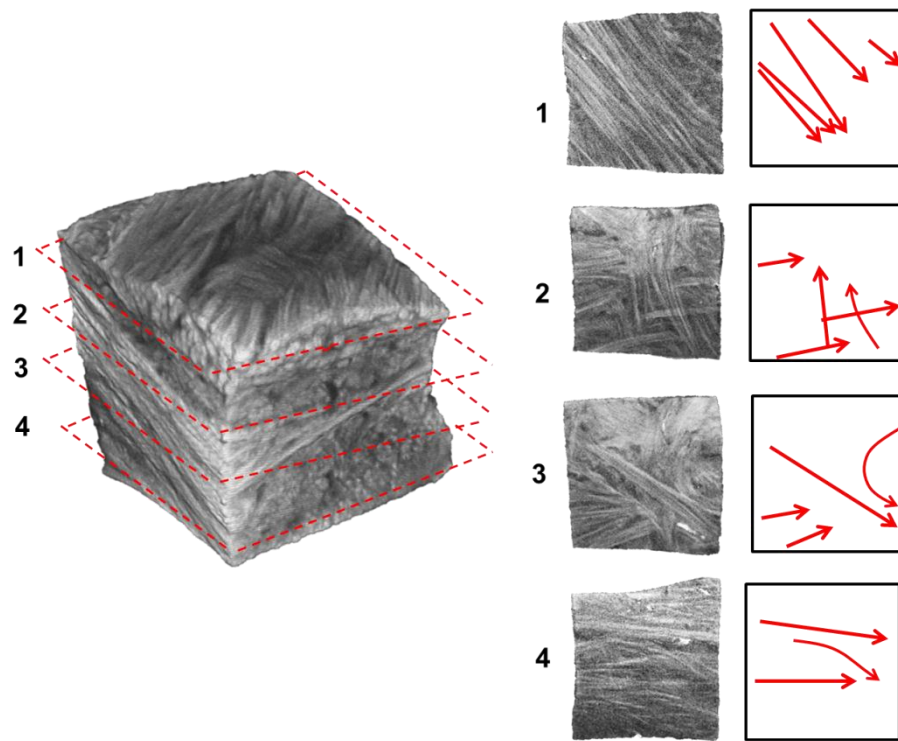
Figure 5.4 A meniscal sample taken from the inner one-third of the main body of the meniscus. Varying fibre orientations can be observed in planes 1-4, moving in the superior to inferior direction. Red arrows to the right indicate the predominant fibre directions in each breakout section image.
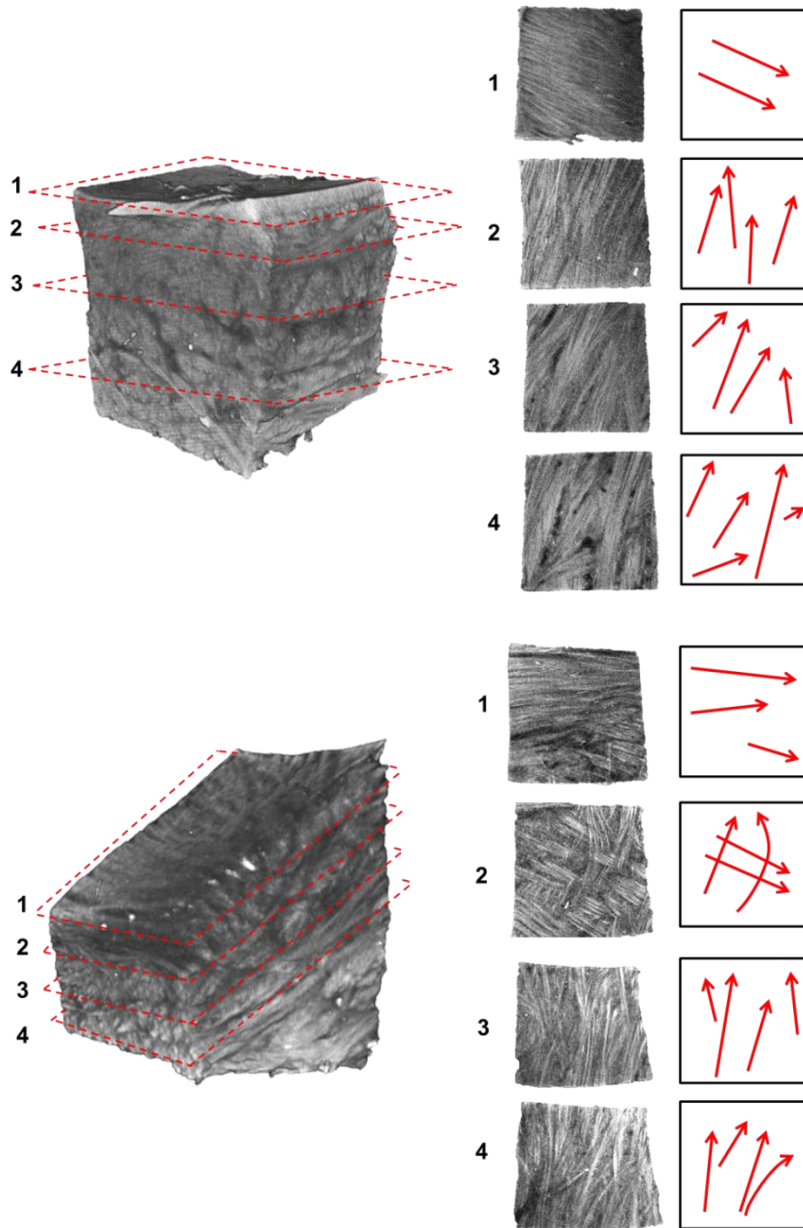
Figure 5.5 Meniscal specimens dissected from the femoral surface (top) and tibial surface (bottom) of a medial meniscus. Fibre bundles at the lamellar layer are oriented in the radial direction parallel to the meniscal surface (1). Moving through the tissue, in the direction normal to the surfaces, the fibre directions transition to braided organizations: sections 2-3 (top), sections 3-4 (bottom) in a direction oblique to the lamellar layer. Woven fibre organization can be seen in both specimen; section 4 (top) and section 2 (bottom).

5.4 Discussion

This study has evaluated the ability of optical projection tomography to visualize the collagenous fibre structure of meniscal specimen. The technique was able to resolve meniscal collagen fascicle orientation, differences between structural layers and blood vessels in three-dimensional space. Specimens dissected from the tibial and femoral surfaces demonstrated a highly aligned lamellar layer at the contact surfaces. This finding agrees with previous findings that showed a distinct layer (150-200 μm thick) with fibres oriented in the radial direction along the surface of human menisci (Petersen and Tillmann 1998).

The maximum resolution of the system is approximately 5 μm. The resolution of the images obtained here ranged from 13.6-20 μm. Due to the limitation of this resolution, the imaging of individual collagen fibres (5 μm diameter (Rattner, Matyas et al. 2011)) is not possible, but collagen fascicles which have a diameters of 100-400 μm can be visualized. Further, visualizing the surface layer identified by Peterson and Tillman (10 μm thick) is not practical with samples of this size. This layer may be visible in smaller samples where the system resolution can be maximized. A scoping analysis of several images indicated fascicle size from 5-25 pixels in diameter, which is consistent with previous findings of fascicle diameters (Petersen and Tillmann 1998). It is also not known if the sample preparation (i.e. BABB clearing) affects collagen architecture. However, qualitatively, sample size and shape did not change from the time of harvest to the images obtained from OPT. Sample dimensions were consistent with those measured prior to clearing and the collagen architecture observed is consistent with 2D imaging techniques which have been subsequently completed (Chapter 6 and Chapter 8).

The specimen from the outer third of the main body demonstrated the highly aligned circumferential fibre direction described previously (Bullough, Munuera et al. 1970; Skaggs, Warden et al. 1994; Rattner, Matyas et al. 2011). This specimen also contained multiple blood vessels which were situated within a collagen-sparse void space. Recent unpublished work from our lab has indicated that this void space is likely a proteoglycan rich region which may play a protective role for blood vessels by shielding them from shear stresses. Blood vessels were also seen along the femoral and tibial surfaces. The position of the vasculature within the tissue agree with the findings of Arnoczky and Warren in the human meniscus (Arnoczky and Warren 1982). Further evaluation of the vascularization of the bovine meniscus would need to be carried out to confirm these findings.
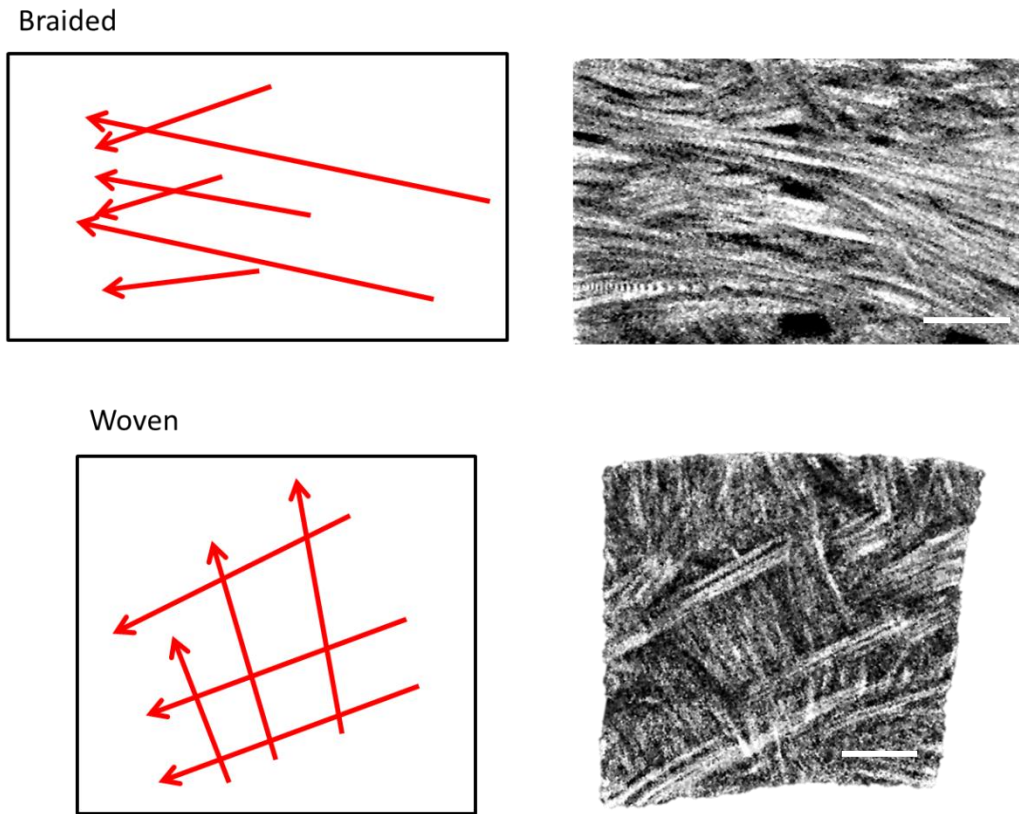
Braided

Woven

Figure 5.6 Schematic representation (left) of braided and woven fibre organizations with associated sections from meniscal samples illustrating these arrangements (right). Scale bars 1 mm.

We have identified two major types of fibre organizations, braided and woven (Figure 5.6), not previously described in the meniscus. These organizations were identified in the surface specimen and the specimen harvested from the main body of the inner third. These two fibre organizations could play a significant role in the load bearing mechanism and the fracture toughness of the meniscus. Braiding and weaving are observed in many materials in which material toughness is required. The braided fibre organization is common in various types of rope (Leech 1987). This organization results in a non-linear stiffness which increases with increasing deformation. As the fibres are stretched axially, they compress against adjacent fibres

increasing the friction between them, thereby increasing the stiffness. This is a mechanical behaviour also observed in meniscal samples in tension (Fithian, Kelly et al. 1990; Tissakht and Ahmed 1995). The woven arrangement is a common in fabrics and in structures that withstand compressive loading onto a flat structure (e.g. a basket). This fibre arrangement allows for the conversion of compressive forces into tensile forces in the weave via attachments to a rigid supporting structure. In the case of the menisci, the ligamentous attachments to the tibial plateau would provide a sufficient supporting structure. The woven arrangement may also play a role in fibre recruitment, as the loading of an individual fibre bundle would result in the recruitment of the entire woven network. This would be an advantageous load bearing mechanism in the meniscus, as if only a portion of the meniscus were loaded, the tissue could recruit many structural units throughout the tissue and limit localized deformation. These two fibre organizations could also play a role in increasing the fracture toughness of the menisci. The compressive forces between fibres under tension in the braided organization would reduce the ability of a crack to propagate through the tissue. Further, a crack passing through a woven arrangement would encounter fibres perpendicular to the direction of crack propagation, which would increase the size of deformation zone and divert energy away from the crack tip (Briscoe, Court et al. 1993). The bending of fibres around one another would also increase the path length and direction a crack would have to follow in order to separate the fibres. These combined the menisci's resistance to failure under physiologic loading conditions.

Although it was outside the scope of this study, the data obtained from this imaging modality could be implemented to develop more accurate computer models of meniscal function. Quantitative data such as 3 dimensional fascicle direction and density could be calculated using segmentation and image processing techniques. This type of analysis could develop site-specific

material behavior based on local fibre architecture. Further the mechanical effects of braiding and weaving could also be evaluated as it relates to force transmission throughout regions of varying fibre organization.

These findings identify the transitional nature of the menisci. Tissue composition varies from the inner cartilage-like tip, to the outer edge of the meniscus (McDevitt and Webber 1990; Nakano, Dodd et al. 1997; Sanchez-Adams and Athanasiou 2012). The results of this study have demonstrated that the structure of the tissue is also transitional. Moving from the outer third of the meniscus to the inner third the fibre arrangement changes from being highly aligned in the circumferential direction to being a woven, less organized structure at the inner third. The inner tip is similar to hyaline cartilage in both composition and structure (Nakano, Dodd et al. 1997; Kambic and McDevitt 2005; Melrose, Smith et al. 2005). Taken together, it can be observed that from the inner tip to the outer edge, the meniscus transitions from a hyaline cartilage-like tissue through an intermediate structure in the inner-portion to a highly aligned ligament-like portion at the outer edge. Further, at the contact surfaces there is a transition from the radially oriented lamellar layer at the surface to the woven or braided orientations seen in the sub-lamellar main body. Benjamin and Ralphs previously described fibrocartilage as a transitional tissue, as it is commonly seen in the interface between different tissue types (i.e. at the tendinous junctions with bone) and because of changes in tissue structure throughout development (Benjamin and Ralphs 2004). It has been demonstrated here that the structure within the meniscus also fits the paradigm of fibrocartilage as a transitional tissue.

This study has expanded the knowledge of bovine meniscal fibre structure using OPT, a novel technique not previously used in the study of connective tissues. We have visualized two fibre organizations, not previously described in the menisci: braided and woven which may help

in further elucidating the load bearing mechanisms within this highly complex tissue. Optical projection tomography is a promising technique in the evaluation of the organization of other connective tissues and changes that occur due to injury or disease processes. For example, changes that occur to tendons after implantation as anterior cruciate ligament (ACL) autografts could be examined to understand remodeling that occurs in soft tissue. This technique could also be used to visualize collagen organization throughout the healing of extra-capsular ligaments (i.e. medial collateral ligament) or tendons. The technique also has potential in developmental studies, evaluating collagenous matrix organization of connective tissues throughout the process of growth and maturation.

Chapter 6

Distribution of structural proteins in the bovine meniscus

Chapter Six:

Abstract

The solid matrix of the knee menisci is composed primarily of type I collagen. However, the 'minor' structural matrix molecules (so-called due to their low abundance in the meniscus): type II collagen, aggrecan and elastin may play significant roles in the overall function of the meniscus. This study evaluated the localization and colocalization of type II collagen and aggrecan as well as the localization of elastin in the bovine meniscus.

Bovine medial menisci were dissected and prepared for fast green and safranin-O histological staining, indirect immunofluorescence (IIF) and orcein staining for elastin. Meniscal cells were cultured from explants and protein expression evaluated using IIF.

Proteoglycan (PG) staining showed a distinct pattern which varied amongst sections prepared from the anterior central and posterior regions. Immunofluorescence revealed colocalization of collagen II and aggrecan in many regions throughout the meniscus, consistent with previous findings in other fibrocartilagenous tissues and articular cartilage. We have identified a new region in the meniscus; an aggrecan rich milieu that surrounds blood vessels in the tissue. This peri-vascular, PG-rich region was not previously identified in the meniscus. Elastin fibres were observed to be oriented parallel to the architectural sub-units of the meniscus, including tie-fibres and circumferential fibres and the surface layer; a novel finding which clarifies conflicting previous results and may indicate a mechanical role for this protein in meniscal function. The findings reported here further our knowledge of bovine meniscal composition and set the groundwork for future evaluation of human menisci.

6.1 Introduction

The menisci are hydrated soft-tissues of the knee, composed of approximately 65% water (Djurasovic, Aldridge et al. 1998). The solid matrix is composed of a network containing primarily collagen type I (the most abundant solid component), collagen type II in smaller amounts, proteoglycan (PG), elastin and other non-collagenous proteins (McDevitt and Webber 1990).

Proteoglycans (PGs) play important roles in the menisci and other connective tissues, including contributions to compressive stiffness through osmotic swelling pressure (Venn and Maroudas 1977; Williamson, Chen et al. 2001), governing fibril formation (Kadler, Holmes et al. 1996), and aiding in joint lubrication (Swann and Radin 1972; Schmidt, Gastelum et al. 2007). Various PG have been identified in the knee menisci, including aggrecan, biglycan, fibromodulin, decorin and lubricin (Ingman, Ghosh et al. 1974; McNicol and Roughley 1980; Schumacher, Schmidt et al. 2005). These molecules vary in their abundance from the inner to outer regions of the menisci (Nakano, Dodd et al. 1997). Generally, the total amount of proteoglycan decreases with increasing distance from the inner tip (in the radial direction), however not all of the component proteoglycans follow this trend. Aggrecan has been shown to decrease toward the outer edge, while fibromodulin and biglycan are most prevalent in the mid portion of the menisci and decorin is most abundant in the outer third (Nakano, Dodd et al. 1997; Valiyaveettil, Mort et al. 2005). This variation in the PG of the menisci is also related to variation in the material properties within these regions (Sanchez-Adams, Willard et al. 2011). Specifically, aggrecan has been identified for its role in compressive stiffness in menisci and articular cartilage due to its high glycosaminoglycan (GAG) content (Williamson, Chen et al. 2001; Sanchez-Adams, Willard et al. 2011). It is hypothesized that the inner portion of the

menisci, which contains more aggrecan, experiences greater compressive loads than the outer portion of the tissue. Further similarities with articular cartilage are seen in this inner region, as the proportion of type II collagen is much higher than in the outer regions, which are predominantly type I collagen (Cheung 1987).

Observations in connective tissues that undergo compressive loading, including menisci, intervertebral disc and articular cartilage and the areas of tendons where they wrap around boney landmarks, reveal that these tissues contain increased levels of aggrecan and type collagen II compared to tension only tissues (tendons and ligaments that do not wrap around bones) (Benjamin and Ralphs 1998). Both type II collagen and aggrecan are commonly found in the same tissues and there is evidence to support the idea that compressive load is required for the maintenance of these molecules in the tissue matrix (Vogel 1996; Milz, McNeilly et al. 1998). Collagen II and aggrecan are both found in the bovine meniscus (Vanderploeg, Wilson et al. 2012); however it is not yet known if they are colocalized within the meniscal extra-cellular matrix (ECM). The previous study that evaluated aggrecan and type II collagen in bovine composition was conducted on very young animals (2-4 weeks old) (Vanderploeg, Wilson et al. 2012). It is known that the composition and distribution of matrix components varies with age in the ovine menisci and similar age related effects may be present in bovine menisci.

Many tissues that display elastic mechanical behaviour including blood vessels, lung, ligament and menisci contain elastin (Peters and Smillie 1972; Hopker, Angres et al. 1986; Rosenbloom, Abrams et al. 1993). Within the menisci the composition is low (0.6%), despite the diffuse vascularization which is known to contain significant amounts of elastin (Peters and Smillie 1972). The role of elastin within connective tissues is not well understood but is hypothesized to play a role in tissue recovery after loading (Peters and Smillie 1972). There is

contradictory information on elastin's orientation within the meniscus ECM. One previous study reported that elastin is oriented obliquely to the collagenous matrix in human menisci using histological staining (Hopker, Angres et al. 1986), while another identified elastin parallel to tie-fibre sheets using scanning electron microscopy (Rattner, Matyas et al. 2011). Elastin fibrils have been observed within cross-sections of collagen fibres of lapine and human menisci using electron microscopy (Ghadially, Lalonde et al. 1983; Ghadially, Wedge et al. 1986) which indicates that elastin may be directly associated with individual collagen fibres or fascicles. Thus, findings of these previous studies are conflicting and further investigation is warranted.

The purpose of this study was to evaluate the localization of GAGs within the tissue's gross structure. Further, the co-localization of the PG, aggrecan, and type II collagen was examined. It was hypothesized that these matrix molecules will be strongly colocalized, similar to that seen in articular cartilage. This study also evaluated the localization of elastin in the tissue with respect to the larger collagenous network. It was hypothesized that elastin fibres would be oriented parallel to both tie-fibres and circumferential fascicles in the meniscus. Understanding the specific organization of these molecules may have implications on understanding their function within the various regions of the meniscus.

6.2 Methods

Bovine stifle joints were obtained from a local abattoir (1.5 - 2.5 years of age, n=6). Stifles were carefully dissected and the menisci removed. For PG staining, specimen were immediately fixed in 100% methanol and refrigerated at 4˚C for at least 24 hours prior to staining. For elastin, collagen II and aggrecan, radial and circumferentially oriented samples were cut, placed in optimal cutting temperature (OCT) compound, snap frozen in liquid nitrogen and stored at -80˚C.

6.2.1 Proteoglycan Staining

To observe the PG distribution in the tissue, radially oriented sections were manually prepared by carefully cutting thin sections using a standard razor blade (from the anterior, middle and posterior portions of 3 stifles) and stained with fast green (collagen) and safranin-o (proteoglycan). Samples were washed in phosphate buffered saline and placed in fast green for 5 minutes, followed by an acetic acid wash (1% v/v) for 1 minute. Sections were dipped in dH_2O and then placed in safranin-O for 3 minutes then washed in PBS for 5 minutes. Sections were then imaged and photographed using a Zeiss Stemi SV8 Microscope with moticam 5.0M Pixel camera. Images were merged using Adobe Photoshop Elements 9.0 (Adobe Systems Inc.).

6.2.2 Collagen II / Aggrecan Indirect Immunofluorescence

Medial menisci were prepared for IIF using the following method: frozen sections were cut (10 µm) using a Microm HM 500 OM Cryostat and fixed in cold methanol (-20 ˚C). Sections were then washed in PBS for 15 minutes, treated with triton X-100 0.1% for 15 minutes, washed again in PBS and placed in primary antibodies (Anti Collagen Type II monoclonal, MAB8887 Millipore, dilution 1:100 and Aggrecan C-20 goat polyclonal IgG, Santa Cruz Laboratories, dilution 1:100) for 1 hour. Sections were again washed in PBS and placed in secondary antibodies (Alexa Fluor 488, Goat Anti-Mouse IgG, Invitrogen and Cy3 AffinPure Donkey Anti-Goat IgG, Jackson ImmunoResearch, dilutions 1:250) for 1 hour. Samples were washed for 15 minutes in PBS for a final time and mounted with the DNA stain DAPI, and an anti-fade agent and imaged using a Zeiss Axioskop 2 plus microscope with a Zeiss AxioCam digital camera. A negative control without primary antibody was imaged to ensure no cross-reactivity of the tissue with the secondary antibody.

6.2.3 Elastin Staining

Thin sections (7-10 μm) were cut using a Microm HM 500 OM, cryostat and fixed in cold methanol (-20 ˚C) to limit shrinkage artifact. The samples were then washed in PBS for 15 minutes. Sections were placed in Orcein solution for 24 hours, dehydrated with a graded ethanol series, cleared in xylene and mounted with Permount solution. Imaging was completed using a Leica DMRE microscope coupled with a Leica DFC420 C camera.

6.2.4 Cell Indirect Immunofluorescence

One piece of the mid-substance of one medial meniscus was sterilely dissected and placed on sterile cover slips with a drop of media. The tissue was allowed to adhere for 30 minutes. Additional media (Delbecco'sDMEM supplemented with 10% fetal calf serum) was added and cell outgrowth was monitored over a 2 week period. Following adequate outgrowth, the cells were fixed with 3% paraformaldehyde. Cover slips were washed in PBS and treated with triton X-100 0.1% for 15 minutes, washed again and placed primary antibody for 30 minutes (type II collagen and aggrecan as previously described and elastin C-21, goat polyclonal IgG dilution 1:100) . Coverslips were washed again and placed in secondary antibodies (as described previously) for 30 minutes. Coverslips were then mounted on microscope slides in the DNA stain, DAPI and imaged using a Zeiss Axioskop 2 plus microscope with a Zeiss AxioCam digital camera. Negative controls without primary antibody were imaged to ensure no cross-reactivity of the cells with the secondary antibody.

6.3 Results

6.3.1 Proteoglycan stain

Safranin-O, is a cationic dye which binds with high specificity to GAGs, a major component of PG (Kiviranta, Jurvelin et al. 1985). Staining identified a unique GAG distribution

within meniscal sections. GAG staining varied amongst anterior, central and posterior sections of the menisci (Figure 6.1). In all sections however, positive staining was observed near the contact surfaces the meniscus, adjacent to the lamellar layer and was commonly associated with the arborizing fibres emanating from the lamellar layer (Figure 6.1). This staining stopped abruptly approaching the outer portion of the meniscus. In the posterior meniscus the staining showed a different pattern, where the entire body of the section stained, while in the anterior and central portions, areas in the mid body did not stain strongly for GAG. While the distribution did vary marginally amongst menisci, all menisci exhibited the distinct pattern described above. The shape of the posterior section of the bovine medial meniscus was also different than the anterior and central sections. The aspect ratio in the posterior section appeared greater in the superior-inferior direction whereas the other sections were greater in the medio-lateral direction (Figure 6.1). At the posterior portion of the medial meniscus, the meniscofemoral attachment inserts in a vertical (superior-inferior) orientation (Figure 6.2). In this posterior region it appears that the meniscal shape transitions as it blends into this vertically oriented attachment.
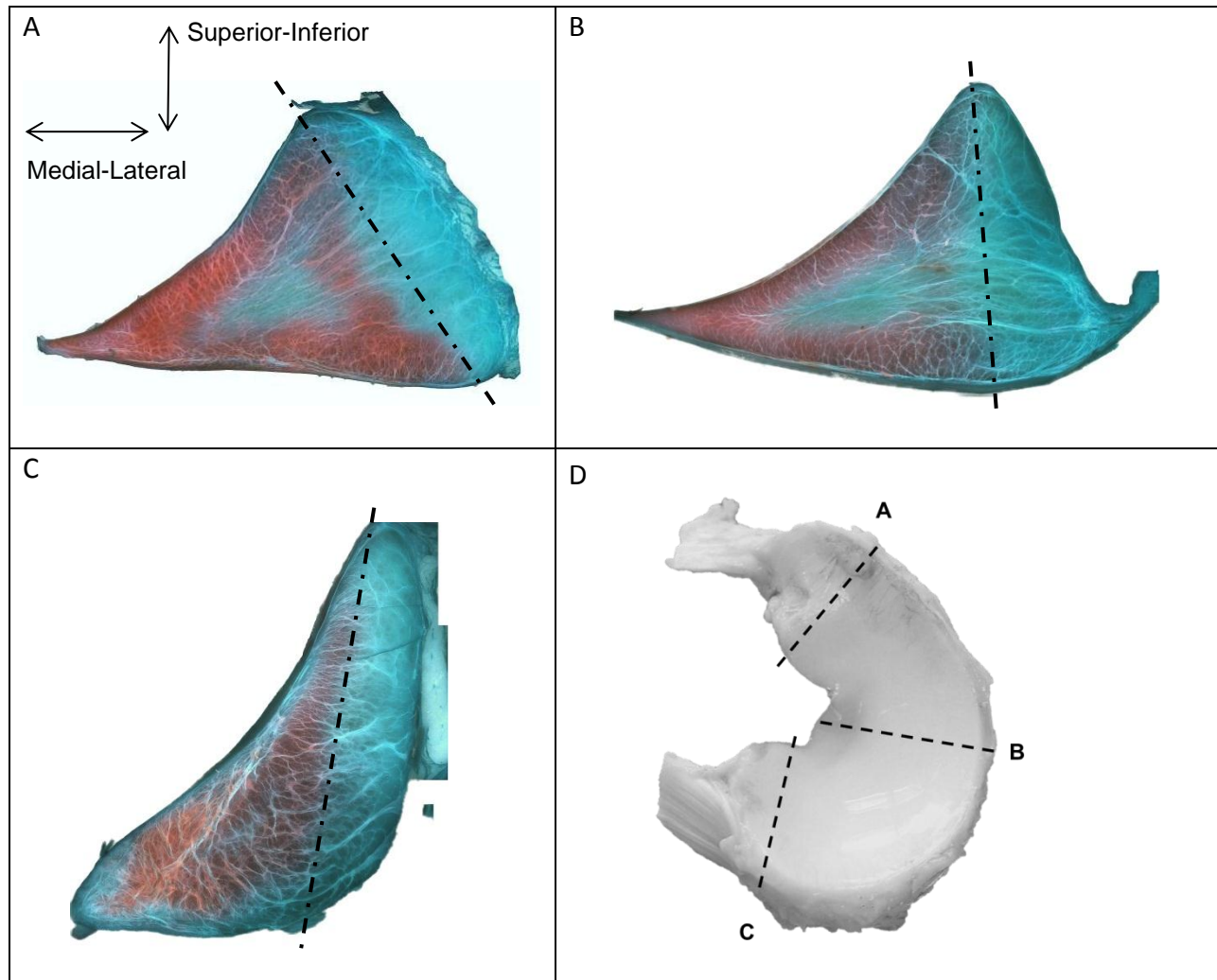
Figure 6.1 Fast green and safranin-O staining of meniscal sections taken from A) anterior B) central and C) posterior portions of the medial meniscus of a bovine stifle. D) A photo of a medial meniscus identifying the locations of the sections stained for histology. Dashed lines in A-C indicate the boundary where safranin-O staining halts abruptly. These patterns were comparable amongst in all specimens that were evaluated.

GAG staining appeared to surround circumferentially oriented bundles in the main body of the sections (Figure 6.3). GAG staining was also evident around blood vessels which tended to be associated with collagen fibres that also surrounded them. This GAG-blood vessel relationship could be seen when sections were cut perpendicular to the blood vessel orientation (Figure 6.3), as well as when sections were cut obliquely to the vessel, where elongated GAG

regions were observed (Figure 6.3). We have identified a unique GAG staining pattern in the bovine meniscus which varies by location as well as identifying locations around fascicles and blood vessels in which GAGs are localized.
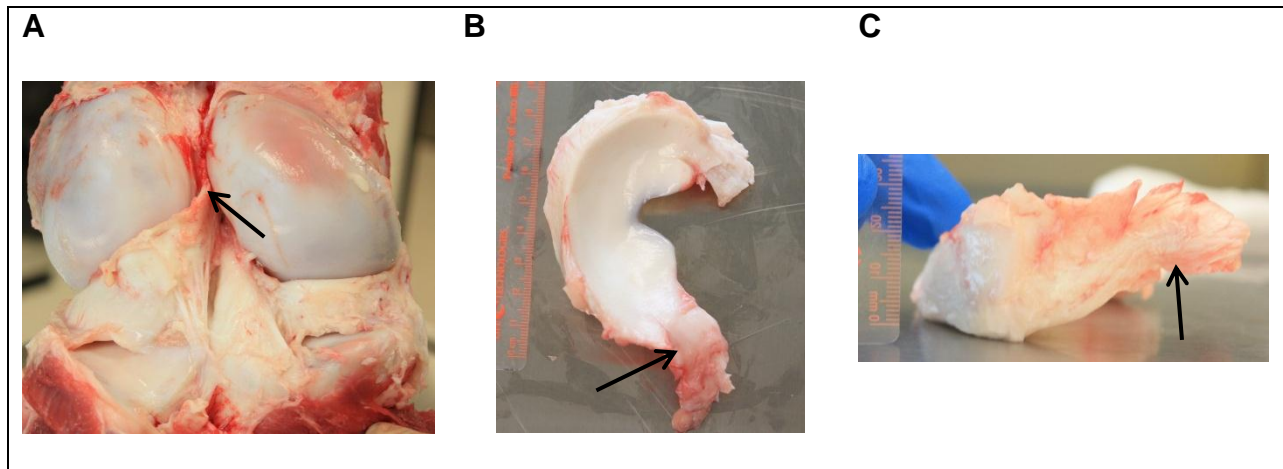
Figure 6.2 Images from the bovine stifle joint A) Posterior view indicating the insertion of the medial meniscus on the lateral femoral condyle (arrow). The ligament near the insertion has a vertical orientation which can be observed in the meniscus upon removal from the joint (B-C). The arrows indicate the meniscofemoral ligament located at the posterior portion of the stifle joint.

6.3.2 Collagen II / Aggrecan Indirect Immunofluorescence

Sections imaged using immunofluorescence microscopy identified antibodies against type II collagen and aggrecan co-localized in several regions in the meniscus (Figure 6.4 A-L). Type II collagen and aggrecan were seen in the tie-fibres, in the areas surrounding circumferential fascicles and within the circumferential fascicles. Punctate fluorescence for both molecules was seen within the circumferential fascicles. Collagen II was also seen to surround highly cellular regions, consistent with blood vessel histology (Figure 6.5 A). Aggrecan was also seen to surround the blood vessels colocalized with collagen II; however in some regions it was not co-localized with the collagen (Figure 6.4 B, D). Regions adjacent to the blood vessel inside the tie-fibre matrix signaled strongly for aggrecan without type II collagen. All blood vessels observed were associated with tie-fibres in the matrix. Indirect immunofluorescence also resulted

in positive cellular staining for both aggrecan and type II collagen in cells cultured from the meniscus (Figure 6.6). Aggrecan and type II collagen were colocalized several structure in the meniscus including tie-fibre, circumferential fascicles and blood vessels.
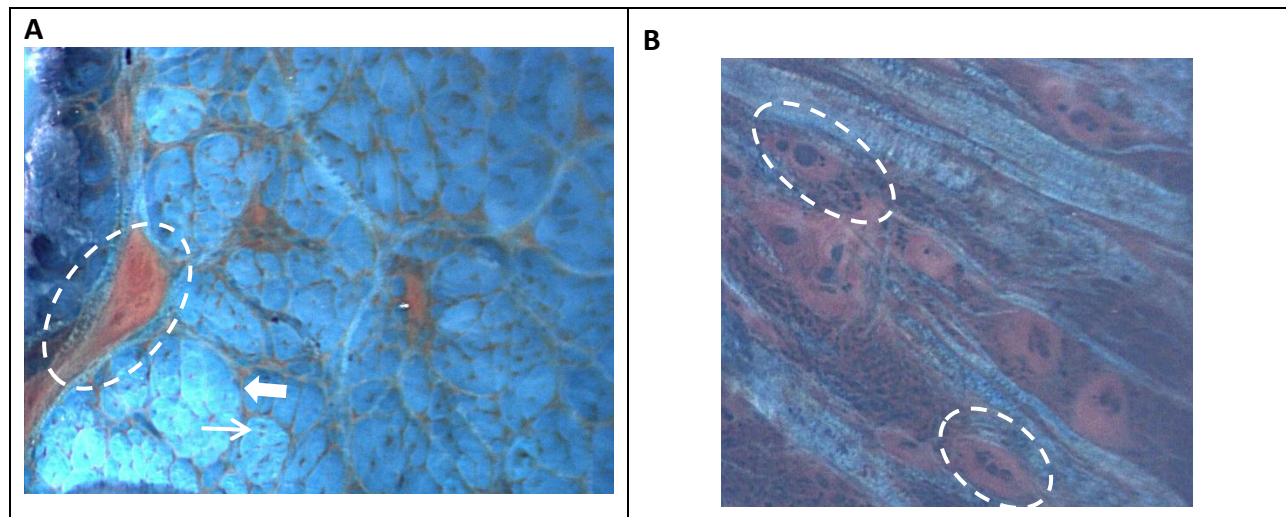
Figure 6.3 Histological images of meniscal sections stained with fast green and safranin-O. Proteoglycan rich regions surrounding blood vessels denoted by dashed ellipses (A) along a cut oblique to the blood vessel orientation (B) cut is perpendicular to the predominant blood vessel direction. Safranin-O staining identified PG surrounding (block arrow) and in punctate regions within circumferential fascicles (arrow). PG staining was also observed to surround blood vessels dashed.

6.3.3 Elastin Staining

Elastin fibres were identified in the meniscus in both the circumferential and radial directions. The fibres were oriented along the radial tie-fibres and seen within the circumferentially oriented fascicles (Figure 6.5). Elastin fibres in circumferentially oriented sections were also oriented in the direction of the fibres within the fascicles. Elastin fibres were also observed in the peri-fascicular region, where they appear to surround the fascicles (Figure 6.5 B). In addition, elastin staining was observed in sections containing blood vessels and near the surface layer and lamellar layer of the meniscus (Figure 6.5 E). Using indirect immunofluorescence, elastin was observed cytoskeletally in cells cultured from the meniscus (Figure 6.6). Elastin fibres were identified in five predominant regions with distinct orientations in each region, indicating potentially distinct elastic mechanical properties for the tissue in those locations.

Aggrecan	Type II Collagen	DAPI	Merge
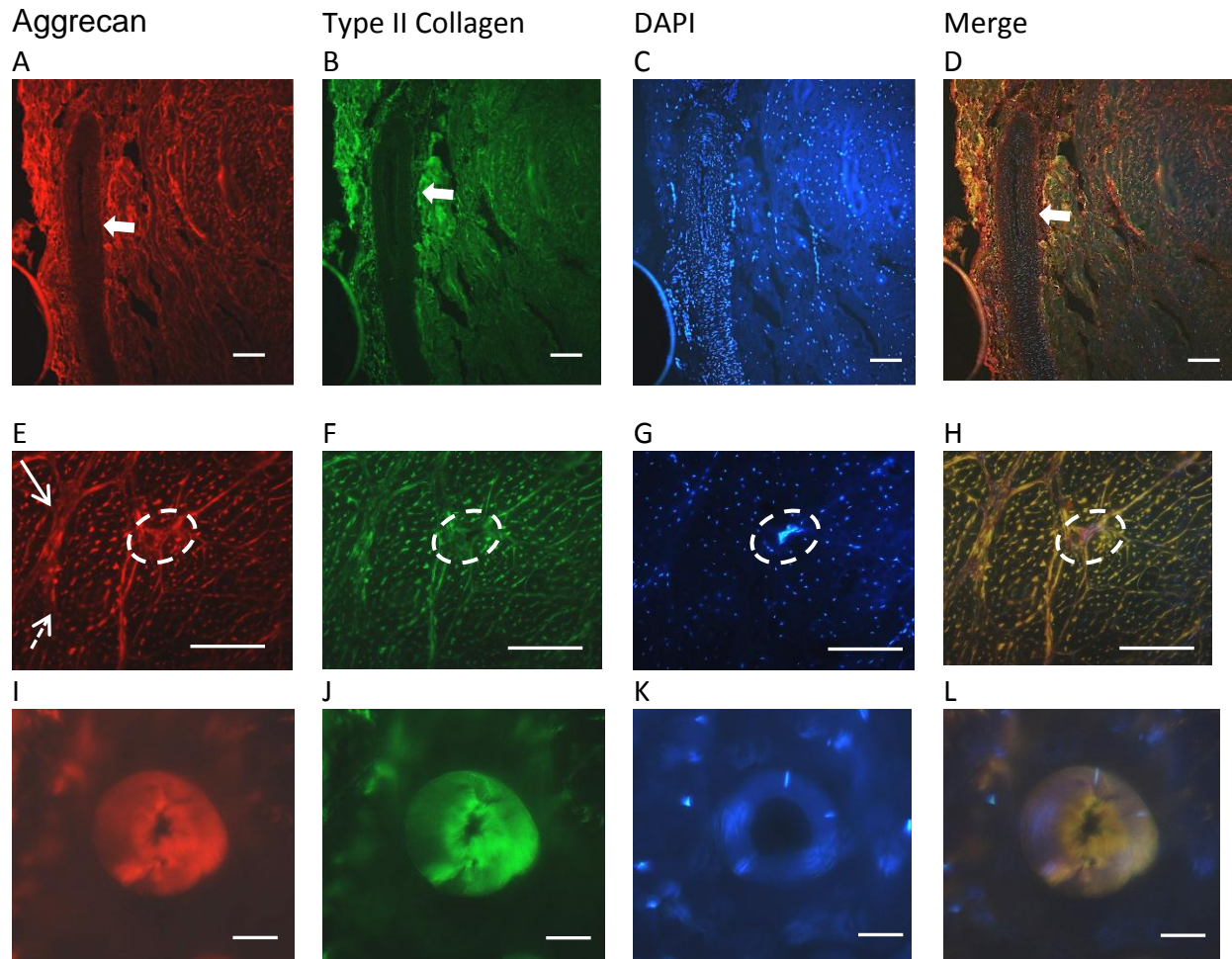
Figure 6.4 Immunofluorescence of radial sections of bovine meniscus. In A-D a section containing a blood vessel cut obliquely. Aggrecan and collagen II are observed to colocalized around the circumference of the vessel (block arrows A-B) Colocalization appears yellow. A thin layer of aggrecan can be observed inside the colocalized region in the merge image (block arrow D), scale bars 100 µm. A radial section shows aggrecan and collagen II colocalization in tie-fibres (arrow) and surrounding fascicles (dashed arrow) (E-H). Dashed ellipses indicate a region of blood vessel, identified by dense cellular staining (G). Collagen II is absent in this region, but aggrecan was localized here. Cells and aggrecan are observed merged image in this region (H). Some small areas fluoresced with aggrecan only, but the two proteins are predominantly colocalized in the section. Scale bars 100 µm Images I-L show an individual fibre that was released from the section as shown previously (Rattner, Matyas et al. 2011), identifying regions of collagen II and aggrecan within the fibre and outside of the cell (L) scale bars 10 µm.
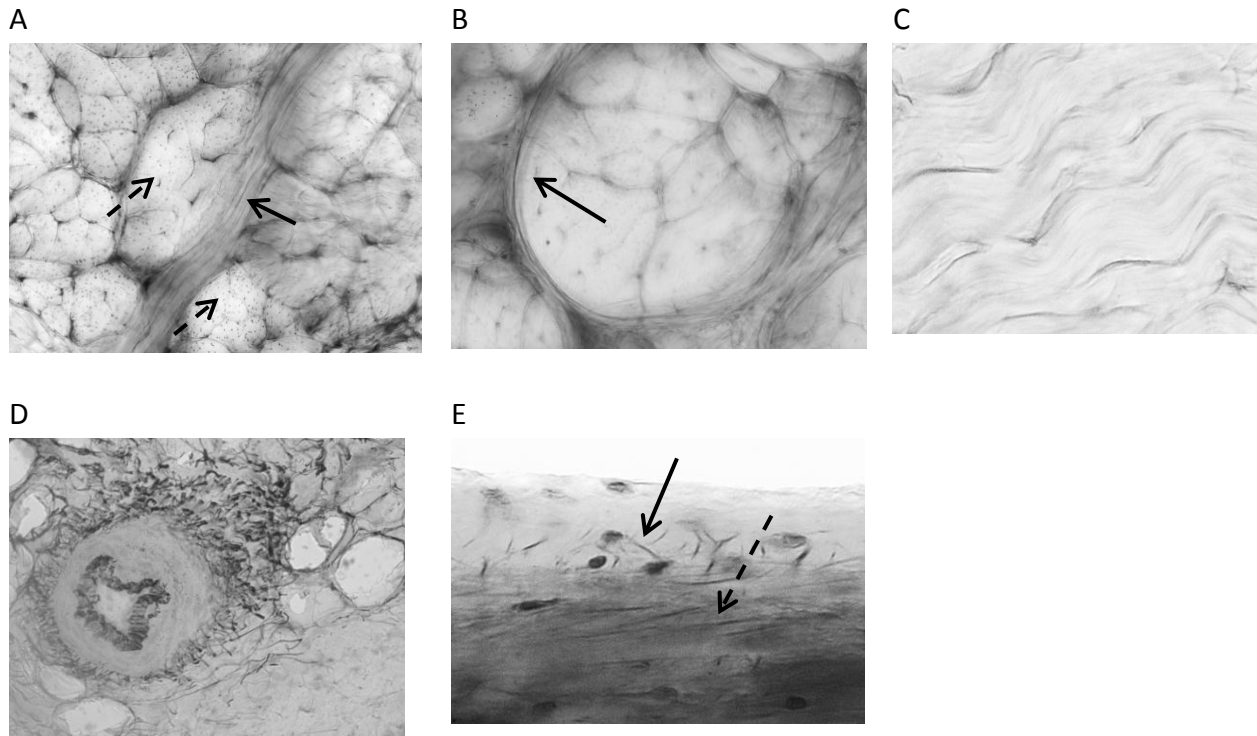
Figure 6.5 Orcein staining for elastin fibres in A-B) radial cross-section C) circumferential cross-section and D) radial cross-section containing a blood vessel, E) Surface layer. In radial cross-section (A), elastin was observed to orient along the direction of the tie-fibres (arrow) and in punctate regions with circumferential fascicles (dashed arrows). Elastin was also identified surround circumferential fascicles in radial cross section (B) (arrow). In circumferential sections, elastin fibres were observed to run in parallel with the collagen fibres. Punctate staining in (A) indicates the cut ends of fibres with orientation similar to that seen in (A). (E) Surface fibres appear randomly oriented (arrow) while fibres in the lamellar layer appear to be aligned, near parallel to the surface (dashed arrow)

A (Aggrecan) B C

D (Coll II) E F

G (Elastin) H I
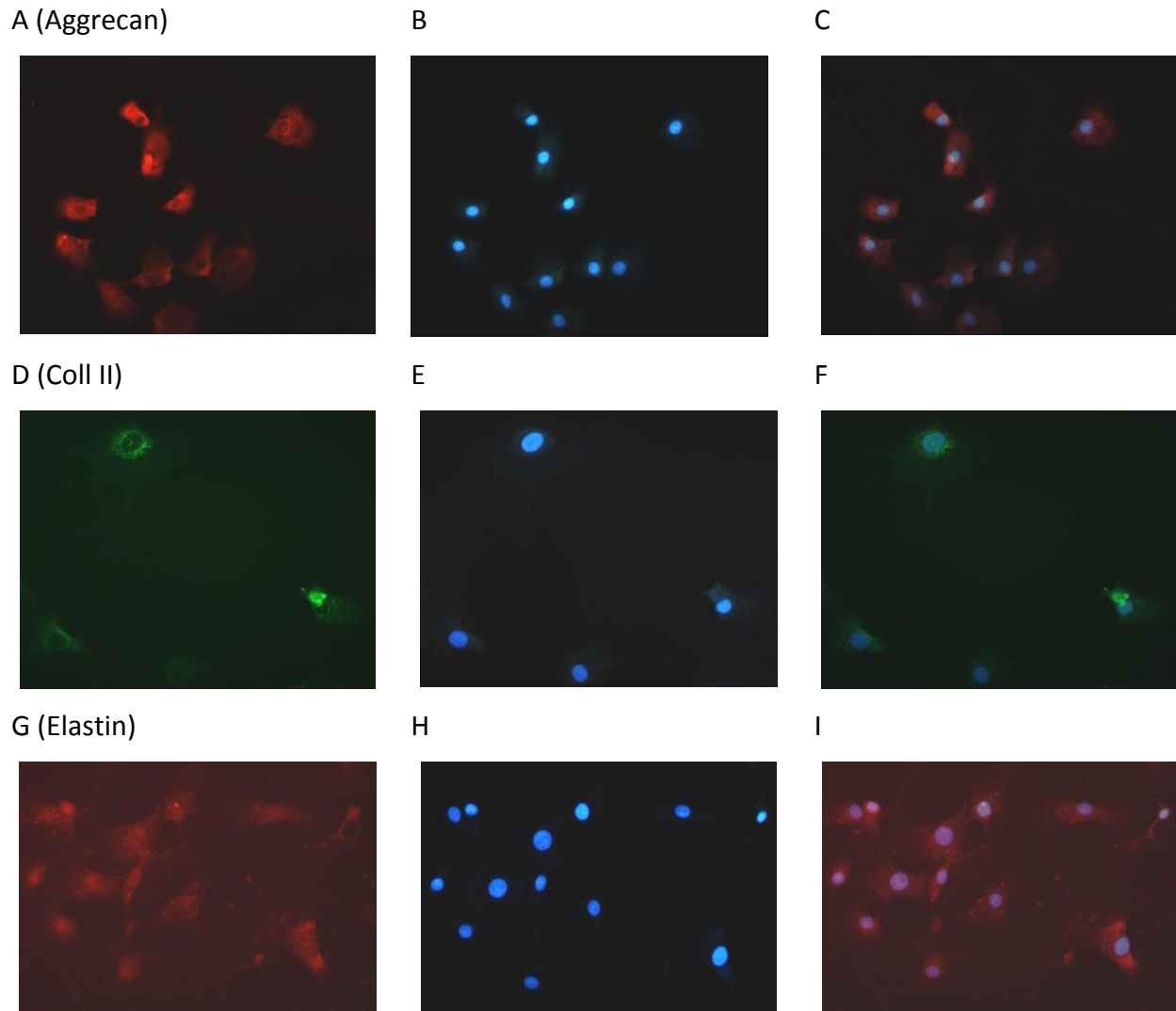
Figure 6.6 Immunofluorescence of meniscal cells. Images of cells stained for aggrecan, collagen II and elastin (left) and the associated nuclear DAPI stain (middle) and merged images (right). All cells fluoresced cytoskeletally, indicating production of each of the proteins by the meniscal cells.

6.4 Discussion

The identification of distinct and unique patterns of PG localization is important to better understanding the complex structure-function relationships within the menisci. GAGs associated with the lamellar layer and the arborizing fibres near the contact surfaces are in locations that would be directly compressed between the femoral condyles and tibial plateau. GAG content has been shown to be correlated with compressive stiffness in articular cartilage and in the menisci

(Williamson, Chen et al. 2001; Sanchez-Adams, Willard et al. 2011). Further, the arborizing fibres are generally oriented perpendicular to the articulating surfaces may indicate that this region is organized in such a fashion as to withstand compressive loading, similar to the deep layer of articular cartilage (Jeffery, Blunn et al. 1991). In all sections, a region could be identified after which the PG staining halted abruptly (Figure 6.1). Interestingly, this region corresponded with the superior outer margin of the meniscus where the meniscus is likely not directly compressed by the femur, as the shape of the tissues would no longer be congruous beyond this superior margin. This finding may indicate that regions of the menisci compressed by the femur and tibia express higher levels of PG than regions not directly compressed by boney contact. The localization of PG at the gross histological level is in agreement with findings in both sheep and rabbit menisci (Chevrier, Nelea et al. 2009). However, these findings are different from those seen in humans, where PG was localized in the main body of the menisci not at the surfaces (Chevrier, Nelea et al. 2009). The observed differences may be species related, but also may be due to the age of the specimen; rabbit and sheep menisci were obtained from skeletally mature, yet relatively young animals (average age 6.9 months and 2.9 years respectively) whereas human specimen were obtained from older patients (average age 54 years). Melrose et al. revealed significant changes in PG distribution using toluidine blue staining in 2 day, 19 month and 10 year old ovine menisci; identifying age-dependence on the localization of PG in meniscal tissue (Melrose, Smith et al. 2005).

At higher magnification, the staining of GAG with safranin-O was observed surrounding circumferential fascicles, in punctate regions within fascicles and in tie-fibres (Figure 6.3). The safranin-O findings corresponded well with the aggrecan IIF results, where immunofluorescence for aggrecan was observed in all of these regions. The colocalization IIF results also identified

type II collagen in these regions. The correspondence of collagen II and aggrecan molecules within tissues that withstand compressive forces (Vogel 1996; Milz, McNeilly et al. 1998) may identify a functional role for this peri-fascicular region in the meniscus. Collagen II and aggrecan were also observed to be colocalized around blood vessels in the outer and middle thirds of the meniscus (Figure 6.4). Findings from safranin-O stained sections also identified PG rich regions surrounding blood vessels. Recent observations from meniscal imaging using optical projection tomography (OPT) identified collagen-sparse void spaces in which blood vessels resided (Chapter 5). Results from PG stained sections indicate that the void space may be PG filled which would not have been visualized with the OPT technique. IIF results indicate that in the collagenous matrix surrounding the vessels, type II collagen and aggrecan were colocalized, however in some regions signal for aggrecan was observed in the absence of collagen II. These aggrecan rich regions corresponded with regions of high cellularity identified using DAPI stain, which is consistent with blood vessel histology (Figure 6.4). IIF results for aggrecan coupled with the PG staining and OPT results may indicate that blood vessels reside in a aggrecan-rich milieu surrounded by a type II collagen matrix, that is associated with the larger tie-fibre network. A recent study by Vanderploeg et al. that evaluated collagen II distribution in juvenile (2-4 week) bovine menisci showed collagen II around a highly cellular region, however this was not discussed as being associated with blood vessels (Vanderploeg, Wilson et al. 2012). We propose that these previous results correspond with the findings presented here. This previous study also evaluated aggrecan distribution in this tissue, but did not present any findings that contained images consistent with blood vessel histology. While both matrix molecules were presented in that study individually, their colocalization was not assessed. In the ovine meniscus,

toludine blue staining for PG and collagen II immunohistochemistry results corresponded quite well (Melrose, Smith et al. 2005).

Results from orcein staining for elastin clarify previous conflicting results regarding elastin organization within the meniscus, where fibres were seen to run obliquely to the predominant fibre direction (Hopker, Angres et al. 1986). This study demonstrated that elastin fibres were oriented in a region specific manner. Elastin fibres were identified along both circumferential fascicles and tie-fibres as well as surrounding circumferential fascicles, in blood vessels and near the surface layers. This result is intuitive from both a biological and mechanical perspective. Since collagen aligns in the direction of greatest tensile stress (Tillman 1991), it is likely that elastin would as well, to impart an elastic function to the matrix in those directions. Populations of cells were also observed along each of the architectural subunits in which elastin was observed. Ghadially et al. previously identified elastin fibrils incorporated with the collagenous matrix surrounded by cellular projections (Ghadially, Lalonde et al. 1983; Ghadially, Wedge et al. 1986). These results, as well as the findings of Rattner et al., which demonstrated elastin fibres oriented along tie-fibres (Rattner, Matyas et al. 2011), support the findings presented here. The elastin fibre alignment indicates a mechanical role within the tissue. The menisci has a low shear modulus perpendicular to the circumferential fascicles (Proctor, Schmidt et al. 1989); elastin in tie-fibres could aid in recovery of tissue shape after loading. In the circumferential direction, elastin may aid in tissue recovery after tissue creep from prolonged loading. Further elastin was observed in the intima and adventitia of blood vessels. These regions of the blood vessel are well known to contain large amounts of elastin (Karnik, Brooke et al. 2003) and play a significant role in the recovery of blood vessel shape in pulsatile flow (Wagenseil and Mecham 2009). As elastin is cross-linked to collagen matrix in blood vessels, it may also play a role in

collagen recruitment under load (Wagenseil and Mecham 2009). Although, the total content of elastin in the meniscus is small (~ 0.6%) (Peters and Smillie 1972), its localization identified here indicates that it may play a significant role in meniscal mechanics and function.

This new understanding of the organization of the structural matrix molecules in the meniscus may lead to new models of meniscal function, which includes the sub-regions and their compositional and organizational variations.

6.5 Conclusion

This study has identified a new region not previously identified in the meniscus. This aggrecan-rich peri-vascular region may play a role in protecting blood vessels in the mechanically active environment of the meniscus. We have further identified a unique glycosaminoglycan staining pattern in the bovine meniscus which varied in the anterior-posterior direction. Immunofluorescence revealed colocalization of collagen II and aggrecan in many regions throughout the meniscus, consistent with previous findings in other fibrocartilagenous tissues that experience compressive load (Vogel 1996; Milz, McNeilly et al. 1998). Further, GAG rich regions were observed surrounding the network of blood vessels within the meniscus; which are hypothesized to play a role in the protection of blood vessels from localized high stresses. Elastin fibres were observed in several locations with region specific orientations. This orientation was parallel to the collagen in the architectural sub-units of the meniscus; a novel finding which may indicate a mechanical role for this protein in meniscal function. This evaluation of bovine menisci has led to a series of discoveries of composition and organization which may lay the groundwork for investigations in human meniscal composition and organization. A more complete knowledge of healthy meniscus composition and organization is

required to fully understand changes that occur during degenerative processes and to set targets

for engineering meniscal replacements.

Chapter 7

Distribution of proteoglycan 4 in the bovine meniscus

Chapter Seven:

7.1 Introduction

Proteoglycan 4 (PRG4) has been identified as an important lubricating protein in many tissues of synovial joints (Jay 2004). It appears that this molecule aids in friction reduction in areas of relative movement between structures and structural elements, including the articulating surfaces of the knee (Flannery, Hughes et al. 1999). Clearly defining the localization of this protein within the menisci may help to identify sites of relative movement of fibres or fascicles within the tissue and elucidate mechanical function therein. PRG4 has previously been studied in the juvenile bovine meniscus; at this point in development the protein is localized to the meniscal surfaces, in the circumferential fibres, radial tie-fibres and in some cells associated with these fibres (Schumacher, Schmidt et al. 2005). It is unclear if this distribution continues or changes during maturation. Therefore, the purpose of this study was to evaluate PRG4 distribution within 2-year old bovine menisci using indirect immunofluorescence (IIF). Specific attention was paid to those structural components of the tissue that were previously identified as well as other sites within the tissue (Schumacher, Schmidt et al. 2005). We hypothesized that the distribution of PRG4 is conserved as the animal ages and found wherever major architectural elements of the tissue interact.

7.2 Methods

Bovine stifle joints (n=5, 1.5 − 2 years old) were obtained at a local abattoir within 48 hours of slaughter. The medial menisci were carefully dissected and prepared for IIF using the following method: intact menisci were fixed in methanol for 24 hours at 4 $^\circ$C ; then whole mount sections (~30 − 40 µm in thickness) were cut manually in either the circumferential or radial

directions using a single edge razor blade (~10 sections in each direction for each meniscus). Sections were then washed in PBS for 30 minutes, and placed in primary antibody (PRG4 H-140 Santa Cruz Laboratories, dilution 1:100) for 48 hours. Sections were again washed in PBS and placed in secondary antibody (Alexa Fluor 488 goat–anti rabbit IgG, Invitrogen) for 1 hour. Samples were washed for 30 minutes in PBS for a final time and mounted with the DNA stain DAPI, and an anti-fade agent and imaged using a Zeiss Axioskop 2 plus microscope with a Zeiss AxioCam digital camera. A negative control without primary antibody was imaged to ensure no cross-reactivity of the tissue with the secondary antibody. SDS-PAGE Western blotting (3-8% TrisAcetate, Life Technologies) was used to determine the MW distribution of the PRG4 species recognized by Ab H-140 (dilution 1:500, with secondary Ab goat-anti rabbit IgG-HRP at 1:2000), using bovine PRG4 purified from media conditioned by cartilage explants (Ludwig, McAllister et al. 2012), as described previously (Abubacker, Ham et al.).

A piece of the mid-substance of the medial meniscus was sterilely dissected and placed on sterile cover slips with a drop of culture medium. The cells were allowed to adhere to the cover slips for 30 minutes. Additional medium (Delbecco's Modified Eagle Medium supplemented with 10% fetal calf serum) was added and cell outgrowth was monitored over a 2 week period. Following adequate outgrowth, the cells were fixed with 100% methanol and stored in PBS at 4˚C. On the day of testing, cover slips were placed in primary antibody (PRG4 H-140 Santa Cruz Laboratories, dilution 1:100) for 30 minutes at room temperature, then washed in PBS. Slides were then placed in secondary antibody (Cy3 AffinPure Goat Anti-Rabbit IgG, Jackson ImmunoResearch, dilutions 1:250) for 30 minutes, then washed and mounted with the DNA stain DAPI and imaged as above.

7.3 Results

We first determined the specificity of the antibody used in this study using purified bovine PRG4. A high MW immunoreactive species was observed by western blotting, with an apparent MW of ~ 460kDa, a MW consistent with PRG4 (Figure 1b). Sections imaged using immunofluorescence microscopy revealed that PRG4 was distributed at the surface of the menisci as well as at the junction between all the major structural elements of the menisci including the radial tie fibres (Figure 7.2b), the fascicles containing the circumferentially arranged collagen fibres (Figure 7.2a) and the individual collagen fibres that are arranged in parallel within the fascicle (Figure 7.2c, d). Interestingly, these sites coincided with the site of the various cell populations that are found within the menisci and all of these cells populations stained positive for PRG4. Unexpectedly, blood vessels also showed reactivity with the antibody at sites along the surface of the intimal wall, in the cells within the tunica media of the vessel, on the outer surface of the vessel (tunica adventitia) as well as diffusely in the matrix surrounding the vessel (Figure 7.1a). Non-immune IgG showed no reactivity within the samples (data not shown). Cells isolated from meniscal explants fluoresced positively for PRG4 antibody. Fluorescence was observed extensively in the cytoskeleton including along stress fibres, and in vesicles in the cellular processes (Figure 7.3).
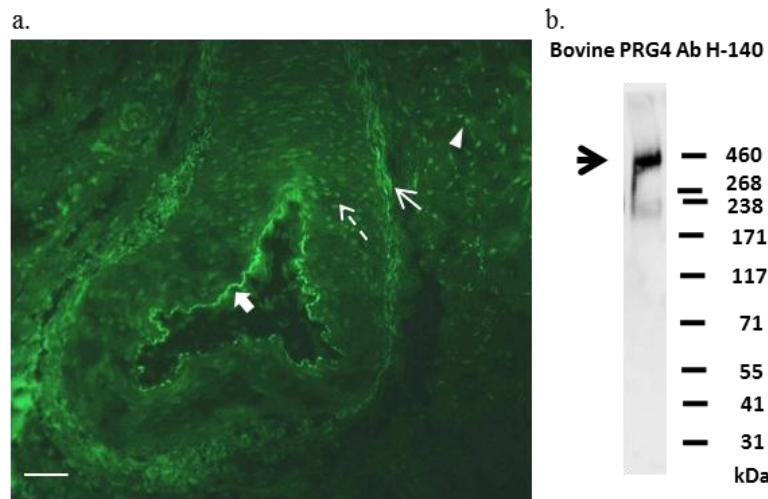
Figure 7.1 Scale bar 100 μm. Blood vessel staining for PRG4 within the menisci at sites along the intima (thick arrow), media cells (dashed arrow), adventitia (arrow) and in the surrounding matrix (arrow head).
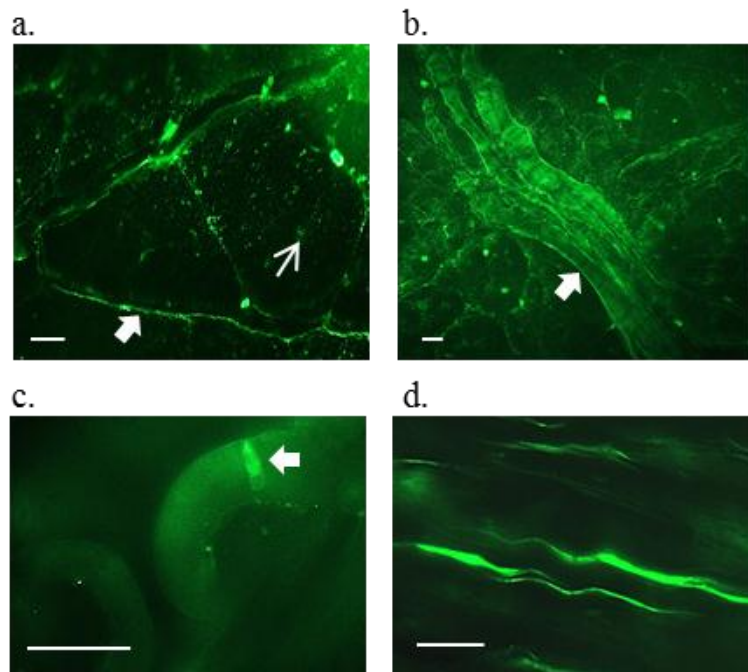
Figure 7.2. All scale bars 50 μm. (a) Radial sections identifying PRG4 staining around circumferential fascicles (thick arrow) and within the fascicles (thin arrow) (b) PRG4 signal along tie-fibres in radial sections (arrow) (c) Individual circumferential fibre with its associated cell staining for PRG4 (thick arrow) (d) PRG4 on individual fibres of a circumferentially oriented fascicle

A   B
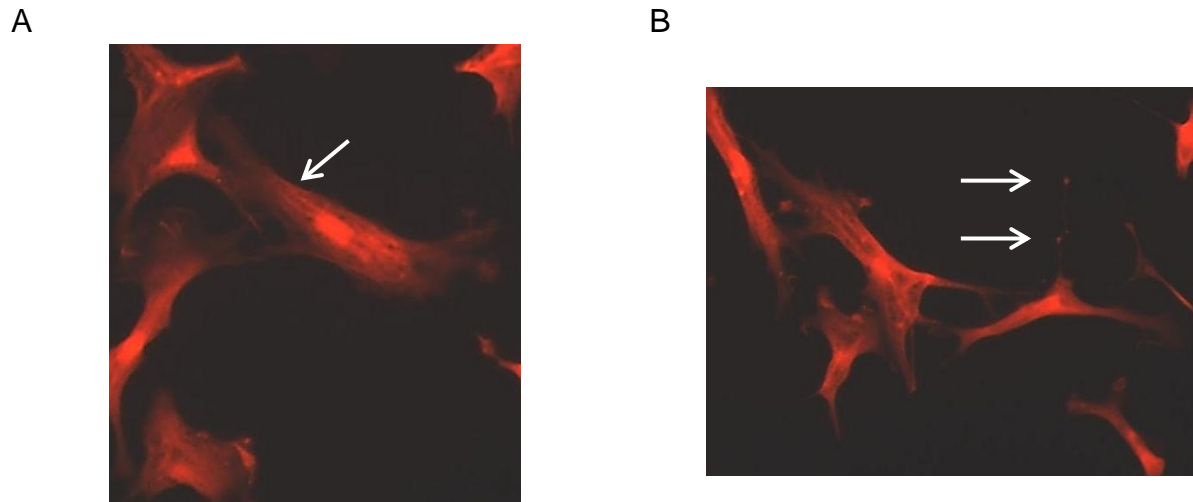
Figure 7.3 Cell fluorescence for PRG4 antibody. All cells signalled positively for PRG4. In some cells, it was observed along stress fibres (arrow A); in others it was observe in vesicles in cellar processes (arrows right).

7.4 Discussion

These findings support the hypothesis that the distribution of PRG4 in the meniscus is conserved as the animal ages and in general agree with previous findings (Schumacher, Schmidt et al. 2005). However, this study identified areas not previously shown, including areas around circumferential fascicles and in blood vessels. Further, PRG4 was immunolocalized within all of the cells associated with both the circumferential and radial tie-fibres and around the circumferential fascicles. These differences could be due to changes due to the age of the animals or the methodology used and requires further examination. PRG4 was also highly expressed in and around blood vessels in the menisci which was not hypothesized. This novel finding also warrants further exploration in its applicability to blood vessels outside of the meniscus. The high apparent MW of the immunoreactive band identified by Ab H-140 suggests that full length PRG4 is being observed in these tissues (Ludwig, McAllister et al. 2012). The expression of PRG4 between all of the architectural sub-units of the meniscus (Rattner, Matyas et al. 2011), the

site of populations of meniscal cells raised the possibility that PRG4 may not only play role in facilitating the movement between architectural units but also in protecting meniscal cells from shear forces generated during loading. The extensive cellular fluorescence coupled with the observation of fluorescence in cell-rich regions in the tissue may indicate that a large amount of observed signal is actually cytoskeletal rather than extracellular PRG4.

7.5 Significance

A complete understanding of the distribution of PRG4 within the menisci may elucidate mechanical loading interactions within the tissue. This understanding is an important benchmark in the development of tissue engineered constructs as well as changes that occur in aging, injury or disease processes.

Chapter 8

Discussion

Chapter Eight:

8.1 Summary of Findings

In this body of work we have implemented an integrated approach in the analysis of the meniscus. This approach has led to several novel findings regarding meniscal structure, function and composition. The following list provides a summary of the main findings:

1. The menisci do not act as shock absorbers in the femorotibial joint.

2. Meniscal sample swelling is not osmolarity independent.

   a. A pre-stressed state within the menisci is implied by this result.

   b. A structural basis for swelling was identified where swelling is predominantly in the direction perpendicular to the circumferential fascicles

   c. Tie-fibre network may play a role in limiting swelling.

3. Swelling strongly influenced compressive properties:

   a. Swollen samples were $1/3^{rd}$ as stiff in bulk modulus compared to samples recompressed to their non-swollen thickness prior to test initiation.

   b. Swollen samples were $1/9^{th}$ as stiff in dynamic (secant) modulus compared to samples recompressed to their non-swollen thickness prior to test initiation.

4. Optical projection tomography (OPT) was capable of visualizing the three-dimensional, collagenous structure of the meniscus.

   a. Braided and woven fibres were identified for the first time in the circumferential fascicles of the meniscus.

   b. Blood vessels were visualized in meniscal tissue.

   c. Blood vessels reside in a collagen-spare void space.

5. Proteoglycans (PG) have a distinct distribution in radial cross-section in the bovine meniscus which varies amongst anterior, mid and posterior regions.

    a. The PG rich milieu that surrounds blood vessels throughout the tissue was identified as a new region of the meniscus. This region is speculated to play a role in the protection of blood vessels from mechanical loading.

    b. Aggrecan, and type II collagen were generally colocalized in the meniscus.

    c. Elastin fibres were oriented along the direction of the collagenous matrix in each region of the meniscus.

    d. PRG4 localized where architectural subunits interact as well as around blood vessels.

8.2 Discussion of Results

The multi-faceted approach taken in this work led to a number of results which supported findings from previous studies. Results from the osmotic swelling study indicate that menisci behave like both articular cartilage and intervertebral disc under iso-osmotic conditions (Venn and Maroudas 1977; Race, Broom et al. 2000). The presence and colocalization of aggrecan and type II collagen in the meniscus may form the basis for a mechanism of swelling similar to that found in articular cartilage and the annulus fibrosis of the IVD [Chapter 6]. The abundance of PGs, and specifically aggrecan, identified in Chapter 6 would result in osmotic pressure gradients that could induce swelling in meniscal samples if the collagenous matrix were compromised by the cutting process required to prepare the samples. The non-uniform distribution of PGs throughout the menisci, observed using safranin O staining, may have played a role in the significant inter-sample variability in swelling which was observed in Chapter 3. The distribution of PG content and tie-fibre organization between samples could have been

responsible for the variability observed in results from Chapter 3; as each sample could contain a unique combination of PG content and tie-fibre architecture. Optical projection tomography (OPT) results visualized braided and woven fibre organizations in localized regions within the menisci [Chapter 5]. These fibre organizations would resist swelling very differently than highly aligned fibres, and may have also influenced the swelling of meniscal samples. While care was taken to sample from the same regions between animals, individual variations coupled with complex tissue architecture would make consistent sample composition impracticable. Swelling appears to be strongly affected by the highly variable, local composition and architecture in the region from which the sample is prepared. These findings may suggest region-specific tissue properties that play different roles within the tissue.

The mechanical properties of a test sample would also be affected by its specific microarchitecture and composition (see Chapter 3 and 4 results). Aggrecan content and collagen fibre organization have been demonstrated to influence the mechanical properties of connective tissue (Skaggs, Warden et al. 1994; Williamson, Chen et al. 2001). Consequently, the variability that is observed in previous mechanical testing studies may not only be influenced by mechanical protocols, as described in Chapter 1, but also by the specific architecture and composition in the regions from which the samples are harvested. Bursac et al. summarized some of the coefficients of variation (COV) of studies of the menisci (Bursac, Arnoczky et al. 2009). They identified a range of COV between 50 -150% in mechanical tests. Small variations in sample location could result in significantly different sample structure, resulting in large variability in the material behaviour (Figure 6.3). The complex microarchitecture and distribution of proteins within the menisci may indicate that it is not a good candidate for isolated sample testing to extrapolate on the behaviour of the tissue as a whole. As was described in Chapter 1, mechanical testing within

the same animal populations has led to vastly different results in material properties. For example, the previous studies of bovine menisci have resulted in bulk moduli of 410 kPa, 110 kPa and 28 kPa from samples prepared from comparable regions in the tissue in the same animal model (Proctor, Schmidt et al. 1989; Joshi, Suh et al. 1995; Nguyen and Levenston 2012). The results of Chapter 4 identified stiffness in swollen samples of 50 kPa compared to 156 kPa when samples were recompressed to their fresh height prior to stress relaxation testing. Further, the dynamic stiffness values were 300 kPa swollen and 2700 kPa in the recompressed condition; an order of magnitude difference between the two test conditions. The variability within these results identifies the difficulty in developing an accurate model of meniscal behaviour in compression using standard techniques. Further, the variability of composition and structure throughout the tissue may also suggest a basis for the large range of values reported in tension and shear as summarized in Chapter 1.

8.3 Limitations

There are several key limitations to the collection of studies that have been presented. First, the use of a bovine model has significant limitations in its application to the human condition. The animal's size and quadrupedal nature limit the cross over between human and bovine comparisons. This model however has been used extensively in previous work and was held consistent throughout the studies. This approach has allowed for the integration of results between studies. Further, only one age of animal was used throughout the study which gives a compositional and structural snapshot for one time period in the development of the tissue. It is known that meniscal structure and composition changes with growth, development and aging in other animal models (Melrose, Smith et al. 2005).

The compressive behaviour study [Chapter 4], provided several unique challenges. The attempts to test samples fresh at low strain levels may have led to incomplete confinement in the test chamber and affected the dynamic response of the tissue as fluid would be free to flow radially and vertically. Another limitation was that the permeability of these samples was not calculated using biphasic theory; instead it was inferred from the time constants from a Prony series model. Poor agreement between the rapidly applied loading data and biphasic theory precluded its use in numerically determining sample permeability. Further investigation should be carried out to evaluate the ability of this theory and the applied boundary conditions to model rapidly applied loads.

The OPT study was conducted as a pilot study to evaluate the effectiveness of the technique in visualizing collagenous structure [Chapter 5]. As a pilot study, the medial menisci from only two animals of were evaluated. Further work is required to evaluate the variability in structure throughout the meniscus and between animals.

Indirect immunofluorescence (IIF) is limited by the accessibility of the antibody to the specific binding sites on the proteins of interest [Chapters 6 and 7]. Collagen fascicles are tightly bound structures and may not allow adequate penetration of antibodies into the tissue. The low permeability of the meniscus may also reduce antibody accessibility. In cases where fibres were released from the tissue, they often fluoresced throughout the fibres as compared to the punctate staining seen in sections [Figure 6.4]. Much of the fluorescence in the tissue occurred in cell-rich regions and may have been predominantly cytoskeletal signal for the proteins observed. However, it can be speculated that if the cells in a region are producing a specific protein, then it is likely that the protein itself will be found in the adjacent matrix.

8.4 Model of meniscal function

Taken together, the results of this work have provided new knowledge regarding the structure of the meniscus. However, to date there has been minimal attempt to integrate the function of each architectural sub-unit and its inherent biomechanical properties into a combined description of meniscal function. The currently accepted mechanical model for the menisci, suggests that circumferential hoop stress is generated via axial loading; and this hoop stress is borne by the circumferentially oriented fibres and their attachments to the tibia and femur (Fairbank 1948; Bullough, Munuera et al. 1970; Shrive, O'Connor et al. 1978). It is also proposed that the radial tie-fibres resist radial splitting of the circumferential fibres. The complexity of the matrix architecture and composition revealed in this work has provided new insights which enable the development of a more complete model of meniscal function.

In many analyses of the mechanics of tissues, the loading is determined via purely mechanical principles, i.e. static and dynamic analyses. In the case of the menisci, this analysis is problematic, due to the complex shape of the menisci and their various attachments to the tibia and femur. According to Pauwel's theory of causal histogenesis, the structure of a tissue is determined by the stress it experiences (Pauwels 1960). This theory is analogous to Wolff's Law for bone adaptation to load. Further, the findings of Tillman and Schunke identified that collagens align along the direction of greatest tensile stress (Tillman 1991). The model that is proposed here was developed keeping Pauwel's theory of causal histogenesis in mind. The model is summarized below (Figure 8.1) and the following sections will summarize what I consider the key features of each region of the meniscus and its proposed mechanical function.
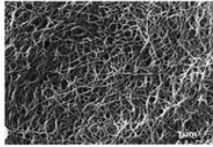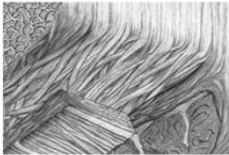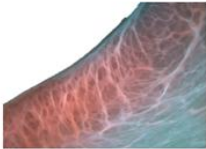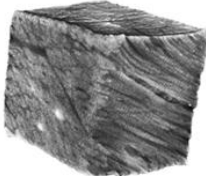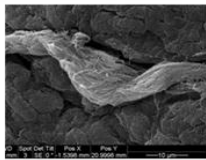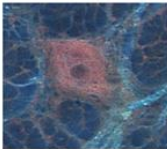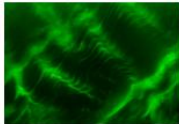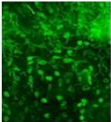
Region	Structure	Function
Surface Layer	Tightly woven fibers Fusiform Cells (Petersen and Tillmann 1998)	Low friction surface Wear resistance Possible flow regulation
Lamellar Layer	Radially oriented fascicles Arborizing fibers Braided organization (Petersen and Tillmann 1998)	Prevent radial splitting Increase fracture toughness
Arcade Region	Fibers perpendicular to surface Abundant PG	↑ Compressive stiffness Transition between layers
Circumferential Fibers	Large fiber bundles (fascicles) Aligned in outer 1/3 Various organizations in inner 2/3	Resist extrusion Hoop stress ↑ Tensile stiffness ↑ Fracture toughness
Tie-Fibers	Fibers form sheets Weave between and around fascicles Contain elastic fibers	↑ Radial stiffness Segregate fascicles ↓ Shear stiffness ↓ Bending stiffness
Peri-Vascular Region	PG rich Collagen II and aggrecan surround blood vessels	↑ Osmotic pressure Blood vessel protection
PRG4	Found where architectural subunits interact	Facilitates sliding between adjacent structures
Cellular Network	Variable morphology Site dependent (Hellio Le Graverand, Ou et al. 2001)	Produce and maintain ECM Sense and respond to load

Figure 8.1 Summary of the proposed mechanical model of the meniscus, including: Left: Region, Center: Structure and Right: Function of each of the regions in the meniscus.

8.4.1 Surface Layer

The surface layer is composed of a fine mesh of fibrils approximately 35 nm in diameter and is 10 µm thick (Petersen and Tillmann 1998). The surface layer is also populated by a large number of fusiform cells (Ghadially, Lalonde et al. 1983). The cells on the surface have been shown to produce proteoglycan 4 (PRG4), a molecule shown to have lubricating properties in synovial joints (Schumacher, Schmidt et al. 2005; Sun, Berger et al. 2006). PRG4 may also interact with hyaluronic acid in the synovial fluid to further decrease friction between articulating surfaces (Schmidt, Gastelum et al. 2007). The tightly woven surface mesh may also play a role in the regulation of flow across the surface. This fine mesh combined with cells that produce lubricating molecules result in a surface capable of providing low-friction, wear resistant properties that are integral to maintaining long term joint health.

8.4.2 Lamellar Layer

Beneath the surface is a 150-200 µm thick layer of woven bundles (20-50 µm wide) composed of 120 nm fibrils (Figure 1.3) (Petersen and Tillmann 1998). This superficial layer surrounds the main body of the meniscus. The woven bundle pattern is aligned radially along the surface of the meniscus. This fibre orientation may imply that this layer experiences a stress state that tends to splay the tissue radially as it is loaded by the femur.

There are vertical, arborizing, fibres which project from this lamellar layer in the main body of the meniscus from both the femoral and tibial surfaces (Figure 8.2). The presence of the vertical projections from the surface may have several mechanical functions. These fibres would tie together the lamellar and central portions of the tissue, integrating the two regions and allowing force transmission between the layers. This interconnectivity would distribute lamellar stresses through the circumferentially oriented fascicles and resist failure between layers with

oblique fibre directions. Our observations have identified that the orientation of the fibres near the surface is analogous to the collagen arcades of articular cartilage described by Benninghoff (Figure 8.2 E) (Benninghoff 1925). The PG distribution in the meniscus appeared to be strongly linked with the arborizing fibres from the surface [Chapter 6]. The osmotic swelling pressure developed by the abundant PG in those regions could be resisted by the vertically oriented fibres in that region. The result would be analogous to articular cartilage with a pre-stressed vertically oriented matrix with high concentrations of PG. It appears that fibres from the radially oriented tie-fibres also integrate with the lamellar layer through branches that are oriented perpendicularly to the surface (Figure 8.2 B). The Benninghoff arcade model includes the rigid subchondral bone, to which the fibres are anchored; in the meniscus, the vertically oriented fibres appear to be integrated with the main body of the tissue. Vertically oriented fibres could also act to limit swelling of the meniscus. Water may be reabsorbed into the tissue in long periods of unloading due to the osmotic swelling pressure; similar to other fibrocartilages, such as the intervertebral disc (Adams, Dolan et al. 1990); the arborizing fibres could act to limit this swelling.
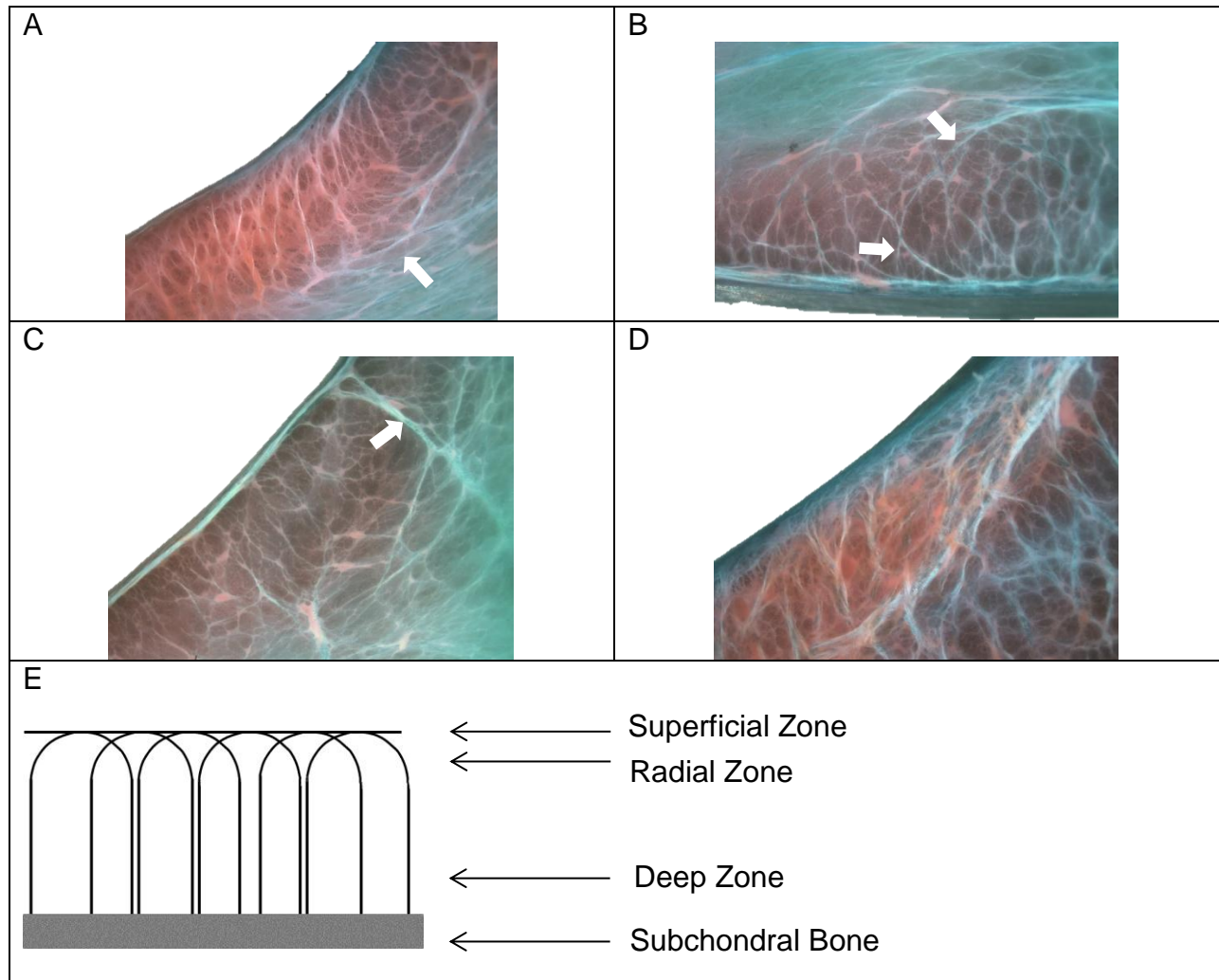
Figure 8.2 Fast green and safranin O whole mount sections from the femoral surfaces of the anterior (A), central (C) and posterior surfaces (D) of a medial meniscus and the tibial surface from the anterior portion of the same meniscus (B). (E) A schematic illustrating the Benninghoff arcade previously described for articular cartilage (Benninghoff 1925). Safranin O staining for PG and perpendicularly oriented fibres stops abruptly in the main body (arrow A). Fibres from the radially oriented tie fibres appear to branch and interact with the lamellar layer near the tibial surface (arrows B). A thick arborizing fibre emanates from the femoral surface into the main meniscal body (arrow C). Arborizing fibres and PG staining spread deeper into the tissue in the posterior portion of the meniscus (D).

8.4.3 Main Body

8.4.3.1 Circumferential Fascicles

The current paradigm regarding meniscal structure is that the majority of fibres are oriented in the circumferential direction. Imaging using OPT has illustrated that this is generally true in the outer third of the bovine meniscus however; it is a gross oversimplification of the complexity observed in the inner two-thirds of the tissue. OPT images identified non-uniform fibre organization in the inner third and in the regions near the femoral and tibial surfaces (Figure 5.3). These images contained braided and woven fibre organizations. These organizations would increase fibre recruitment under various loading conditions and act as a transition between regions containing different fibre orientations [Chapter 5]. Observations of a dimethylene blue (DMB) stained, transverse section of the meniscus identified bifurcation of fascicles in the circumferential direction toward the inner portion of the meniscus (Figure 8.3A). This organization would allow further integration between the outer and in inner regions and increase the number of fascicles recruited under varying loading conditions. A fast green and safranin O section of the posterior portion of a bovine meniscus identified a fascicle bundle oriented in the inferior/superior direction. This bundle appeared to branch in various directions in the section (Figure 8.3 B) and further identifies the variability in the orientation of the circumferential fascicles.
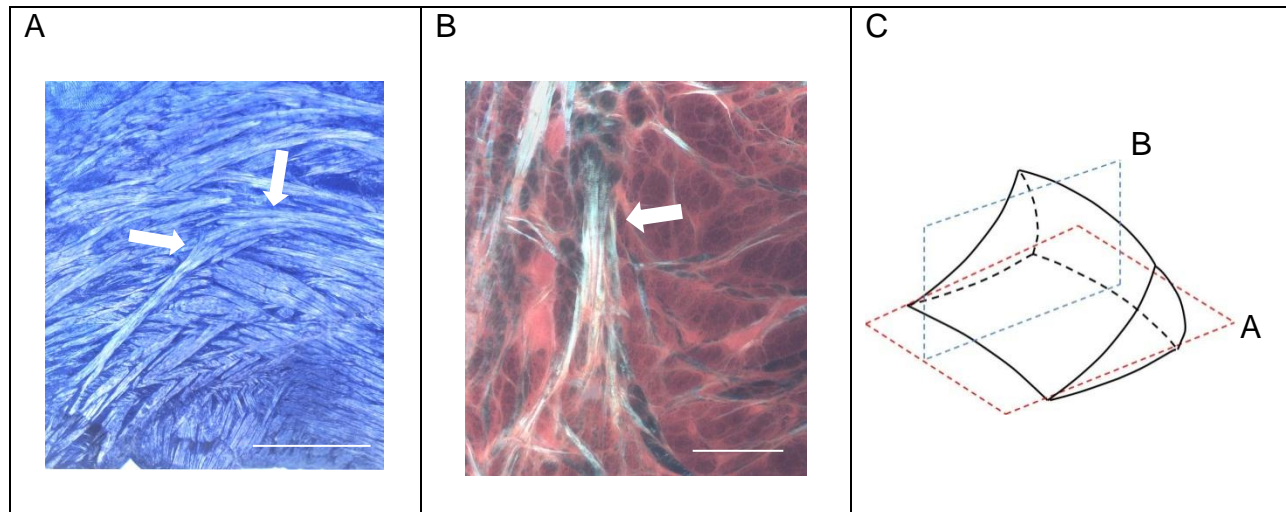
Figure 8.3 Scale bars 1 mm. A dimthylene blue stain transverse section identifying a circumferential fascicle which bifurcates toward the inner tip of the meniscus (arrows A). Safranin O and fast green stained radial section from the posterior medial meniscus. Circumferential fascicles appear to be oriented vertically downward and branches into the section (arrow B). A schematic of the section orientations (C).

The organization of the circumferential fibres becomes more uniform toward the outer edge of the meniscus [Chapter 5]. By evaluating the relative vertical and extrusive forces exerted on the surface of the meniscus, it becomes apparent that the radial extrusive forces increase toward the outer edge as the slope of the surface of the meniscus steepens (Figure 8.4). Interestingly, the proportion of collagen stained regions to PG stained region also increases toward the outer edge. Based on these results, it is proposed that as the radial extrusive force increases as the slope increases, the state of stress in the outer portion of the meniscus becomes more uniform in tension and consequently the fibre alignment is also more uniform as seen in Chapter 5. The inner portion of the meniscus experiences a more uniform compressive stress with minimal radial stress, and the presence of circumferential fibres is minimal in this region. The fibre organization may transition from the inner tip to the outer edge as a function of the shape and stresses experienced by these regions.
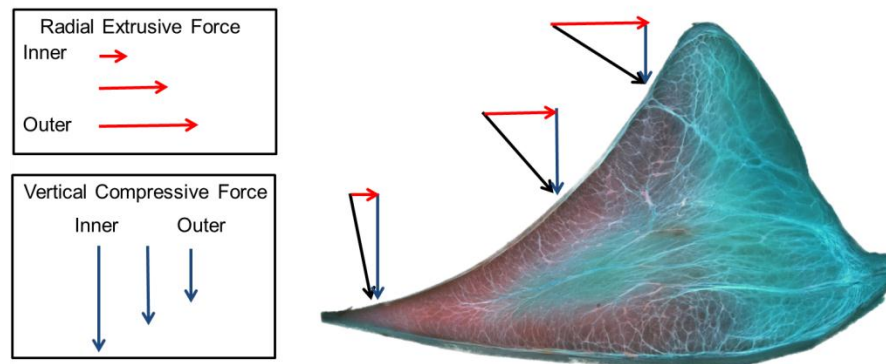
Figure 8.4 Fast green and safranin O stained radial section of the middle portion of a medial meniscus. Black arrows indicate the applied load from the femur, perpendicular to the meniscal surface. Red arrows identify the radial component of the applied load and blue arrows identify the vertical component of the applied load.

PRG4 has been observed to be localized between circumferential fascicles as well as between the fibres [Chapter 7]. This molecule has been shown to decrease the coefficient of friction between articular cartilage surfaces (Schmidt, Gastelum et al. 2007). Within tissues it has been speculated to decrease the sliding resistance between collagen fascicles (Schumacher, Schmidt et al. 2005; Sun, Berger et al. 2006). The collagen organization described here, coupled with the presence of PRG4, could indicate that fascicles may be recruited individually and move relative to one another under load. The presence of PRG4 at the fibre level may also indicate that the fibres within a fascicle are also differentially recruited and may slide relative to one another. This may also play a role in reducing the shear modulus of the menisci by enabling the reorganization of fascicles, thereby allowing changes in shape of the tissue. Populations of cells also reside at each of these hierarchical levels. Therefore, while facilitating sliding and reorganization, PRG4 may also reduce shear stresses on the cells in these regions.

8.4.3.2 <u>Tie-Fibres</u>

Extensive tie-fibre networks were observed in the bovine meniscus. Tie-fibres may play several important roles in the menisci. Tie-fibres appear to interact with the lamellar layer and may contribute to the compressive properties of the tissue. These fibres have been previously shown to organize into sheets. A model was previously proposed in which the sheets form a honeycomb like structure through which the circumferential fascicles pass (Rattner, Matyas et al. 2011). Based on the findings of the current studies, a modification to this model is proposed, in which the tie fibres form a three-dimensional net-like organization composed of ribbons of tie-fibres. This tie-fibre net would give the tissue the radial tensile strength required to resist radial splitting of the meniscus and also facilitate the woven and bifurcating orientation of circumferential fascicles. Another significant function of this network would be to segregate circumferential fascicles. The segregation of circumferential fascicles would result in two mechanical phenomena. First, segregation of fascicles would allow for reorganization of fascicles under load, resulting in the low shear modulus previously identified in the meniscus (Proctor, Schmidt et al. 1989; Nguyen and Levenston 2012). The low shear modulus may be required to accommodate the varying shape of the femur from extension to flexion to ensure even load distribution in the tissue (Figure 1.9). Second, PRG4 was also identified between the tie-fibre network and the circumferential fascicles, which may indicate sliding between the structures [Chapter 7]. From the observations of elastin organization, significant amounts were seen within the tie-fibre network, indicating an elastic function of this structure. Elastin may allow the menisci to return to a "zero-position" after changes in shape from loading. As pure shear would not result in fluid exudation, an elastic network would be required to regain the tissue's original shape after loading. The segregation of fascicles also gives the structure a low

bending stiffness, by reducing the moment of inertia within each fascicle. The menisci bend in the transverse plane throughout flexion as the anterior horn moves closer to the posterior horn which increases the joint congruency throughout flexion. This low bending stiffness would also be accommodated by the segregation of circumferential fascicles.

Finally, we have identified a new region in the menisci, the PG-rich region surrounding blood vessels [Chapter 6]. This PG rich milieu surrounds the blood vessels, inside a type II collagen rich matrix, and tends to be oriented along the tie-fibre network. The PG matrix would increase the osmotic pressure in the peri-vascular region which would then be constrained by the surrounding collagen matrix. This region may have a mechanical function in pressurizing the region around the blood vessel to protect it from compression resulting from contact forces or from the circumferential fascicles in the outer region.

8.4.4 Model Summary

An updated working model of meniscal function has been proposed based on findings from the collection of work contained within this thesis combined with previous work in this field. Using the theory of causal histogenesis, combined with information from previous mechanical studies and the functional requirements of the menisci, a novel model of meniscal behaviour has been described. Identifying specific building blocks within the menisci, enables speculation about the behaviour of the region of interest (i.e. PG and type II collagen for compressive properties and type I collagen and elastin for tensile properties). By investigating the tissue structure and mechanics using an integrated approach we have gleaned greater knowledge of meniscal behaviour.

8.5 Future Work

The results presented here provide new information about meniscal structure and function; however there are many questions which require further investigation. Understanding the changes that occur in structure and composition during meniscal development and subsequent breakdown are integral to developing repair or replacement strategies (i.e. tissue engineered constructs). To date, no thorough investigation has been conducted to evaluate meniscal development from the embryologic stage through to skeletal maturity. Knowledge of the spatial and temporal changes that occur in the menisci may elucidate strategies for growth of tissue engineered constructs.

The IIF findings from Chapters 6 and 7 identify colocalization of proteins within specific regions in the meniscus (i.e. the surface, tie-fibres, circumferential fascicles and PG rich peri-vascular regions). Investigations into the specific proteins within each of these regions may further differentiate the building blocks of the meniscus. We have conducted a pilot study on the composition of individual tie-fibres and circumferential fibres using mass spectrometry and have received preliminary results. These results indicate compositional differences as well as similarities between these constituent units. A full investigation of the differences at structural and hierarchical levels within the tissue may further explain the organization of the meniscus.

From a mechanical perspective a variety of studies would be required to support the model proposed in this chapter. A study on the relative movement of fibres in normal and PRG4 deficient animals would further support the hypothesis that PRG4 does facilitate sliding between architectural subunits. Further, the use of various proteases including elastase and chondroitinase could be used to investigate the specific roles of elastin and aggrecan in meniscal mechanics.

From a structural perspective, OPT could be used to visualize the transition between the insertional ligaments and the meniscal body. This technique could also be used to attempt to visualize the length and continuity of collagen fascicles. The highly three-dimensional organization of the matrix does not allow visualization of whole fascicles over long distances in two-dimensional sections. These evaluations could also be implemented on tendon and ligament to understand the specific arrangement of these tissues.

Information gleaned from mechanical, structural and compositional studies could be used to increase the accuracy and complexity of computer models of meniscal mechanics. Further quantification of the orientation of fibre bundles and the region specific differences in material properties may allow for better understanding of the load bearing mechanisms in the meniscus. As discussed in Chapter 4, the direction and density of the collagen fascicles could be quantified through segmentation and image processing techniques. If the constituent material properties of these fibers were determined, more accurate models of the menisci could be developed and the mechanics developed by the local architecture could be evaluated within sub-regions of the tissue. Further, the localization of compositional differences identified in Chapter 6 could also further the accuracy of these models. Relationships have been studied between PG content and compressive stiffness in articular cartilage (Williamson, Chen et al. 2001). These relationships could also be studied in a region specific manner in the meniscus to determine the role of these regions play in overall meniscal function. Moreover, these models would facilitate studies on the effect of matrix degradation or compositional changes on the overall mechanics of the tissues. These types of models have been developed for the evaluation of the mechanics of both articular cartilage (Li, Cheung et al. 2009) and bone (MacNeil and Boyd 2008). Predictive models may identify regions of weakness in the menisci which could be compared against injured or diseased

tissues. Further, these models could be used to evaluate the effect of surgical repair techniques on the mechanics of the remaining, intact tissue. As current measurement techniques are unable to measure strain in the body of the meniscus under load; accurate computer models would be a valuable addition in the evaluation of meniscal mechanics.

The collection of work described in this thesis has identified several novel findings in the meniscus, including concepts regarding overall function, mechanics, structure and composition. This integrated approach has led to the development of a new descriptive model of meniscal function and has set the groundwork for future evaluations of the menisci and other connective tissues.

REFERENCES

Abubacker, S., H. O. Ham, et al. "Cartilage boundary lubricating ability of aldehyde modified proteoglycan 4 (PRG4-CHO)." Osteoarthritis and Cartilage(0).

Adams, M., P. Dolan, et al. (1990). "Diurnal changes in spinal mechanics and their clinical significance." Journal of Bone & Joint Surgery, British Volume **72-B**(2): 266-270.

Adeeb, A. M., E. Y. Sayed, et al. (2004). "Congruency effect on load bearing in diarthrodial joints." Computer Methods in Biomechanical and Biomedical Engineering **7**(3): 147-157.

Alexander, R. M. (1991). "Energy-saving mechanisms in walking and running." J Exp Biol **160**: 55-69.

Allen, C. R., E. K. Wong, et al. (2000). "Importance of the medial meniscus in the anterior cruciate ligament-deficient knee." J Orthop Res **18**(1): 109-115.

Andrews, S., N. Shrive, et al. (2011). "The shocking truth about meniscus." J Biomech **44**(16): 2737-2740.

Andrews, S. H. J., Ronsky, J.L. (2011). Strain rate dependence of bovine medial menisci in circumferential tension. Alberta BME Conference. Banff, AB.

Arnoczky, S. P. (1990). Animal models for knee ligament research. Knee Ligaments: Structure, Function, Injury and Repair. D. W. Daniel, Akeson, W., O'Connor, J. . New York, Raven Press**:** 401-417.

Arnoczky, S. P., J. L. Cook, et al. (2010). "Translational models for studying meniscal repair and replacement: what they can and cannot tell us." Tissue Eng Part B Rev **16**(1): 31-39.

Arnoczky, S. P. and R. F. Warren (1982). "Microvasculature of the human meniscus." Am J Sports Med **10**(2): 90-95.

Ateshian, G. A., W. H. Warden, et al. (1997). "Finite deformation biphasic material properties of bovine articular cartilage from confined compression experiments." J Biomech **30**(11-12): 1157-1164.

Athanasiou, K. A. and J. Sanchez-Adams (2009). "Engineering the Knee Meniscus." Synthesis Lectures on Tissue Engineering **1**(1): 1-97.

Augat, P., T. Link, et al. (1998). "Anisotropy of the elastic modulus of trabecular bone specimens from different anatomical locations." Medical Engineering & Physics **20**(2): 124-131.

Baratz, M. E., F. H. Fu, et al. (1986). "Meniscal tears: the effect of meniscectomy and of repair on intraarticular contact areas and stress in the human knee. A preliminary report." Am J Sports Med **14**(4): 270-275.

Benjamin, M. and E. J. Evans (1990). "Fibrocartilage." J Anat **171**: 1-15.

Benjamin, M. and J. R. Ralphs (1998). "Fibrocartilage in tendons and ligaments--an adaptation to compressive load." J Anat **193 (Pt 4)**: 481-494.

Benjamin, M. and J. R. Ralphs (2004). "Biology of fibrocartilage cells." Int Rev Cytol **233**: 1-45.

Benninghoff, A. (1925). "Form und bau der Geleknorpel in ihren Bezeihungen zur Funktion." Z Zellforsch Mikrosk
 2: 783-825.

Best, B. A., F. Guilak, et al. (1994). "Compressive mechanical properties of the human anulus fibrosus and their relationship to biochemical composition." Spine (Phila Pa 1976) **19**(2): 212-221.

Biot, M. A. (1941). "General Theory of Three-Dimensional Consolidation." J. Appl. Phys. **12**(2).

Brandt, J. M., L. K. Brière, et al. (2010). "Biochemical comparisons of osteoarthritic human synovial fluid with calf sera used in knee simulator wear testing." Journal of Biomedical Materials Research Part A **94A**(3): 961-971.

Brantigan, O. C. and A. F. Voshell (1943). "THE TIBIAL COLLATERAL LIGAMENT: ITS FUNCTION, ITS BURSAE, AND ITS RELATION TO THE MEDIAL MENISCUS." The Journal of Bone & Joint Surgery **25**(1): 121-131.

Bray, D. F., J. Bagu, et al. (1993). "Comparison of hexamethyldisilazane (HMDS), Peldri II, and critical-point drying methods for scanning electron microscopy of biological specimens." Microsc Res Tech **26**(6): 489-495.

Briscoe, B. J., R. S. Court, et al. (1993). "The effects of fabric weave and surface texture on the interlaminar fracture toughness of aramid/epoxy laminates." Composites Science and Technology **47**(3): 261-270.

Bullough, P. G., L. Munuera, et al. (1970). "The strength of the menisci of the knee as it relates to their fine structure." J Bone Joint Surg Br **52**(3): 564-567.

Bursac, P., S. Arnoczky, et al. (2009). "Dynamic compressive behavior of human meniscus correlates with its extra-cellular matrix composition." Biorheology **46**(3): 227-237.

Buschmann, M. D., J. Soulhat, et al. (1998). "Confined compression of articular cartilage: linearity in ramp and sinusoidal tests and the importance of interdigitation and incomplete confinement." J Biomech **31**(2): 171-178.

Cameron, H. U. and I. Macnab (1972). "The structure of the meniscus of the human knee joint." Clin Orthop Relat Res **89**: 215-219.

Canatrow, A., Tumper, M (1978). Water, Sodium, Chloride, Potassium,: Physiological Considerations. Clinical Biochemistry. A. L. Latner. Philadelphia, W. B. Saunders Company**:** 339-367.

Cappozzo, A., Figura, F., Leo, T., and Marchetti, M. (1978a). Movements and mechanical energy changes in the upper part of the human body during walking. Biomechanics VI-A. E. A. a. K. Jorgensen. Baltimore, University Park Press**:** 272.

Carton, R. W., J. Dainauskas, et al. (1962). "Elastic properties of single elastic fibers." J Appl Physiol **17**: 547-551.

Cheung, H. S. (1987). "Distribution of type I, II, III and V in the pepsin solubilized collagens in bovine menisci." Connect Tissue Res **16**(4): 343-356.

Chevrier, A., M. Nelea, et al. (2009). "Meniscus structure in human, sheep, and rabbit for animal models of meniscus repair." J Orthop Res **27**(9): 1197-1203.

Chia, H. N. and M. L. Hull (2008). "Compressive moduli of the human medial meniscus in the axial and radial directions at equilibrium and at a physiological strain rate." J Orthop Res **26**(7): 951-956.

Chimich, D., N. Shrive, et al. (1992). "Water content alters viscoelastic behaviour of the normal adolescent rabbit medial collateral ligament." J Biomech **25**(8): 831-837.

Cottrell, J. M., P. Scholten, et al. (2008). "A new technique to measure the dynamic contact pressures on the Tibial Plateau." J Biomech **41**(10): 2324-2329.

Djurasovic, M., J. W. Aldridge, et al. (1998). "Knee Joint Immobilization Decreases Aggrecan Gene Expression in the Meniscus." Am J Sports Med **26**(3): 460-466.

Donahue, T. L. H., M. L. Hull, et al. (2002). "A Finite Element Model of the Human Knee Joint for the Study of Tibio-Femoral Contact." Journal of Biomechanical Engineering **124**(3): 273-280.

Eisenberg, S. R. and A. J. Grodzinsky (1985). "Swelling of articular cartilage and other connective tissues: electromechanochemical forces." J Orthop Res **3**(2): 148-159.

Englund, M. (2009). "The role of the meniscus in osteoarthritis genesis." Med Clin North Am **93**(1): 37-43.

Englund, M., A. Guermazi, et al. (2009). "The meniscus in knee osteoarthritis." Rheum Dis Clin North Am **35**(3): 579-590.

Evans, B. G. (2007). The Knee. Essentials of Orthopedic Surgery. S. Wiesel, Delahay, J. New York, Springer Sceince**:** 454-471.

Eyre, D. R. and J. J. Wu (1983). "Collagen of fibrocartilage: a distinctive molecular phenotype in bovine meniscus." FEBS Lett **158**(2): 265-270.

Fairbank, T. J. (1948). "Knee joint changes after meniscectomy." J Bone Joint Surg Br **30B**(4): 664-670.

Fernández, P., M. J. Lamela Rey, et al. (2011). "Viscoelastic Characterisation of the Temporomandibular Joint Disc in Bovines." Strain **47**(2): 188-193.

Fithian, D. C., M. A. Kelly, et al. (1990). "Material properties and structure-function relationships in the menisci." Clin Orthop Relat Res(252): 19-31.

Flannery, C. R., C. E. Hughes, et al. (1999). "Articular cartilage superficial zone protein (SZP) is homologous to megakaryocyte stimulating factor precursor and Is a multifunctional proteoglycan with potential growth-promoting, cytoprotective, and lubricating properties in cartilage metabolism." Biochem Biophys Res Commun **254**(3): 535-541.

Fleming, B. C., P. A. Renstrom, et al. (2001). "The effect of weightbearing and external loading on anterior cruciate ligament strain." J Biomech **34**(2): 163-170.

Fukubayashi, T. and H. Kurosawa (1980). "The contact area and pressure distribution pattern of the knee. A study of normal and osteoarthrotic knee joints." Acta Orthop Scand **51**(6): 871-879.

Gabrion, A., P. Aimedieu, et al. (2005). "Relationship between ultrastructure and biomechanical properties of the knee meniscus." Surg Radiol Anat **27**(6): 507-510.

Galante, J. O. (1967). "Tensile properties of the human lumbar annulus fibrosus." Acta Orthop Scand: Suppl 100:101-191.

Ghadially, F. N., J. M. Lalonde, et al. (1983). "Ultrastructure of normal and torn menisci of the human knee joint." J Anat **136**(Pt 4): 773-791.

Ghadially, F. N., J. H. Wedge, et al. (1986). "Experimental methods of repairing injured menisci." J Bone Joint Surg Br **68**(1): 106-110.

Goertzen, D. J., D. R. Budney, et al. (1997). "Methodology and apparatus to determine material properties of the knee joint meniscus." Med Eng Phys **19**(5): 412-419.

Hellio Le Graverand, M. P., Y. Ou, et al. (2001). "The cells of the rabbit meniscus: their arrangement, interrelationship, morphological variations and cytoarchitecture." J Anat **198**(Pt 5): 525-535.

Higuchi, H., M. Kimura, et al. (2000). "Factors affecting long-term results after arthroscopic partial meniscectomy." Clin Orthop Relat Res(377): 161-168.

Holmes, M. H. (1986). "Finite deformation of soft tissue: analysis of a mixture model in uni-axial compression." J Biomech Eng **108**(4): 372-381.

Holmes, M. H. and V. C. Mow (1990). "The nonlinear characteristics of soft gels and hydrated connective tissues in ultrafiltration." J Biomech **23**(11): 1145-1156.

Hopker, W. W., G. Angres, et al. (1986). "Changes of the elastin compartment in the human meniscus." Virchows Arch A Pathol Anat Histopathol **408**(6): 575-592.

Huang, K. and L. D. Wu (2008). "Aggrecanase and aggrecan degradation in osteoarthritis: a review." J Int Med Res **36**(6): 1149-1160.

Ingman, A. M., P. Ghosh, et al. (1974). "Variation of collagenous and non-collagenous proteins of human knee joint menisci with age and degeneration." Gerontologia **20**(4): 212-223.

Jay, G. D. (2004). "Lubricin and surfacing of articular joints." Curr Opin Orthop **15**(5): 355-359.

Jeffery, A. K., G. W. Blunn, et al. (1991). "Three-dimensional collagen architecture in bovine articular cartilage." J Bone Joint Surg Br **73**(5): 795-801.

Jones, R. S., G. C. Keene, et al. (1996). "Direct measurement of hoop strains in the intact and torn human medial meniscus." Clin Biomech (Bristol, Avon) **11**(5): 295-300.

Joshi, M. D., J. K. Suh, et al. (1995). "Interspecies variation of compressive biomechanical properties of the meniscus." J Biomed Mater Res **29**(7): 823-828.

Kadler, K. (1994). "Extracellular matrix. 1: fibril-forming collagens." Protein Profile **1**(5): 519-638.

Kadler, K. E., D. F. Holmes, et al. (1996). "Collagen fibril formation." Biochem J **316 (Pt 1)**: 1-11.

Kambic, H. E. and C. A. McDevitt (2005). "Spatial organization of types I and II collagen in the canine meniscus." J Orthop Res **23**(1): 142-149.

Karnik, S. K., B. S. Brooke, et al. (2003). "A critical role for elastin signaling in vascular morphogenesis and disease." Development **130**(2): 411-423.

Kelly, M. A., Fithian, D.C., Mow, V.C. (1990). Structure and Function of the Meniscus: Basic and Clinical Implications. Biomechanics of Diarthrodial Joints. V. C. Mow, Ratcliffe, A., Woo, S.L-Y. New York, Springer-Verlag. **I:** 1911-1211.

Kempson, G. E., H. Muir, et al. (1970). "Correlations between stiffness and the chemical constituents of cartilage on the human femoral head." Biochim Biophys Acta **215**(1): 70-77.

Kettelkamp, D. B. and A. W. Jacobs (1972). "Tibiofemoral contact area--determination and implications." J Bone Joint Surg Am **54**(2): 349-356.

Kiviranta, I., J. Jurvelin, et al. (1985). "Microspectrophotometric quantitation of glycosaminoglycans in articular cartilage sections stained with Safranin O." Histochemistry **82**(3): 249-255.

Kohn, D. and B. Moreno (1995). "Meniscus insertion anatomy as a basis for meniscus replacement: a morphological cadaveric study." Arthroscopy **11**(1): 96-103.

Krause, W. R., M. H. Pope, et al. (1976). "Mechanical changes in the knee after meniscectomy." J Bone Joint Surg Am **58**(5): 599-604.

Kurosawa, H., T. Fukubayashi, et al. (1980). "Load-bearing mode of the knee joint: physical behavior of the knee joint with or without menisci." Clin Orthop Relat Res(149): 283-290.

Kwan, M. K., W. M. Lai, et al. (1984). "Fundamentals of fluid transport through cartilage in compression." Ann Biomed Eng **12**(6): 537-558.

Kwan, M. K., W. M. Lai, et al. (1990). "A finite deformation theory for cartilage and other soft hydrated connective tissues--I. Equilibrium results." J Biomech **23**(2): 145-155.

Lanzer, W. L. and G. Komenda (1990). "Changes in articular cartilage after meniscectomy." Clin Orthop Relat Res(252): 41-48.

Lechner, K., M. L. Hull, et al. (2000). "Is the circumferential tensile modulus within a human medial meniscus affected by the test sample location and cross-sectional area?" J Orthop Res **18**(6): 945-951.

Lee, S. J., K. J. Aadalen, et al. (2006). "Tibiofemoral contact mechanics after serial medial meniscectomies in the human cadaveric knee." Am J Sports Med **34**(8): 1334-1344.

Leech, C. M. (1987). "THEORY AND NUMERICAL-METHODS FOR THE MODELING OF SYNTHETIC ROPES." Communications in Applied Numerical Methods **3**(5): 407-413.

Li, L. P., J. T. M. Cheung, et al. (2009). "Three-dimensional fibril-reinforced finite element model of articular cartilage." Med Biol Eng Comput **47**(6): 607-615.

Light, L. H., G. E. McLellan, et al. (1980). "Skeletal transients on heel strike in normal walking with different footwear." J Biomech **13**(6): 477-480.

Lohmander, L. S., P. M. Englund, et al. (2007). "The long-term consequence of anterior cruciate ligament and meniscus injuries: osteoarthritis." Am J Sports Med **35**(10): 1756-1769.

Ludwig, T. E., J. R. McAllister, et al. (2012). "Diminished cartilage lubricating ability of human osteoarthritic synovial fluid deficient in proteoglycan 4: Restoration through proteoglycan 4 supplementation." Arthritis & Rheumatism: n/a-n/a.

MacNeil, J. A. and S. K. Boyd (2008). "Bone strength at the distal radius can be estimated from high-resolution peripheral quantitative computed tomography and the finite element method." Bone **42**(6): 1203-1213.

Mak, A. F. (1986). "The apparent viscoelastic behavior of articular cartilage--the contributions from the intrinsic matrix viscoelasticity and interstitial fluid flows." J Biomech Eng **108**(2): 123-130.

Maquet, P., A. Van De Berg, et al. (1976). "[The weight-bearing surfaces of the femoro-tibial joint]." Acta Orthop Belg **42 Suppl 1**: 139-143.

Maroudas, A. and M. Venn (1977). "Chemical composition and swelling of normal and osteoarthrotic femoral head cartilage. II. Swelling." Ann Rheum Dis **36**(5): 399-406.

Maroudas, A. I. (1976). "Balance between swelling pressure and collagen tension in normal and degenerate cartilage." Nature **260**(5554): 808-809.

Masouros, S. D., I. D. McDermott, et al. (2008). "Biomechanics of the meniscus-meniscal ligament construct of the knee." Knee Surg Sports Traumatol Arthrosc **16**(12): 1121-1132.

Matava, M. J. (2007). "Meniscal Allograft Transplantation: A Systematic Review." Clin Orthop Relat Res **455**: 142-157 110.1097/BLO.1090b1013e318030c318024e.

McDermott, I. D. and A. A. Amis (2006). "The consequences of meniscectomy." J Bone Joint Surg Br **88**(12): 1549-1556.

McDermott, I. D., Masouras, S.D., Bull, A.M.J., Amis, A.A. (2010). Anatomy. The Meniscus. P. Beaufils, Vwrdonk, R. Berlin, Springer-Verlag.

McDermott, I. D., S. D. Masouros, et al. (2008). "Biomechanics of the menisci of the knee." Current Orthopaedics **22**: 9.

McDevitt, C. A. and R. J. Webber (1990). "The ultrastructure and biochemistry of meniscal cartilage." Clin Orthop Relat Res(252): 8-18.

McNicol, D. and P. J. Roughley (1980). "Extraction and characterization of proteoglycan from human meniscus." Biochem J **185**(3): 705-713.

Melrose, J., S. Smith, et al. (2005). "Comparative spatial and temporal localisation of perlecan, aggrecan and type I, II and IV collagen in the ovine meniscus: an ageing study." Histochem Cell Biol **124**(3-4): 225-235.

Melrose, J., S. Smith, et al. (2005). "Perlecan displays variable spatial and temporal immunolocalisation patterns in the articular and growth plate cartilages of the ovine stifle joint." Histochem Cell Biol **123**(6): 561-571.

Milz, S., C. McNeilly, et al. (1998). "Fibrocartilages in the extensor tendons of the interphalangeal joints of human toes." Anat Rec **252**(2): 264-270.

Mow, V. C., W. Y. Gu, et al. (2005). Structure and Function of Articular Cartilage and Meniscus. Basic Orthopaedic Biomechanics and Mechano-Biology. V. C. Mow and R. Huiskes. Philadelphia, Lippincott Williams & Wilkins**:** 182-258.

Mow, V. C., S. C. Kuei, et al. (1980). "Biphasic creep and stress relaxation of articular cartilage in compression? Theory and experiments." J Biomech Eng **102**(1): 73-84.

Mow, V. C., A. Ratcliffe, et al. (1992). "Cartilage and diarthrodial joints as paradigms for hierarchical materials and structures." Biomaterials **13**(2): 67-97.

Muratsu, H., K. Ishimoto, et al. (2000). The mechanical mapping of the meniscus. 46th annual meeting of the Orthopaedic Research Society. Orlando. FL: Orthopaedic Research Society.

Nakano, T., C. M. Dodd, et al. (1997). "Glycosaminoglycans and proteoglycans from different zones of the porcine knee meniscus." J Orthop Res **15**(2): 213-220.

Nakano, T. and P. G. Scott (1986). "Purification and characterization of a gelatinase produced by fibroblasts from human gingiva." Biochem Cell Biol **64**(5): 387-393.

Nguyen, A. M. and M. E. Levenston (2012). "Comparison of osmotic swelling influences on meniscal fibrocartilage and articular cartilage tissue mechanics in compression and shear." Journal of Orthopaedic Research **30**(1): 95-102.

O'Connor, B. L. (1976). "The histological structure of dog knee menisci with comments on its possible significance." Am J Anat **147**(4): 407-417.

Parsons, J. R. and J. Black (1979). "Mechanical behavior of articular cartilage: quantitative changes with alteration of ionic environment." J Biomech **12**(10): 765-773.

Pauwels, F. (1960). "[A new theory on the influence of mechanical stimuli on the differentiation of supporting tissue. The tenth contribution to the functional anatomy and causal morphology of the supporting structure]." Z Anat Entwicklungsgesch **121**: 478-515.

Peters, T. J. and I. S. Smillie (1972). "Studies on the chemical composition of the menisci of the knee joint with special reference to the horizontal cleavage lesion." Clin Orthop Relat Res **86**: 245-252.

Petersen, W. and B. Tillmann (1998). "Collagenous fibril texture of the human knee joint menisci." Anat Embryol (Berl) **197**(4): 317-324.

Piersol, A. G. P., T.L. (2010). Harris' Shock and Vibration Handbook. New York, McGraw-Hill Companies Inc.

Proctor, C. S., M. B. Schmidt, et al. (1989). "Material properties of the normal medial bovine meniscus." J Orthop Res **7**(6): 771-782.

Race, A., N. D. Broom, et al. (2000). "Effect of loading rate and hydration on the mechanical properties of the disc." Spine (Phila Pa 1976) **25**(6): 662-669.

Rattner, J. B., J. R. Matyas, et al. (2011). "New understanding of the complex structure of knee menisci: implications for injury risk and repair potential for athletes." <u>Scand J Med Sci Sports</u> **21**(4): 543-553.

Richards-Kortum, R. and E. Sevick-Muraca (1996). "Quantitative optical spectroscopy for tissue diagnosis." <u>Annu Rev Phys Chem</u> **47**: 555-606.

Rodeo, S. A., Warren, R.F. (1994). "Indications and techniques for use of a fibrin clot in meniscal repair." <u>Operative Techniques in Sports Medicine</u> **2**(3): 217-222.

Røhl, L., E. Larsen, et al. (1991). "Tensile and compressive properties of cancellous bone." <u>J Biomech</u> **24**(12): 1143-1149.

Roos, E. M., A. Ostenberg, et al. (2001). "Long-term outcome of meniscectomy: symptoms, function, and performance tests in patients with or without radiographic osteoarthritis compared to matched controls." <u>Osteoarthritis Cartilage</u> **9**(4): 316-324.

Roos, H., M. Lauren, et al. (1998). "Knee osteoarthritis after meniscectomy: prevalence of radiographic changes after twenty-one years, compared with matched controls." <u>Arthritis Rheum</u> **41**(4): 687-693.

Rosenbloom, J., W. R. Abrams, et al. (1993). "Extracellular matrix 4: the elastic fiber." <u>FASEB J</u> **7**(13): 1208-1218.

Sanchez-Adams, J. and K. A. Athanasiou (2012). "Biomechanics of meniscus cells: regional variation and comparison to articular chondrocytes and ligament cells." <u>Biomech Model Mechanobiol</u>.

Sanchez-Adams, J., V. P. Willard, et al. (2011). "Regional variation in the mechanical role of knee meniscus glycosaminoglycans." <u>J Appl Physiol</u> **111**(6): 1590-1596.

Scarvell, J. M., P. N. Smith, et al. (2007). "Magnetic resonance imaging analysis of kinematics in osteoarthritic knees." <u>J Arthroplasty</u> **22**(3): 383-393.

Schmidt, T. A., N. S. Gastelum, et al. (2007). "Boundary lubrication of articular cartilage: role of synovial fluid constituents." <u>Arthritis Rheum</u> **56**(3): 882-891.

Schumacher, B. L., T. A. Schmidt, et al. (2005). "Proteoglycan 4 (PRG4) synthesis and immunolocalization in bovine meniscus." <u>J Orthop Res</u> **23**(3): 562-568.

Scowen, E. F., J. F. Brailsford, et al. (1948). "Discussion on generalized diseases of bone in the adult." <u>Proc R Soc Med</u> **41**(11): 735-744.

Seedhom, B. B., D. Dowson, et al. (1974). "Proceedings: Functions of the menisci. A preliminary study." <u>Ann Rheum Dis</u> **33**(1): 111.

Sharpe, J., U. Ahlgren, et al. (2002). "Optical projection tomography as a tool for 3D microscopy and gene expression studies." <u>Science</u> **296**(5567): 541-545.

Sheehan, F. T. and J. E. Drace (2000). "Human patellar tendon strain. A noninvasive, in vivo study." <u>Clin Orthop Relat Res</u>(370): 201-207.

Shrive, N. G., J. J. O'Connor, et al. (1978). "Load-bearing in the knee joint." <u>Clin Orthop Relat Res</u>(131): 279-287.

Skaggs, D. L., W. H. Warden, et al. (1994). "Radial tie fibers influence the tensile properties of the bovine medial meniscus." <u>J Orthop Res</u> **12**(2): 176-185.

Sun, Y., E. J. Berger, et al. (2006). "Mapping lubricin in canine musculoskeletal tissues." <u>Connect Tissue Res</u> **47**(4): 215-221.

Sun, Y., E. J. Berger, et al. (2006). "Expression and mapping of lubricin in canine flexor tendon." <u>J Orthop Res</u> **24**(9): 1861-1868.

Sun, Y. L., Z. P. Luo, et al. (2002). "Direct quantification of the flexibility of type I collagen monomer." <u>Biochem Biophys Res Commun</u> **295**(2): 382-386.

Swann, D. A. and E. L. Radin (1972). "The molecular basis of articular lubrication. I. Purification and properties of a lubricating fraction from bovine synovial fluid." <u>J Biol Chem</u> **247**(24): 8069-8073.

Sweigart, M. A., C. F. Zhu, et al. (2004). "Intraspecies and interspecies comparison of the compressive properties of the medial meniscus." <u>Ann Biomed Eng</u> **32**(11): 1569-1579.

Thornton, G. M., N. G. Shrive, et al. (2001). "Altering ligament water content affects ligament pre-stress and creep behaviour." <u>J Orthop Res</u> **19**(5): 845-851.

Tillman, B., Schunke, M. (1991). "Struktur and Funktion extra-zellularer Matrix." <u>Anat Anz [Suppl]</u> **168**: 23-26.

Tissakht, M. and A. M. Ahmed (1995). "Tensile stress-strain characteristics of the human meniscal material." <u>J Biomech</u> **28**(4): 411-422.

Valiyaveettil, M., J. S. Mort, et al. (2005). "The concentration, gene expression, and spatial distribution of aggrecan in canine articular cartilage, meniscus, and anterior and posterior cruciate ligaments: a new molecular distinction between hyaline cartilage and fibrocartilage in the knee joint." <u>Connect Tissue Res</u> **46**(2): 83-91.

Vanderploeg, E. J., C. G. Wilson, et al. (2012). "Regional variations in the distribution and colocalization of extracellular matrix proteins in the juvenile bovine meniscus." <u>J Anat</u> **221**(2): 174-186.

Vedi, V., A. Williams, et al. (1999). "Meniscal movement. An in-vivo study using dynamic MRI." <u>J Bone Joint Surg Br</u> **81**(1): 37-41.

Venn, M. and A. Maroudas (1977). "Chemical composition and swelling of normal and osteoarthrotic femoral head cartilage. I. Chemical composition." <u>Ann Rheum Dis</u> **36**(2): 121-129.

Verdonk, P. C., R. G. Forsyth, et al. (2005). "Characterisation of human knee meniscus cell phenotype." <u>Osteoarthritis Cartilage</u> **13**(7): 548-560.

Vogel, K. G. (1996). "The effect of compressive loading on proteoglycan turnover in cultured fetal tendon." <u>Connect Tissue Res</u> **34**(3): 227-237.

Voloshin, A. S. and J. Wosk (1983). "Shock absorption of meniscectomized and painful knees: a comparative in vivo study." <u>J Biomed Eng</u> **5**(2): 157-161.

Wagenseil, J. E. and R. P. Mecham (2009). "Vascular Extracellular Matrix and Arterial Mechanics." <u>Physiological Reviews</u> **89**(3): 957-989.

Walker, P. S. and M. J. Erkman (1975). "The role of the menisci in force transmission across the knee." <u>Clin Orthop Relat Res</u>(109): 184-192.

White, S. C., H. J. Yack, et al. (1998). "Comparison of vertical ground reaction forces during overground and treadmill walking." <u>Med Sci Sports Exerc</u> **30**(10): 1537-1542.

Williamson, A. K., A. C. Chen, et al. (2001). "Compressive properties and function-composition relationships of developing bovine articular cartilage." <u>J Orthop Res</u> **19**(6): 1113-1121.

Winter, D. A. (1983). "Energy generation and absorption at the ankle and knee during fast, natural, and slow cadences." <u>Clin Orthop Relat Res</u>(175): 147-154.

Woo, S. L., S. D. Abramowitch, et al. (2006). "Biomechanics of knee ligaments: injury, healing, and repair." <u>J Biomech</u> **39**(1): 1-20.

Zaffagnini, S., G. M. Marcheggiani Muccioli, et al. (2011). "Prospective Long-Term Outcomes of the Medial Collagen Meniscus Implant Versus Partial Medial Meniscectomy." <u>Am J Sports Med</u> **39**(5): 977-985.

Zhu, W., K. Y. Chern, et al. (1994). "Anisotropic viscoelastic shear properties of bovine meniscus." <u>Clin Orthop Relat Res</u>(306): 34-45.

APPENDIX A: ALBERTA BME (2011) ABSTRACT

Stephen Andrews, Dr. Janet Ronsky

INTRODUCTION

A complete understanding of the material properties of the menisci of the knee is integral for the development of accurate computer models, bioengineered materials or synthetic materials appropriate for grafting in orthopaedic procedures. While the material properties of the menisci have been evaluated, most studies are completed at very slow, non-physiological strain rates (Fithian, Kelly et al. 1990; Tissakht and Ahmed 1995). Therefore, the goal of this study was to determine strain rate-dependence of bovine medial menisci in tension and develop and mathematical technique to analyze said data.

METHODS

Tensile testing was conducted on bovine medial meniscal samples (n=9). Specimens were obtained from the outer edge of the menisci using a series of custom designed cutting jigs. The specimen were dimensions were approximately (10 mm x 5 mm x 2 mm, length x width x thickness). Testing was completed using a Bose Electroforce 3200 apparatus (Bose Corp., Eden Prairie, USA). The specimens' dimensions were first measured using a photogrammetric technique developed with custom Matlab code. Specimens were mounted and a tare load of 0.03 N was applied, then preconditioned (3% strain, 15 cycles @ 1 Hz) and allowed to recover for 120 s. The samples were then tested at four different extension rates (0.005, 0.05, 0.5 and 5 mm/s) to approximately 8% strain, and the resulting force-displacement curves were recorded with 120 s recoveries between each test. Grip-to-grip displacement and the cross-sectional area were used to convert the force-displacement to stress-strain. This data was then fit to a sigmoidal function using Matlab curve fitting function. To calculate the tangent modulus, the analytical function describing the stress-strain curve was then differentiated to obtain the function describing the tangent modulus. T-tests ($\alpha = 0.05$) were used to compare the normalized increase in stiffness (normalized to the lower strain rate). A Bonferroni correction was applied to account for multiple comparisons.

RESULTS

There was a substantial and significant increase in the tangent modulus with increasing strain rate. Modulus at 7% strain was 37% greater at 0.5 mm/s and 20% stiffer at 0.05 mm/s than at 0.005 mm/s ($p < 0.001$ and $p < 0.001$, respectively). Modulus was also greater for 0.5 mm/s strain rate compared to 0.05 mm/s ($p < 0.001$). The sigmoidal fit of the stress-strain data was excellent (figure 1), with average $R^2 = 0.9999$, [0.9994 – 1.000]. The tangent modulus obtained from analytical differentiation (figure 2) was compared to the numerical derivative of the filtered stress-strain curve, and the values were in good agreement.

CONCLUSIONS

Bovine medial menisci were sensitive to strain rate in circumferential tension with a 37% increase in modulus from the slowest to fastest strain rate. The sigmoid fit proved to be an excellent approximation of the experimental data
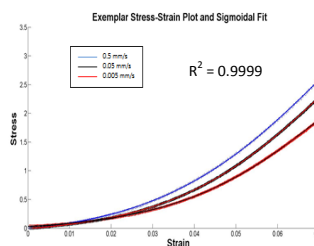
FIGURES

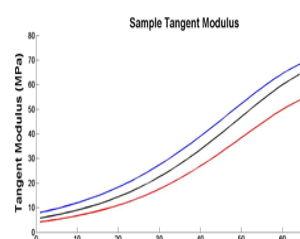
Figure 1. Exemplar stress-strain plot with sigmoid fit.

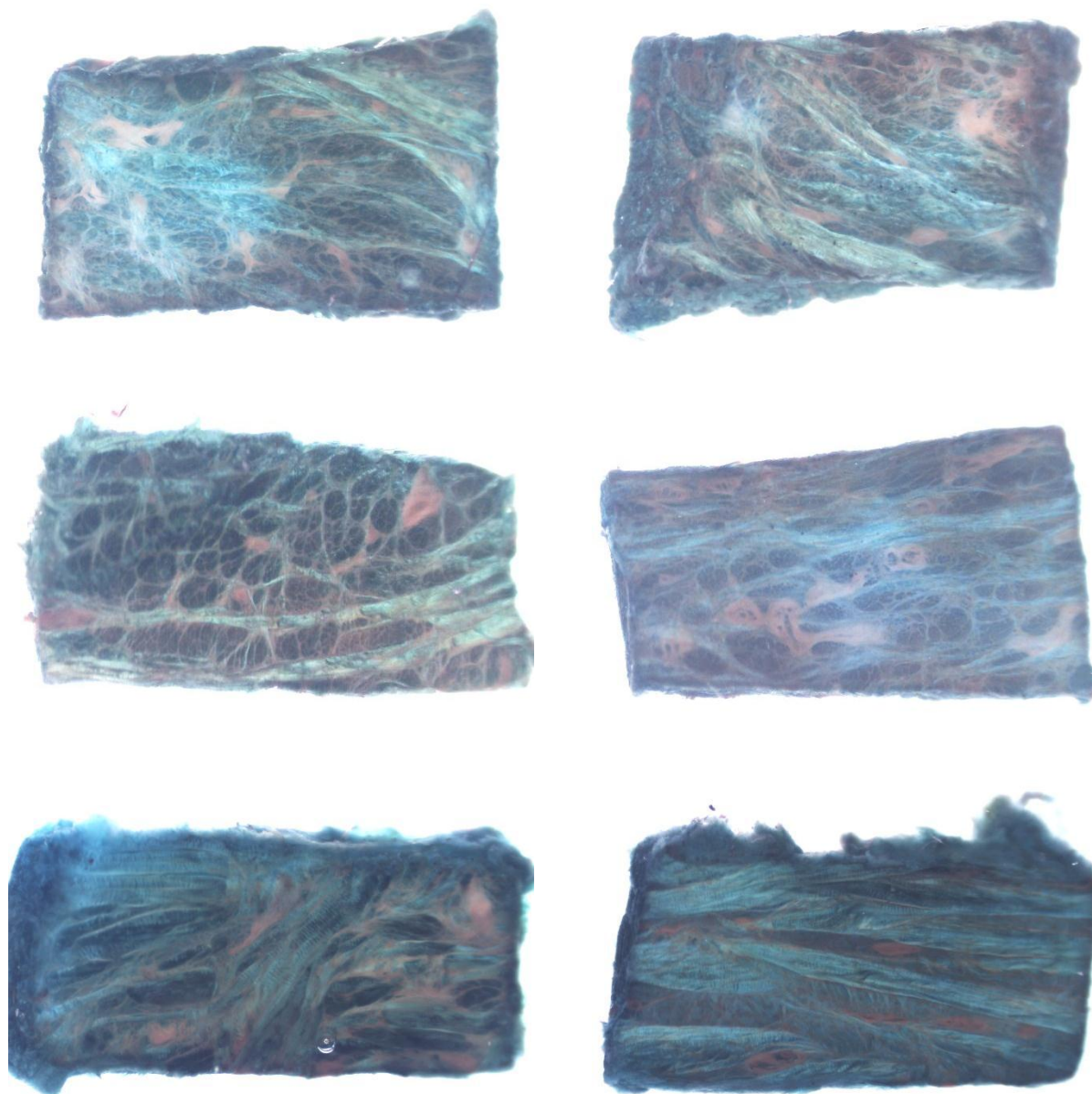Figure 2. Sample tangent modulus plot for increasing strain rate

APPENDIX B: FAST GREEN AND SAFRANIN O SUPPLEMENTAL IMAGES

(CHAPTER 3)

Figure B.1   Example cross sections of 6 samples after swelling for 1 hour in PBS with PI stained with Fast Green (collagen) and Safranin O (proteoglycan). Images illustrate the heterogeneity between and within samples for collagen architecture and PG distribution